

**Isolation and screening of selenium nanoparticles synthesizing
marine bacteria**

A Dissertation for

Course code and Course Title: MMI-651 Discipline Specific Dissertation

Credits: 16

Submitted in partial fulfillment of Master's Degree

M.Sc. In Marine Microbiology

by

PRERANA PIPI MURGAONKAR

Seat NO: 22P0390010

ABC ID: 991544168409

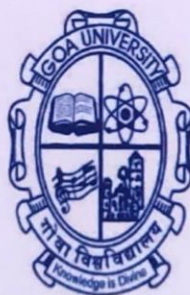
PRN: 201910396

Under the Supervision of

DR. DIVIYA VAIGANKAR

School of Earth, Ocean and Atmospheric Sciences

Marine Microbiology



GOA UNIVERSITY, TALEIGAO PLATEAU

GOA, INDIA

APRIL, 2024

Examined by:

Diviyavankar



Seal of the School

DECLARATION

I hereby declare that the data presented in this Dissertation report entitled, "Isolation and screening of selenium nanoparticles synthesizing marine bacteria" is based on the results of investigations carried out by me in the Marine Microbiology at the School of Earth, Ocean and Atmospheric Sciences, Goa University, under the supervision of Dr. Diviya Vaigankar and the same has not been submitted elsewhere for the award of a degree or diploma by me. Further, I understand that Goa University or its authorities will not be responsible for the correctness of observations / experimental or other findings given the dissertation.

I hereby authorize the University authorities to upload this dissertation on the dissertation repository or anywhere else as the UGC regulations demand and make it available to anyone as needed.



Prerana Pipi Murgaonkar

22P0390010

Date: 02-05-2024

Place: Goa University

COMPLETION CERTIFICATE

This is to certify that the dissertation report “Isolation and screening of selenium nanoparticles synthesizing marine bacteria” is a bonafide work carried out by Ms Prerana Pipi Murgaonkar under my supervision in partial fulfillment of the requirements for the award of the degree of **Master of Science** in the Discipline of Marine Microbiology at School of Earth, Ocean and Atmospheric Sciences, Goa University, Goa.

Prerana Pipi Murgaonkar
02/05/24
Dr. Diviya Vaigankar

Marine Microbiology

School of Earth, Ocean and Atmospheric Sciences

Date: 02.05.2024

Sanjeev C. Ghadi
31/07/24

Sr. Prof. Sanjeev C. Ghadi

(Dean, School of Earth, Ocean and Atmospheric Sciences)

Date:

Place: Goa University



School Stamp

CONTENTS

CHAPTER	PARTICULARS	PAGE NO.
	Preface	i
	Acknowledgments	ii - iii
	List of tables	iv
	List of figures	v - ix
	Abbreviations used	x - xii
	Abstract	xiii - xiv
1	Introduction	1-9
2	Literature Review	10-20
3	Methodology	21-38
4	Results	39-101
5	Discussion and Conclusion	102-112
	References	115 - 125
	Appendix	I-XI

PREFACE

In the field of nanotechnology, the synthesis of nanoparticles holds immense promise for numerous applications ranging from biomedical to environmental sectors. Selenium, a trace element, plays a crucial role in various biological processes, including antioxidant defence mechanisms, stress tolerance and nutrient metabolism. In recent years, selenium nanoparticles have garnered considerable attention due to their unique physicochemical properties and potential applications in biomedicine, environmental remediation, agriculture and nanotechnology. The study deals with the isolation and screening of marine bacteria for selenium nanoparticle synthesis involving a multifaceted approach encompassing microbiology, nanotechnology, and environmental science.

The work on selenium nanoparticles synthesized by marine bacteria indicates promises of discovery, innovation, and sustainable solutions. It promises biotransformation of toxic selenite to non-toxic elemental Se. Thus, assuring the potential of strains to be used for bioremediation in contaminated marine and estuarine environments. Furthermore, it also demonstrates the formation of selenium nanoparticles concurrently with their promising environmental applications in agriculture through seed priming highlighting its potential to address key challenges facing modern agriculture, including food security and environmental sustainability. It is my sincere hope that this preface explodes curiosity and inspires readers to enlighten exploration of this fascinating field, contributing to the advancement of knowledge.

ACKNOWLEDGEMENT

Success is not measured by what you accomplish but by the opposition you have encountered, and the courage with which you have maintained the struggle against overwhelming odds. Believe you can and you're halfway there. I take this opportunity to sincerely thank everyone who directly or indirectly landed helping hands in various disciplines in completing this thesis. Every project is successful largely due to the efforts of many people who have always given their valuable advice or a helping hand. I sincerely appreciate the inspiration, support and guidance of all those people who have been instrumental in making this project a success.

I would like to express my deepest gratitude to my God for the blessings and good health throughout this journey. In moments of doubt and uncertainty, I found comfort in the belief that there is a higher power overseeing every step of this work. First and foremost, my sincere thanks to our present Dean Sr. Prof. Sanjeev C. Ghadi and formal Dean Sr. Prof. C. U. Rivonker for providing the infrastructure to carry out my work. I would also like to thank Dr. Varda Damare, Program Director, Marine Microbiology, SEOAS for providing the required materials for the completion of my project.

I would like to record my deep gratitude to my guide, Dr. Diviya Vaigankar, Assistant Professor, Marine Microbiology program, SEOAS, Goa University for valuable support and guidance throughout this Master's degree. Your expertise, patience, and encouragement have helped shape my work and refine my ideas, pushing me to strive for excellence every step of the way. Throughout this journey, you have generously shared your knowledge and insights, providing valuable feedback and constructive criticism that have undoubtedly enhanced the quality of my work. You have been a constant source of inspiration and motivation for me. I am truly grateful for the time and efforts that you have invested in me and for sharing your knowledge and expertise so generously. I am very grateful for the efforts you have put in bringing up the best in me without your support and efforts this journey would have not been possible to achieve success. Thank you so much Ma'am for being there for me through all the highs and lows of my work.

I would like to thank all the faculty members of the Marine Microbiology program. I would like to show my gratitude towards the Laboratory assistants and office staff, Ms. Vaishali Merchant and Rohan Marshelkar for helping me throughout.

I am thankful to Mr. Linus Coelho research scholar, Department of Microbiology, Goa University for providing space in their orbital shaker and for helping and supervising me whenever I approached.

I am also thankful to the non-teaching staff Ms. Tulsi, Department of Applied Zoology, Goa University for allowing me to use their weighing balance.

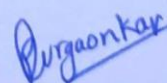
I am grateful for the SEM analysis carried out by M.G. Lanjewar (Technical Officer-I) at the University Science Instrumentation Center (USIC), Goa University.

I am grateful to Ms. Yarram Jyothi, Technical In-charge, Central Sophisticated Instrumentation facility, for helping me carry out SEM-EDX and XRD analysis at BITS Pilani K K Birla Goa Campus.

I would like to thank my few friends and batchmates from Marine Microbiology for their encouragement and support in making all this possible.

I would like to express my deepest gratitude to the two main pillars of my life my lovely mom and dad for their sincere encouragement and inspiration throughout my work and for lifting me uphill during this phase of life. I owe everything to them for all the support and help given throughout. Also, my siblings thank you so much for being there whenever I needed.

Last but not least, I would like to thank all my other family members, cousins, friends and my well-wishers for their moral support and also for motivating and encouraging me throughout my work. Lastly, I offer my heartfelt gratitude to the Almighty God whose grace and guidance have illuminated my path throughout this journey.



Prerana Pipi Murganekar

LIST OF TABLES

TABLE NO.	DESCRIPTION	PAGE NO.
	CHAPTER 2: LITERATURE REVIEW	
2.1	National and international status of research	13
	CHAPTER 3: METHODOLOGY	
3.1	Various treatments used for rice and mung seeds	38
	CHAPTER 4: RESULTS	
4.1	Physicochemical parameters of various samples used	42
4.2	List of the twenty-five selected bacterial isolates	45 - 46
4.3	Colony characteristics of isolated bacterial strains	46 - 47
4.4	Gram character of selected isolates	48
4.5	Biochemical characteristics of selenite-resistant marine bacterial isolates	60 - 61
4.6	Antibiotic susceptibility of selected bacterial isolates.	63

LIST OF FIGURES

FIGURE NO.	DESCRIPTION	PAGE NO.
CHAPTER 3: METHODOLOGY		
3.1	Sampling sites selected for collection of water and sediment samples	22
CHAPTER 4: RESULTS		
4.1	(a) to (i) Sampling sites used for isolation of selenite-reducing marine bacterial isolates & (j) codes used against the respective sites	40 - 41
4.2	Enriched flasks: (a) water and (b) sediment samples (Control and Test) after 48 h of incubation	43
4.3	ZMA plates: (a) without Na ₂ SeO ₃ , (b) with (2 mM) Na ₂ SeO ₃ showing brick red colonies	44
4.4	ZMA plates - (a) without Na ₂ SeO ₃ , (b) with (2 mM) Na ₂ SeO ₃ showing brick red colonies	44
4.5	ZMA Slants containing isolated bacterial strains	45
4.6	Gram stain images of 25 different bacterial isolates	49 - 50
4.7	Growth of selected bacterial isolates on ZMA with increasing concentrations of Na ₂ SeO ₃ (5,10 and 20 mM)	51
4.8	Growth of selected bacterial isolates on ZMA with increasing concentrations of Na ₂ SeO ₃ (30-80 mM)	52
4.9	Growth of 14 bacterial isolates on ZMA with increasing concentrations of Na ₂ SeO ₃ (100-200 mM).	53
4.10	Growth of 8 bacterial isolates on ZMA with increasing concentrations of Na ₂ SeO ₃ (220-360 mM)	54
4.11	MTC of selected potential selenite-reducing bacterial isolates	55

4.12	MIC of 5 bacterial isolates selected out of 8 inoculated in ZMB with increasing concentrations of Na ₂ SeO ₃ (2-40 mM)	56
4.13	Isolates grown in the presence of 50-120 mM Na ₂ SeO ₃	57
4.14	Isolates grown in the presence of 145-195 mM Na ₂ SeO ₃	57
4.15	Bacterial isolate PMVW ₃ grown in the presence of 220-380 mM concentrations of Na ₂ SeO ₃	58
4.16	Bacterial isolate PMBW ₃ grown in the presence of 220-320mM Na ₂ SeO ₃	58
4.17	MIC of selected potential selenite-reducing bacterial isolates	59
4.18	Congo red staining of the <i>Shewanella</i> sp. indicating EPS production	59
4.19	A few biochemical tests of selected bacterial isolates for PMVW ₃ and PMChW ₂	62
4.20	Antibiotic disks used to carry out antibiotic sensitivity testing of the bacterial isolates	64
4.21	Bacterial cultures showing zone of inhibition against respective antibiotics; (a-d) antibiotic susceptibility against isolate PMVW ₃ ; (e-h) antibiotic susceptibility against PMChW ₂ ; (i and j) negative control of PMVW ₃ and PMChW ₂ respectively and (k) positive control for both isolates	65-66
4.22	Scanning electron micrographs (SEM) of both the cells of strain PMVW ₃ and PMChW ₂ ; (a) Bacterial cells of PMVW ₃ without Na ₂ SeO ₃ exposure, (b) Bacterial cells with 2 mM Na ₂ SeO ₃ exposure, (c) Bacterial cells of PMChW ₂ without Na ₂ SeO ₃ exposure and (d) Bacterial cells with 2 mM Na ₂ SeO ₃ exposure	67
4.23	Electron dispersive X-ray (EDX) spectrum of both the cells of strain PMVW ₃ and PMChW ₂ ; (a) Bacterial cells	68

	of PMVW ₃ without Na ₂ SeO ₃ exposure, (b) Bacterial cells with 2 mM Na ₂ SeO ₃ exposure, (c) Bacterial cells of PMChW ₂ without Na ₂ SeO ₃ exposure and (d) Bacterial cells with 2 mM Na ₂ SeO ₃ exposure	
4.24	(a) Electrophoresis unit, (b) Agarose gel and (C) Genomic DNA isolation of PMVW ₃ and PMChW ₂	70
4.25	16S rRNA gene amplicon of PMVW ₃ and PMChW ₂	71
4.26	Phylogenetic tree showing relatedness of <i>Pseudoalteromonas</i> sp. strain PMVW ₃ (accession number: 24C110_519_2) with other strains of <i>Pseudoalteromonas</i> , constructed using neighbor joining method (Tamura et al., 2013)	72
4.27	Phylogenetic tree showing relatedness of <i>Shewanella</i> sp. strain PMChW ₂ (accession number: 24C110_520_3) with other strains of <i>Shewanella</i> , constructed using neighbor joining method (Tamura et al., 2013)	73
4.28	Flasks showing (left to right) strain PMVW ₃ grown in ZMB culture (a) containing 0 mM Na ₂ SeO ₃ (b) with 2 mM Na ₂ SeO ₃ ; (c) Harvested SeNPs suspension (d) characteristic absorbance maxima of biogenic SeNPs using UV-Vis spectrophotometry	74
4.29	(a) Colourless culture supernatant; Flasks showing (left to right) culture supernatant of PMVW ₃ (b) containing 0 mM Na ₂ SeO ₃ (c) with 2 mM Na ₂ SeO ₃	75
4.30	Bacterial strain PMChW ₂ grown in ZMB flasks with varying pH 5-10	76
4.31	Bacterial strain PMVW ₃ grown in ZMB flasks with varying pH 5-10	76
4.32	Effect of SeNPs at different pH	77
4.33	UV-Vis absorption spectra acquired at varying pH (a) 6, (b) 7, (c) 8 and (d) 9	77

4.34	Bacterial strain PMVW ₃ grown in ZMB flasks with varying Na ₂ SeO ₃ concentrations, 1- 6 mM with pH 7	78
4.35	Effect of SeNPs at different Na ₂ SeO ₃ concentrations	78
4.36	UV-Vis absorption spectra acquired at varying Na ₂ SeO ₃ concentration with pH 7 at (a) 1mM (b) 2mM, (c) 3mM, (d) 4mM, (e) 5mM and (f) 6mM of Na ₂ SeO ₃	79
4.37	Bacterial strain PMVW ₃ grown in ZMB flasks with pH 7, 2 mM concentration and at different temperatures 28°C, 32°C and 37°C	80
4.38	Effect of SeNPs at different temperatures	80
4.39	UV-Vis absorption spectra acquired for at varying temperatures: (a) 28 °C (b) 32 °C and (c) 37 °C with 2 mM Na ₂ SeO ₃ concentration and pH 7	81
4.40	Time course study of SeNPs biosynthesis under optimized conditions; (a) flask with strain PMVW ₃ grown in ZMB with all optimized conditions, (b) UV-Vis absorption spectra acquired after 48 h and (c) Growth behavior of strain PMVW ₃ in presence of SeNPs	82
4.41	Harvested SeNP powder	83
4.42	Absorbance maxima for biosynthesized SeNPs at 265 nm	84
4.43	SEM-EDX profile of biogenic SeNPs	85
4.44	SEM-EDX profile of strain PMChW ₂	86
4.45	X-ray diffraction profile of <i>Pseudoalteromonas</i> sp. strain PMVW ₃ exposed to 2 mM Na ₂ SeO ₃	87
4.46	The antimicrobial activity of biogenic SeNPs against (a) <i>E.coli</i> , (b) <i>Salmonella</i> sp., (c) <i>Bacillus</i> sp. and (d) <i>S.aureus</i> (with negative control)	88
4.47	The antimicrobial activity of biogenic SeNPs against (a) <i>E.coli</i> , (b) <i>Salmonella</i> sp., (c) <i>Bacillus</i> sp. and (d) <i>S.aureus</i> (with positive control)	89

4.48	Antibiofilm activity against human pathogens with increasing SeNPs concentrations; (a) control plate, (b) <i>E. coli</i> , (c) <i>S.aureus</i> , (d) <i>Bacillus</i> sp. and (e) <i>Salmonella</i> sp.	90
4.49	Antibiofilm activity of the different SeNPs concentration against human pathogens	91
4.50	Free radical scavenging activity of biogenic SeNPs (Ascorbic acid (Aa) served as a standard).	92
4.51	Bacterial cells stained with alcian blue dye; (a) Control, (b and c) showing EPS.	93
4.52	(a) Showing the formation of EPS precipitate and (b) Control	93
4.53	Eppendorf tubes containing dried EPS precipitate	94
4.54	EPS-SeNPs solution	94
4.55	Root length under various treatments after 5 and 10 days of germination	96
4.56	Shoot length under various treatments after 5 and 10 days of germination	97
4.57	Wet weight under various treatments after 10 days of germination	97
4.58	Rice seeds under various treatments after (a) 5 th and (b) 10 th day of germination	98
4.59	Root length under various treatments after 5 and 10 days of germination	99
4.60	Shoot length under various treatments after 5 and 10 days of germination	100
4.61	Wet weight under various treatments after 10 days of germination	100
4.62	Mung beans under various treatments after (a) the 5 th and (b) 10 th day of germination	101

ABBREVIATIONS

ENTITY	ABBREVIATION
%	Percentage
°C	Degree centigrade
µg	Microgram
µl	Microlitre
As	Arsenic
ABTS	2,2'-azino-bis-(3-ethylbenzothiazoline-6-sulfonic) acid
BLAST	Basic local alignment search tool
Cd	Cadmium
DPPH	1, 1-diphenyl-2-picrylhydrazly
DW	Distilled water
DNA	Deoxyribonucleic acid
EDX	Energy-dispersive X-ray
EPS	Extra polymeric substances
FTIR	Fourier Transformed Infrared Spectroscopy
g	Gram
GPx	Glutathione peroxidases
h	Hour
H ₂ O ₂	Hydrogen peroxide
H ₂ S	Hydrogen sulfide
L	Litre
MHA	Muller Hinton agar

MIC	Minimum inhibitory concentration
MTC	Minimum Tolerance concentration
min	Minutes
mL	Millilitre
mM	Milli molar
Mm	Millimeter
Na ₂ SeO ₃	Sodium selenite
NaCl	Sodium chloride
NB	Nitrate broth
NPs	Nanoparticles
NaOH	Sodium hydroxide
OH	Hydroxyl
PBS	Phosphate buffered saline
PCR	Polymerase chain reaction
pH	Potential of hydrogen
ROS	Reactive oxygen species
Rpm	Revolution per minute
RT	Room temperature
Se	Selenium
SeNPs	Selenium nanoparticles
Sp.	Specie
UV	Ultraviolet
Vis	Visible
WHO	World health organization

XRD	X-ray diffraction
ZMA	Zobell marine agar
ZMB	Zobell marine broth

ABSTRACT

Nanoparticle ranges in size from one to one hundred nanometers. Selenium (Se), a vital micronutrient, is found in various forms in the environment, including inorganic, unstable, water-soluble, selenite, and elemental water-insoluble forms. It is considered an essential trace element (< 40 µg/day) for living forms. Se nanoparticles (SeNPs) have numerous applications in electronics, agriculture, food, feed, environmental bioremediation, and medicine, with a particular focus on medicine due to their critical biological role, specificity, selectivity, bioavailability, and low toxicity. Marine microorganisms are known to reduce toxic selenite to elemental Se using various mechanisms and simultaneously produce nanoparticles. In the present study, selenium-resistant bacterial isolates were isolated from the various marine/estuarine habitats of Goa, India. Among these isolates, bacterial strain PMVW₃ was selected based on its ability to tolerate up to 380 mM of selenite in Zobell Marine Broth (ZMB). This strain was identified to be *Pseudoalteromonas* sp. (24C110_519_2) using 16S rRNA gene sequencing. Yet another strain PMChW2, exhibiting MTC of 70 mM for selenite showed Extracellular Polymeric Substance (EPS) formation among all and thus was also selected for further studies. This strain was identified as *Shewanella* sp. (24C110_520_3) using 16S rRNA gene sequencing. The strain PMVW₃ could produce stable SeNPs within 48 h under optimized growth conditions (pH 7, 2 mM sodium selenite and temperature of 28 °C). UV–visible spectrum was used to initially characterize SeNPs showing a peak at 265 nm along with the formation of brick red coloration in the growth medium. SEM analysis of harvested SeNPs revealed rod-shaped morphology and EDX analysis further confirmed SeNPs. Additionally, X-ray diffraction (XRD) analysis also revealed the presence of crystalline SeNPs. For biosynthesis using strain PMChW2 similar synthesis of SeNPs was assured however this strain could synthesize two morphotypes namely Se rods and nanospheres. Further, four antibiotics showed sensitivity against *Pseudoalteromonas* sp. and *Shewanella* sp. Moreover, biogenic

SeNPs showed the highest antibiofilm activity against *E. coli*. SeNPs also showed excellent dose-dependent anti-oxidant potential at 100 µg/mL using DPPH. The EPS composite SeNPs when tested for plant growth promotion demonstrated higher plant growth promotion compared to EPS or sodium selenite (Na₂SeO₃) treated seeds alone. Thus, the study highlighted the potential of marine bacteria in reducing toxic selenite to elemental form suggesting its bioremediation potential with concurrent SeNPs biosynthesis ability.

KEYWORDS

Marine bacterium, Selenium nanoparticles, *Pseudoalteromonas sp.*, *Shewanella sp.*, Antibiofilm, Extracellular polymeric substance, Bioremediation.

CHAPTER 1

INTRODUCTION

1.1 BACKGROUND

Nanotechnology has developed as a rising multidisciplinary area of global interest, with a key impact on agriculture, the environment, food, biology and pharmaceuticals (Shi et al., 2021). The prefix 'nano' is derived from the Greek word dwarf, which is one billionth of a meter. Richard Feynman discussed the core concept of nanotechnology in his 1959 lecture "There's Plenty of Room at the Bottom" at the American Institute of Technology. Nanotechnologies generate nanomaterials with a very small scale of 1 to 100 nm, which may present as any of the following nano forms: nanoparticles, nanofibers, nanotubes, nanowhiskers, fullerenes, and nanosheets (Cushen et al., 2012).

Nanoparticles (NPs) are generally classified into organic and inorganic nanoparticles. Organic nanoparticles include nanoparticles formed of proteins, polysaccharides, lipids, polymers, or any other organic substance (Pan and Zhong, 2016). Dendrimers, liposomes, micelles, and protein complexes such as ferritin are the most well-known examples of this class. These nanoparticles are normally non-toxic and biodegradable (Joudeh, N., and Linke, D. 2022). They are susceptible to thermal and electromagnetic radiation, such as heat and light (Ealia and Saravanakumar, 2017). Furthermore, they are frequently produced by non-covalent intermolecular interactions, which makes them more labile and provides a route for removal from the body (Ng and Zheng, 2015). Composition, surface shape, stability, carrying capacity, and other factors all influence the possible field of application of organic nanoparticles. They are now mostly used in biomedicine for targeted drug delivery (Ealia and Saravanakumar, 2017) and cancer therapy (Gujrati et al., 2014).

Metal and ceramic are common examples of inorganic nanoparticles that are composed of inorganic components. Metal nanoparticles are composed entirely of metal precursors and can be monometallic, bimetallic, or polymetallic (Toshima and Yonezawa 1998; Nascimento et al., 2018). Bimetallic nanoparticles can be produced from alloys or in multiple layers (core-shell) (Toshima and Yonezawa 1998). These NPs have distinct optical and electrical properties due to their localized surface plasmon resonance features (Khan et al., 2019). Furthermore, some metal nanoparticles have distinct thermal, magnetic, and biological properties (Ealia and Saravanakumar, 2017). As a result, they are becoming increasingly essential materials for the development of nanodevices that can be utilized in a wide range of physical, chemical, biological, biomedical, and pharmaceutical applications (Mody et al., 2010; Fedlheim and Foss, 2001).

1.1.1 SYNTHESIS OF NANOPARTICLES

Nanoparticles are broadly synthesized using two approaches viz. bottom-up and top-down. The bulk material is broken down externally using microscopic devices in the top-down technique to achieve the required form and size. In contrast, in the bottom-up technique, atoms or molecules are combined to create nano-dimensions using various chemical and biogenic procedures.

1.1.2 PHYSICAL and CHEMICAL PROCESSES TO SYNTHESIZE NANOPARTICLES

Despite being invisible to the human eye, nanoparticles can behave differently from their larger-than-life counterparts in terms of both physical and chemical processes.

Physical methods mainly encompass laser ablation, inert gas condensation, spray pyrolysis, electrospray, electron beam nanolithography and combustion flames (Kammler et al., 2001; Lamas et al., 2003; Amendola and Meneghetti, 2009; Adhikari et al., 2010; Kang et al., 2011; Pimpin and Srituravanich, 2012). Inert gas condensation is the oldest and most widely used process, in which metals (gold/palladium) are evaporated in high vacuum chambers filled with inert gas. Following this, the nanoparticles are formulated when the evaporated metals condense into small nanocrystals via coalescence and Brownian motion.

Laser ablation (top-down technique) creates nanoparticles by immersing bulk materials in a liquid solution and focusing a laser on it. As a result of the ablation, plasma plumes are formed, which condense to produce nanoparticles. The physical mechanism results in an excellent size distribution of nanoparticles. However, several of these methods require the use of hazardous precursors, and the reactions are typically multistep, which may result in the formation of particles with unfavorable surface chemistry. It also demands the use of high-temperature and pressure devices, as well as the formation of poisonous by-products, limiting its application (Vaigankar, 2020).

The chemical methods mainly involve reduction, sol-gel, solvothermal, hydrothermal, reverse-micelles and co-precipitation (Adschiri et al., 2001; Nahar and Arachchige, 2013). Frequently, a reducing agent (Sodium borohydride, sodium citrate,

hydrazine, Polyethylene glycol, and formaldehyde), metal/metalloid salt precursor, and surfactant or stabilizers (SDS, PVP) are used to prevent aggregation in the chemical reduction technique. Furthermore, heat or catalyst can be used to speed up the reaction and synthesis process, and solvents are employed to stabilize the metal salts (Hu et al., 2015).

Reduction permits the production of huge numbers of nanoparticles with precise control over size and form. However, the method is expensive and involves the use of hazardous precursors, reducing agents, and capping agents. It also requires the use of high-temperature equipment and also generates poisonous byproducts. Because of its low biocompatibility and high toxicity, the use of hazardous stabilizing agents diminishes its potential to be used in the biomedical field (Vaigankar, 2020).

1.1.3 BIOLOGICAL PROCESSES TO SYNTHESIZE NANOPARTICLES

Even though chemical and physical methods are frequently used, the drawbacks associated with them limit their applications, thus suggesting a need to design desirable alternatives that are environmentally friendly and safe. Interestingly, the structural components of the living being are in nano-dimensions. Additionally, Deoxyribonucleic acid (DNA), protein (ferritin, serrapeptase, phytochelatins, and glutathiones), and viral particles (Tobacco mosaic virus) have been studied for the generation of nanoparticles (Douglas et al., 1995; Brelle et al., 1999; Shenton et al., 1999; Ravindra, 2009; Anil Kumar et al., 2007).

Microbes can produce a variety of nanomaterials, including nanoparticles. Inorganic minerals are used in the microbial process and converted into complex or

simpler forms either intracellularly (Baesman et al., 2007; Muthukannan and Karuppiah, 2011) or extracellularly (Oremland et al., 2004; Kathiresan et al., 2010). To accomplish intracellular nanoparticle formation, cells are typically cultured in media supplemented with metal/metalloid salts. Intracellular processes involve the synthesis of NPs within cells, these nanoparticles are typically isolated using either physical or chemical methods, such as cell wall disruption with Triton X-100, SDS, or lysozymes, followed by centrifugation to remove cell debris and subsequent purification of nanoparticles (Kalimuthu et al., 2008; Nangia et al., 2009).

Microbial synthesis of nanoparticles is advantageous due to its cellular-level metabolic process and its role in the biogeochemical cycling of metals, metalloids, and minerals. It is a flexible, organized, and effective process occurring under controlled conditions. Microbial biosynthesis is crucial for applications in biology and medicine, as it does not produce or use external toxic substances.

The marine environment is a unique habitat that is characterized by harsh conditions and retains a vast microbial diversity. It has been observed that these bacteria have unique methods for tolerating high salt concentrations, severe pH, pressure, and high quantities of certain hazardous metals and metalloids (Vaigankar, 2020). However, these marine microorganisms have not been thoroughly explored for nanoparticle production. Therefore, it would be interesting and imperative to study and explore the capability of these metalloid-resistant marine bacteria for synthesizing nanoparticles.

1.1.4 SELENIUM NANOPARTICLES (SeNPs)

Selenium (Se) is a micronutrient necessary for life and it belongs to group 16 (XVI A) of the periodic table, with atomic number 34. In the environment, it exists as elemental water-insoluble selenium (Se^0), water-soluble selenite (SeO_3^{2-}), selenate (SeO_4^{2-}) and inorganic, unstable selenide (Se^{2-}). Selenocysteine and selenomethionine are organic forms. Jacob Berzelius discovered selenium (Se) in 1818. At low concentrations, this element can be regarded as a necessary trace micronutrient for living things; but, at higher doses, it becomes toxic and harmful. The range of dietary deficiency ($< 40 \mu\text{g}/\text{day}$) and excess ($> 400 \mu\text{g}/\text{day}$) is fairly narrow (Fordyce, 2013). Moreover, its excess (less than $400 \mu\text{g}/\text{day}$) results in selenosis, and its deficiency produces "Keshan disease." (Chen, 2012; Morris and Crane, 2013). However, $40 \mu\text{g}/\text{mL}$ of Se is regarded as safe in drinking water as per WHO guidelines (WHO, 2011). Selenium has been recognized as an important cofactor for enzymes including glutathione peroxidases and thioredoxin reductases in animals thereby reducing oxidative stress (Wang et al., 2018).

Selenium in nano-dimensions has received a great deal of attention due to its numerous applications in electronics, agriculture, food, feed, environmental bioremediation, and medicine, with a particular emphasis on medicine due to its critical biological role even at low concentrations (Shirsat et al., 2015). Even though SeNPs have several applications, research on marine bacteria synthesizing SeNPs is limited. SeNPs are one of the most attractive prospects for biomedical applications due to their specificity, selectivity, bioavailability, and low toxicity. They play a functional role in numerous oxidoreductive reactions because they are bioactive and biologically accessible. They also have a variety of regulatory effects that promote the body's (both

plants and animals) healthy functioning and have numerous health benefits (El-Ramady et al., 2016; Schrauzer 2000; Skalickova et al., 2017).

1.2 AIM and OBJECTIVES

1.2.1 Aim

Biosynthesize and characterize selenium nanoparticles from marine bacteria to be used for various applications in biology and the environment.

1.2.2 OBJECTIVES

- Isolation of selenium nanoparticles producing bacteria from the marine environment.
- Identification of selected potential strains synthesizing selenium nanoparticles.
- Characterization of biosynthesized selenium nanoparticles.
- Applications of biosynthesized Selenium nanoparticles.

1.3 HYPOTHESES

Marine bacteria possess the inherent capability to reduce metals/metalloids into their elemental form which can be exploited to simultaneously synthesize nanoparticles to be explored for potent biological and environmental applications.

1.4 SCOPE

This investigation involves the systematic isolation and characterization of marine bacterial strains capable of selenite reduction, along with the screening of selenium nanoparticle synthesis and its optimization. Characterization techniques such as scanning electron microscopy and X-ray diffraction will be employed to assess the physicochemical properties of biogenic selenium nanoparticles. Furthermore, the

biotechnological applications of selenium nanoparticles, including biomedical and environmental will be explored. The research will also consider the environmental implications of nanoparticle synthesis and assess the sustainability of the proposed approach. Overall, this investigation seeks to advance the scientific understanding of microbial nanobiotechnology, contribute to the development of sustainable nanoparticle synthesis methods, and explore innovative applications in healthcare, environmental remediation, and nanotechnology.

CHAPTER 2

LITERATURE REVIEW

2.1 LITERATURE REVIEW

Amongst actinobacteria, cyanobacteria, yeast, and fungi, bacteria are the best choice for the synthesis of nanoparticles (Srivastava and Mukhopadhyay, 2015), due to their fast growth rate, easy handling, low cost, and high productivity (Srivastava and Mukhopadhyay, 2013). Marine microbes such as *Citrobacter freundii strain KP6*, *Streptomyces sp.*, *Lysinibacillus sp.*, *Bacillus amyloliquefaciens*, *Bacillus paramycooides SP3*, *Shewanella sp.*, *Bacillus subtilis BSN313*, *Pseudomonas aeruginosa*, *Bacillus subtilis AS12*, *Halomonas venusta* and *Streptomyces sp.* are known to produce selenium nanoparticles and are reported to have specific mechanisms to tolerate high salt concentrations, extreme pH and high levels of different toxic metals and metalloids (Samant et al., 2018; Bharathi et al., 2020; Keskin et al., 2020; Ashengroph and Hosseini, 2021; Borah et al., 2021; Ho et al., 2021; Ullah et al., 2021; Shakeri et al., 2022; Saad et al., 2022; Vaigankar et al., 2022; Sumithra et al., 2023) (Table 2.1).

The shape and size of nanoparticles can be influenced by controlling pH, temperature, and substrate concentration in the growth medium along with the concentration of metal/metalloid substrates (Gericke and Pinches, 2006). Furthermore, to create homogeneous-sized and shaped nanoparticles, the above conditions must be carefully controlled and monitored. Apart from cell-free supernatant and whole-cell biomass, bacterial metabolites, which mostly contain polysaccharides, proteins, enzymes, and pigments, have also been employed as reducing agents for biosynthesis. For instance, *Bacillus subtilis* MSBN17 has been reported to create polysaccharide bioflocculant, which is responsible for the generation of silver nanoparticles in reverse micelles (Sathiyarayanan et al., 2013). Metal microbial interactions can result in nanoparticle formation, which is governed by several parameters, including the nature

and solubility of metal/metalloid ions, as well as the sort of interactions involved (Haferburg and Kothe, 2007). Adsorption, or the attachment of these metals/metalloids to bacterial surfaces, initiates metal/metalloid interactions. Following adsorption, these metals/metalloids are either carried into cells by various transporters or reduced/oxidized by various microbial components, primarily enzymes, proteins, thiols, and other microbial components. Diverse microorganisms, such as bacteria and fungi, show detoxifying ability when exposed to toxic selenite by converting it to insoluble and less toxic elemental selenium (Ike et al., 2000; Li et al., 2014). In addition, selenide or organic selenium also develops along with elemental selenium (Tan et al., 2018). Bacterial reductions of selenate or selenite occur both anaerobically and aerobically, by non-enzymatic or enzymatic mechanisms. In a study by Ullah et al., (2021) SeNPs were successfully produced using the *Bacillus subtilis* BSN313 through a biosynthetic approach. In yet another study, by Morahem and coworkers, a marine strain of *Bacillus amyloliquefaciens* was isolated and characterized for its ability to convert selenite to SeNPs under aerobic conditions (Ashengroph and Hosseini. 2021).

Additionally, a study using *Halomonas eurihalina* SeNPs reported the synthesis of SeNPs with a spherical shape having an average particle size of 260 nm (Shakeri et al., 2022). Moreover, SeNPs by *Halomonas venusta* using marine bacteria were reported with a diameter in the range of 20-80 nm. (Vaigankar et al., 2022).

Table 2.1: National and international status of research

Marine microbes	Strains	Size (nm)	Intra(I)/ extracellular(E)	References
Bacteria				
	<i>Citrobacter freundii</i> strain KP6	45 -70	E	Samant et al., 2018
	<i>Bacillus</i> sp.	20-50	E	Bharathi et al., 2020
	<i>Lysinibacillus</i> sp.	130	E	Keskin et al., 2020
	<i>Bacillus amyloliquefaciens</i>	45.4–68.3	E	Ashengroph, M., and Hosseini, S. R. 2021
	<i>Bacillus paramycoides</i> SP3	120-170	E	Borah et al., 2021
	<i>Shewanella</i> sp.	30–6	E	Ho et al., 2021
	<i>Bacillus subtilis</i> BSN313	530	E	Ullah et al., 2021
	<i>Pseudomonas aeruginosa</i>	260	I	Shakeri et al., 2022
	<i>Bacillus subtilis</i> AS12	77	E	Saad et al., 2022
	<i>Halomonas venusta</i>	20–80	I	Vaigankar et al., 2022
	<i>Streptomyces</i> sp.	50–70	E	Sumithra et al., 2023

2.2 MECHANISMS INVOLVED IN THE BIOSYNTHESIS OF SELENIUM NANOPARTICLES

2.2.1 Transport of selenate [Se (VI)]

The first phase in selenium metabolism is transport, which includes reduction, methylation, and assimilation. The sulfate ABC transporter complex expressed by the *cysAWTP* operon transports Se (VI) in *Escherichia coli* (*E. coli*) was studied by Turner et al., (1998). *Comamonas testosteroni* strain S44, an obligate aerobic bacterium, appeared to assimilate Se (VI) via the same sulfate transport pathway as *E. coli* (Tan et al., 2018) because of the molecular closeness of Se (VI) to sulfate

2.2.2 Selenate reduction to selenite

Respiratory Se (VI) reductases have been characterized in Gram-negative *Thauera selenatis* (*T. selenatis*) and Gram-positive *Bacillus selenatarsenatis* (*B. selenitireducens*) strain SF-1 under anaerobic conditions by Kuroda et al., in 2011 and Krafft et al., in 2000. Other bacteria, including *Rhodobacter sphaeroides* (*R. sphaeroides*) and *Escherichia coli*, have shown in vitro Se (VI) reduction activity, using potassium selenate and potassium tellurite as electron acceptors (Sabaty et al., 2001). Se (VI) reduction via the sulfate dissimilatory pathway as a detoxifying mechanism could be a widespread mechanism of Se (VI) reduction in aerobic species. The respiratory Se (VI) reductases *SerABC* and nitrite reductase in *T. selenatis* can mediate Se (VI) and Se (IV) reduction to SeNPs independently or synergistically (Sabaty et al., 2001). Additionally, cytoplasmic selenium deposits were formed during respiratory reduction, suggesting two mechanisms. It's unknown if bacteria directly reduce Se (VI) to Se (0) beyond Se (IV).

2.2.3 Transport of selenite [Se (IV)]

In contrast to Se (VI), no particular Se (IV) uptake channel has been identified. Se (IV) may be transported by the sulfate permease in *E. coli* strain K-12, but the *K_m* value indicating substrate affinity to Se (IV) was around 50-fold and 6-fold higher than that to sulfate and Se (VI), implying that the sulfate permease affinity to Se (IV) was lower than that to sulfate and Se (VI) (Lindblow-Kull et al., 1985). Furthermore, repressing sulfate permease expression did not entirely block Se (IV) absorption, indicating the presence of other yet undiscovered transporters (Turner et al., 1998).

2.2.4 Selenite reduction to elemental selenium and selenide

Recent studies have emphasized Se (IV) reduction, with various bacteria involved in dissimilatory reduction to generate SeNPs and selenide intracellularly or extracellularly. The reduction typically occurs in the periplasm and cytoplasm, while extracellular reduction occurs when reductive substances are generated and excreted by bacteria (Dwivedi et al., 2013). Se (IV) can be anaerobically reduced to selenium nanoparticles by respiratory Se (IV) reductase *SrrABC* (sulfite reductase reactivation ABC transporter), *FccA* (fumarate reductase) and *Nir* (nitrite reductase) in the periplasm (Wells et al., 2019). Se (IV) can be aerobically reduced to SeNPs by multiple reductases in the cytoplasm, and/or by thiols such as GSH (glutathione reductase) and bile salt hydrolase (Wang et al., 2019; Piacenza et al., 2019). and aerobically reduced to SeNPs in the periplasm by fumarate reductase and selenite reductase (*SerT*). In the presence of sulfate and Se (IV), a mixture of Se₈-nSn nanoparticles could be produced extracellularly through yet unknown pathways (Wang et al., 2022).

2.2.5 Export

SeNPs have been found in the periplasm, cytoplasm, and exterior of bacterial cells. Most SeNPs generated by microorganisms are spherical, with diameters ranging from 11 to 700 nm (Wadhvani et al., 2016). It is unclear how SeNPs efflux occurred if they were generated intracellularly. Direct secretion, vesicular secretion, and cell lysis are all possible mechanisms.

2.3 CHARACTERIZATION OF SELENIUM NANOPARTICLES

The characterization of metalloids NPs is needed to correlate their physicochemical properties to their biological effects and toxicity. The initial physicochemical characterization of these NPs is carried out by using a myriad of routine lab techniques to analyze their shape, size and size distribution, porosity, surface chemistry, crystallinity, and dispersion pattern (Kapur et al., 2017). The most widely used techniques include UV-visible (UV-Vis) spectroscopy, luminescence spectroscopy (LS), scanning electron microscopy–energy dispersive X-ray spectroscopy (SEM-EDX), transmission electron microscopy (TEM), Fourier transform infrared spectroscopy (FTIR), X-ray diffraction (XRD). XRD confirms the presence of NPs and determines their lattice structure, crystallinity and crystallite size. Electron microscopy techniques, such as TEM and SEM, enable the study of NP shape and size to deduce their size distribution along with elemental composition (EDX) (Estevam et al., 2017). According to Kapur et al., magnified field emission scanning electron microscopy (FESEM) images provide information about the nature and composition of the NPs (Kapur et al., 2017). The FTIR is an efficient technique that provides reproducible analyses used to reveal the presence of functional groups at the NP surface. These

groups may be involved in the reduction of the metal ions and/or the NP capping that ensures colloidal stability (Wadhvani et al., 2017; Rahman et al., 2019). In addition to determining the surface charge (z-potential) of the NPs, dynamic light scattering (DLS) provides the NP hydrodynamic diameter and good insight into their stability/aggregation by measuring their Brownian motion (Kapur et al., 2017). Atomic force microscopy (AFM) provides quantitative information about the length, width, height, morphology, and surface texture of NPs through a tridimensional visualization (Dhanjal and Cameotra 2010).

2.4 APPLICATION OF SELENIUM NANOPARTICLES

SeNPs are one of the most attractive prospects for biomedical applications due to their specificity, selectivity, bioavailability, and low toxicity. Selenium nanoparticles play a function in numerous oxidoreductive reactions because they are bioactive and biologically accessible.

2.4.1 Selenium nanoparticles as antioxidant agents

Antioxidants prevent and scavenge free radicals in plants and animals. There are numerous studies on the antioxidant potential of Selenium nanoparticles. The higher concentration of reaction intermediates such as superoxide and hydrogen peroxide are responsible for cellular damage (Devasagayam et al., 2004; Gutteridge, 1994). Selenium nanoparticle plays a role in the reduction of free radicals to protect cells from damage by regulating reactive oxygen species (ROS) and glutathione peroxidases (GPx). For instance, SeNPs fabricated from *Emblica officinalis* fruit extract, have shown antioxidant activity in DPPH and ABTS assays. These nanoparticles can also scavenge DPPH and reduce ferric acid, demonstrating their potential as antioxidants

(Kokila et al., 2017). In yet another study antioxidant activity of SeNPs by *Streptomyces* sp. against DPPH free radicals was reported to increase with increasing concentrations of SeNPs (Sumithra et al., 2023). Similarly, SeNPs reported good antioxidant activity in terms of DPPH and ABST scavenging action at a concentration of 150 µg/mL, with no significant differences between the 24 and 48-hour incubation periods (Ullah et al., 2021).

2.4.2 Antimicrobial effect of selenium nanoparticles

Microbial infections cause diseases in humans and animals, leading to antibiotic resistance. Multidrug-resistant bacteria are highly infectious, making antibiotics ineffective. Selenium nanoparticles have been used as a therapeutic agent as it is effective in the growth inhibition of pathogenic microbes. Some studies have revealed that the antimicrobial activity of these nanoparticles is due to the generation of reactive oxygen species, but more studies are needed to clarify their antimicrobial mechanisms (Huang et al., 2016). In one of the studies by Sumithra and coworkers, it has been reported that SeNPs synthesized by *Streptomyces* sp. exhibited broad-spectrum antibacterial activity, with a maximum zone of inhibition of 31.3 ± 0.4 mm against *Pseudomonas aeruginosa*. (Sumithra et al., 2023). Additionally, SeNPs synthesized by *Bacillus amyloliquefaciens* exhibited significant antibacterial activity against *Staphylococcus aureus* compared to chloramphenicol, a broad-spectrum antibiotic (Ashengroph and Hosseini. 2021).

2.4.3 Antibiofilm effect of selenium nanoparticles

Biofilms, encompassing complex microbial communities in a self-produced extracellular matrix, pose a formidable challenge in healthcare settings, as they are notoriously resistant to conventional antimicrobial treatments. SeNPs, with their unique

physicochemical properties and biocompatibility, offer a novel approach to disrupt biofilm formation and eradicate established biofilms (Gomez-Gomez et al., 2019). The sensitivity of biofilm-associated microorganisms to antimicrobial agents is considerably decreased. This is due to multiple factors such as the inability of antibiotics to cross the EPS layer; overproduction of efflux pumps; enzymatic modification of the antimicrobial compound; alteration of the membrane lipids preventing entry of the drug into the cell; and the presence of persisters or dormant cells that slow down or shut down metabolism and no longer offer target site/molecules for the action of the antibiotics (Singh 2017; Yu et al., 2020). These attributes render the multidrug-resistant (MDR) status of the biofilms, and the treatment of chronic infections with antibiotics ineffective (Hasani et al., 2021). SeNPs by *Streptomyces* sp. showed inhibitory effects on biofilm formation by *Pseudomonas aeruginosa* at concentrations higher than 25 µg/ml by Sumithra et al., in 2023. Biogenic SeNPs by *Halomonas venusta* exhibited excellent dose-dependent antioxidant potential at 50 µg/mL as studied by Vaigankar et al., (2022).

2.4.5 Agricultural

SeNP could be an excellent fertilizer ingredient, as it is not easily leached from the soil and dissolves in water or aqueous solutions (Sergey et al., 2020). The addition of SeNPs to soil increases fruit, rice, and tea leaf harvests, selenium content, and quality of blueberries (El-Basiouny et al., 2024). This improved uptake of selenium for crop fertilization may have positive effects on the economy and environment. Soil selenium content significantly impacts dietary intake and plasma selenium levels. Fertilizers containing selenium can normalize selenium content. Se can reduce cell membrane damage, enhance photosynthetic activity, and upregulate antioxidant defense systems, supporting overall defense against ROS's tissue-damaging effects (Hasanuzzaman et

al., 2020). The use of SeNPs as a supplement to regular Se fertilizers to boost crops has become a feasible alternative to traditional Se fertilizers as innovative, cutting-edge, and developing technologies, such as nanotechnology, advance. Vaigankar and coworkers conducted a study on rice seeds (var. *Jyoti*) via seed priming reporting enhanced plant growth potential of SeNPs primed seeds they also demonstrated the antagonistic potential of SeNPs when treated with arsenic stress (Vaigankar et al., 2022).

CHAPTER 3

METHODOLOGY

3.1 SAMPLING OF SELENITE-RESISTANT MARINE BACTERIA

Samples of surface water and sediment were taken in sterile polycarbonate bottles and zip-lock bags, respectively, from different marine and estuarine ecosystems in Goa, India (Fig. 3.1). Various physiological measures were recorded, including temperature, pH, latitude, and longitude (Sumithra et al., 2023).

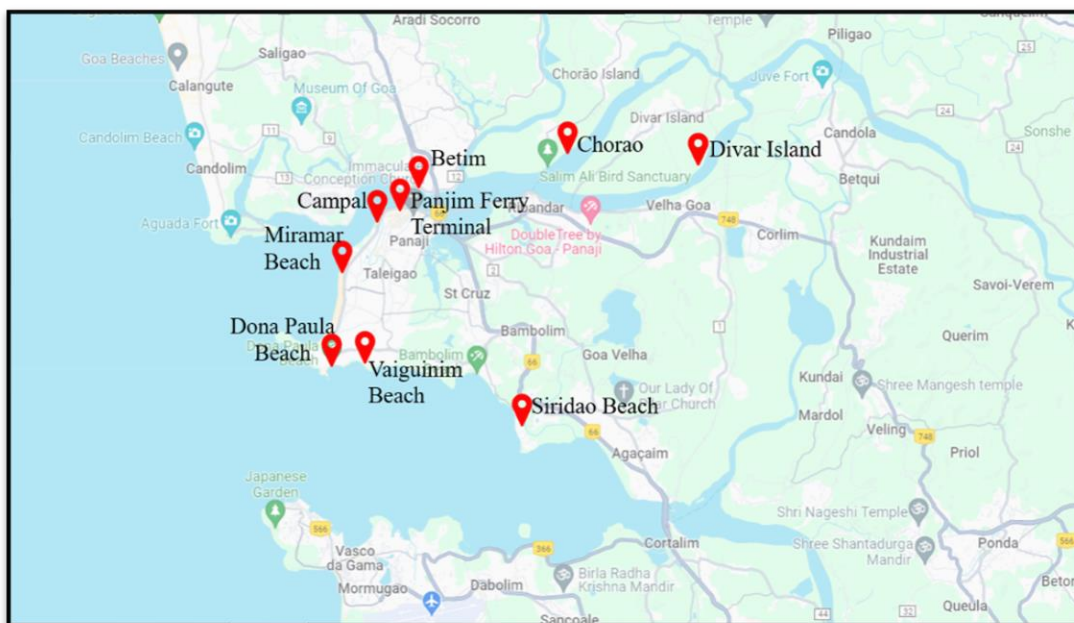


Fig. 3.1: Sampling sites selected for collection of water and sediment samples.

3.2 ENRICHMENT, ISOLATION and SCREENING OF SELENITE-RESISTANT MARINE BACTERIA

Enrichment of the samples was carried out by adding 1mL of water sample and/or 1 g of sediment sample to 50 mL Zobell Marine Broth (ZMB) supplemented with 0.5 mM sodium selenite (Na_2SeO_3) these were then incubated at 28 ± 2 °C on a shaker at 100 rpm for 48 h. Isolation of selenite-reducing bacteria was carried out by dilution plating of the enriched sample on Zobell marine agar (ZMA) plates amended

with 2 mM Na₂SeO₃ and plates were incubated at 28 ± 2 °C for 24 - 48 h. The selected bacterial colonies were sub-cultured on ZMA plates containing 2 mM Na₂SeO₃ and incubated at 28 ± 2 °C for 24 - 48 h (Borah et al., 2021).

3.3 GROWTH and MAINTENANCE CONDITIONS

Selected bacterial isolates were sub-cultured using a sterile wire loop on ZMA slants for short-term storage. The slants were incubated at 28 ± 2 °C for 24 - 48 h and stored in the refrigerator at 4 °C. The purity of the cultures was checked by performing Gram staining and microscopic observations.

3.3.1 Colony characteristics of the selected colonies

- a) **Size**- Measured by scale in millimeters.
- b) **Shape**- Varies from round to irregular.
- c) **Colour**- Pigmentation of colonies (white, cream, yellow, brown, etc).
- d) **Elevation**- How high is the colony above the agar.
- e) **Margin**- The colony was observed under the microscope for fine observation of the margin (raised/convex/flat/umbonate/crateriform).
- f) **Opacity**- The colony was observed and tested for opacity viz. opaque, translucent, transparent.
- g) **Consistency**- The colony was picked and observed for consistency (consistent/mucoid/butyrous).

3.3.2 Gram staining

The selected bacterial isolates were grown on ZMA plates and were incubated at 28 °C for 24 h. A thin bacterial smear was prepared on a clean grease-free glass slide. It was air-dried and heat-fixed. The slide was flooded with crystal violet kept for 2

minutes and later rinsed with distilled water. This was followed by treatment with Gram's iodine for 1 minute. Alcohol was added continuously to the slide for 30 to 45 seconds. The slide was counter-stained with safranin for 2 minutes. It was then rinsed under running distilled water followed by air drying and was visualized under an oil immersion lens.

3.4 DETERMINATION OF MTC (MAXIMUM TOLERANCE CONCENTRATION) and MINIMUM INHIBITORY CONCENTRATION (MIC) OF SELENITE

Bacterial isolates were selected and spot-inoculated on ZMA plates with increasing concentrations of Na_2SeO_3 (0-360 mM). These plates were incubated at 28 °C for 24 h and were checked for the appearance of colonies. The maximum concentration of selenite at which visible colonies were obtained was designated as MTC. For MIC bacterial isolates were selected and inoculated in ZMB with increasing concentrations of Na_2SeO_3 (0-360 mM). These were incubated at 28 °C for 24 h and were observed for growth. The minimum concentration of selenite at which growth did not appear was designated as MIC (Samant et al., 2016).

3.5 PHENOTYPIC ANALYSIS OF EXTRACELLULAR POLYMERIC SUBSTANCE (EPS)

Extracellular polymeric substance (EPS) production was assessed by cultivating the strains on Congo Red Agar (CRA) using a method modified by (Freeman et al, 1989). The medium was prepared by adding 0.08 % of the Congo red dye in ZMA.

The selected bacterial isolates were spot inoculated on Congo Red Agar plates, incubated at 28 °C for 24 h and checked for colonies that appeared black and opaque (Saad et al., 2017).

3.6 BIOCHEMICAL CHARACTERIZATION OF THE BACTERIAL ISOLATES

The selected isolates viz. strains PMVW₃ and PMChW₂ were biochemically and morphologically characterized and identified using *Bergey's Manual of Determinative Bacteriology*.

a. Catalase

The bacterial isolate was tested for the presence of catalase activity by adding a drop of hydrogen peroxide (H₂O₂) solution on a glass slide containing bacterial strains PMVW₃ and PMChW₂ and was observed for effervescence.

b. Hugh Leifson's test

The bacterial cultures were stabbed on Hugh Leifson's medium with, one set overlaid with sterilized paraffin oil. The next day both, the aerobic as well as anaerobic tubes were checked for any change in the color of the medium.

c. Oxidase

Selected isolates were grown for 24 h in nutrient broth and the oxidase discs were immersed in the same and a change of color was observed within 10 seconds.

d. Motility

The motility of the cultures was checked by stabbing the culture on a semi-solid agar medium. The growth of the culture was observed after an incubation of 24 h.

e. Fermentation of sugars

The cultures were inoculated in a medium containing 0.5% of various sugars like glucose, maltose, lactose, and sucrose followed by incubation for 24 h. The medium was observed for a change of color from orange to yellow and the production of bubbles in Durham's tubes. 10% stock solutions of the sugars were prepared and sterilized for 10 minutes at 15 psi.

f. IMViC

Indole

The selected cultures were inoculated in tryptophan broth and incubated for 24 h. After incubation 4-8 drops of Kovac's reagent were added and observed for the development of a ring with a cherry red color.

Methyl red and Voges Proskauer (MR-VP)

The cultures were inoculated in MR-VP broth and incubated for 24 h. The next day the cultural broth was divided into two test tubes. In one methyl red was added and the other Barrit's reagents A and B were added and incubated for 1 h and checked for the presence of red coloration.

Citrate

The cultures were streaked on Simmon's citrate slant and incubated for 24 h. It was then checked for color change from green to deep blue.

g. Nitrate test

The cultures were inoculated in nitrate broth and incubated at room temperature (28 ± 2 °C), the next day equal amount of alpha-naphthyl amine and sulphanilic acid was added and checked for red coloration.

h. Phenylalanine decarboxylase test

The cultures were grown on media containing phenyl pyruvic acid (PPA) on slants. The next day 2% ferric chloride was added and checked for green coloration.

i. Triple Sugar Iron Agar test (TSIA)

The cultures were inoculated in TSIA by stabbing the butt and then streaking on the slant and incubating for 24 h at room temperature (28 ± 2 °C). It was then checked for the color change where yellow indicates acid production and red indicates alkali production in media. The tubes were also checked for H₂S and other gas production.

j. Extracellular polymeric substance (EPS)

Extracellular polymeric substance (EPS) production was assessed by spot-inoculating the strains on ZMA containing 0.08 % of the Congo red dye followed by incubation at 37 °C for 24 h. The plates were checked for the appearance of blackening around the colonies (Saad et al., 2017).

3.7 ANTIBIOTIC SUSCEPTIBILITY OF SELECTED BACTERIA

The sensitivity of selected selenite-resistant bacterial isolates PMVW₃ and PMChW₂ to various antibiotics was determined on Muller Hinton agar (MHA) by the Kirby-Bauer disc diffusion test (Bauer et al., 1966). Bacterial cultures grown overnight

were spread and placed on MHA plates to obtain uniform bacterial lawns subsequently, the antibiotic discs (Himedia, India) were retained on them. The Petri plates were then incubated for 24 h at 28 °C and the zone of clearance due to antibiotics was recorded and compared to the Kirby-Bauer chart (Boyle et al., 1973).

3.8 SEM-EDX ANALYSIS OF SELECTED BACTERIAL STRAINS

The selected bacterial isolates PMVW₃ and PMChW₂ were grown in ZMB supplemented with (2 mM) and 0 mM Na₂SeO₃ (control) and kept for 48 h under constant shaking at 100 rpm and 28 °C. A thin smear of bacterial cells was prepared on a slide and this was then fixed with 2.5 % glutaraldehyde. The cells were washed with PBS (phosphate buffered saline) followed by dehydration using different concentrations of acetone (10 %, 20 %, 30 %, 40 %, 50 %, 60 %, 70 %, 80 %, 90 % and 100 %) for 10 min each. The samples were then gold coated using Blue Quorum Model SC720 and viewed using ZEISS EVO 18 scanning electron microscope and electron dispersive spectroscopic analysis (Quanta FEG 250).

3.9 MOLECULAR IDENTIFICATION OF THE SELECTED BACTERIAL ISOLATES

3.9.1 Extraction of genomic DNA

Genomic DNA extraction of the selenite-reducing bacterial strains was carried out using Dneasy® Blood and Tissue Kit (Qiagen, Hilden, Germany). The cultures were grown in nutrient broth (NB) and incubated at 28 °C for 24 h. Upon centrifuging, cells were resuspended in PBS followed by the addition of proteinase K, Buffer AL, and

ethanol. The mixture was then pipetted into a DNeasy Mini spin column and centrifuged at 4500 rpm for 1 minute. The column was then placed in a new 2 ml collection tube, to which 500 μ l of Buffer AW1 was added and centrifuged for 3 minutes at 4500 rpm (BR -70 BL). The spin column was then transferred to a new 2 ml microcentrifuge tube. The DNA was eluted by adding 200 μ l of Buffer AE to the center of the spin column membrane and incubated for 1 minutes at room temperature (28 ± 2 °C). The DNA sample was electrophoresed using 0.8% agarose gel and visualized by transilluminator (BC- UV-365).

3.9.2 PCR amplification phylogenetic analysis

The bacterial 16S rRNA gene was used as a target and the amplification was carried out using the universal primers 16S27F (5'-CCA GAG TTT GAT CMT GGC TCA G-3') and 16S1492R (5'-TAC GGY TAC CTT GTT ACG ACT T-3') (Weisburg et al. 1991). The amplified PCR product was further purified by salt precipitation. Agarose gel electrophoresis was carried out to determine the quality of PCR amplicons as well as post-purification of the PCR products. Purified amplicons were then subjected to cycle sequencing using BDT v3.1 chemistry and subsequently sequenced on an ABI 3500XL Genetic Analyzer (Himedia, Mumbai India).

3.9.3 Bioinformatic analysis of amplified 16S r RNA gene

The DNA sequence was analyzed by BLAST (Altschul et al., 1990) and submitted to GenBank. The neighbor-joining method was used for the construction of a phylogenetic dendrogram using MEGA11 (Molecular Evolutionary Genetic Analysis, version 11) software (Tamura, Stecher, and Kumar 2021).

3.10 BIOSYNTHESIS OF SELENIUM NANOPARTICLES

3.10.1 To determine the ability of PMVW₃ and PMChW2 strain to biosynthesize SeNPs during growth phase

The potential of the strains PMVW₃ and PMChW2 to synthesize selenium nanoparticles (SeNPs) was studied by inoculating the culture inoculum in ZMB supplemented with 2 mM of Na₂SeO₃ followed by incubation at 28 °C ± 2 at 100 rpm for 24 h. The culture broth after incubation was centrifuged at 4500 rpm, for 20 min at 4 °C. The brick-red colored cell biomass was then lysed in PBS (0.1 M) using a sonicator PRO-650 (Vibronics, 0.5 pulses for 10 min with 5 min intervals) and centrifuged at 4000 rpm for 20 min twice. The resulting supernatant obtained was then scanned in the range of 200-700 nm in UV-Vis spectrophotometer (Shimadzu- UV-1780). The flask containing culture without Na₂SeO₃ and uninoculated media served as controls (Vaigankar. 2020).

3.10.2 To evaluate the ability of PMVW₃ and PMChW2 strain to biosynthesize SeNPs using cell-free culture supernatant

The culture was inoculated in ZMB medium and incubated on an incubator shaker (100 rpm), at 28 °C for 48 h. The fully grown cultures were centrifuged at 4500 rpm, 4 °C for 20 min and the cell-free supernatant was collected into a fresh flask without disturbing the pellet. The supernatant was added to 2 mM of Na₂SeO₃(1:1) and incubated at 28 °C for 48 h. Subsequently, the aliquots (1 mL) were withdrawn and scanned in the range of 200-700 nm using UV-Vis spectrophotometer (Vaigankar. 2020).

3.11. OPTIMIZATION OF MEDIA PARAMETERS FOR SeNPs SYNTHESIS

3.11.1 Varying Sodium selenite concentration

The effect of sodium selenite (Na_2SeO_3) on selenium reduction and nanoparticle synthesis was evaluated by inoculating the bacterial strains PMVW₃ and PMChW₂ in ZMB flasks with varying Na_2SeO_3 concentrations (1, 2, 3, 4, 5 and 6 mM) and incubated at 28 °C, 100 rpm. A nanoparticle containing supernatant was extracted and monitored at 265 nm using UV-Vis spectrophotometer.

3.11.2 The effect of pH

To study the effect of pH on the biosynthesis of SeNPs by strains PMVW₃ and PMChW₂, the pH of the media was adjusted to 5, 6, 7, 8, 9 and 10 using 1 N HCl and 1N NaOH solutions. Bacterial cells were incubated on a shaker (100 rpm) at 28 °C amended with 2 mM Na_2SeO_3 . A nanoparticle containing supernatant was extracted and monitored at 265 nm using UV-Vis spectrophotometer.

3.11.3 The effect of temperature

The strains PMVW₃ and PMChW₂ were inoculated in ZMB flasks with 2 mM Na_2SeO_3 concentration, pH 7 and incubated at various temperatures, namely, 28 °C, 32 °C and 37 °C, 100 rpm and nanoparticles containing supernatant were extracted, and monitored at 265 nm using UV-Vis spectrophotometer.

3.12. GROWTH BEHAVIOUR OF STRAIN PMVW₃ IN PRESENCE OF Na₂SeO₃

SeNPs synthesis during the growth phase of strain PMVW₃ was carried out under optimized conditions obtained from (3.11). The reaction mixture was withdrawn after a specific time interval and was monitored between 200-800 nm using a UV-Vis spectrophotometer (El-deeb et al., 2023).

3.13. HARVESTING OF BIOSYNTHEZIZED SeNPs

To obtain SeNPs, the strain PMVW₃ was harvested by centrifugation at 4500 rpm for 20 min and the resultant brick red colored pellet was washed thrice with 0.1M PBS. The cell pellet was re-suspended in methanol: chloroform (2:1 v/v) and sonicated (0.5 pulses for 10 min with 5 min intervals). After cell lysis, the suspension was subjected to centrifugation at 4000 rpm for 20 min, the supernatant obtained was retained and the pellet containing cell debris was discarded. The brick-red colloidal suspension obtained was further harvested at 4500 rpm for 30 min and the pellet obtained was subsequently washed twice with distilled water and ethanol. The pellet was dried at 60 °C using an oven to get SeNPs and pulverized to obtain the fine powder using agate mortar (Vaigankar. 2020).

3.14. CHARACTERIZATION OF BIOGENIC SeNPs

3.14.1 UV-Vis spectroscopic analysis

The biogenic SeNPs were suspended in methanol: chloroform solvents (2:1 v/v) and absorbance was recorded in the range of 200- 700 nm with methanol: chloroform (2:1 v/v) as blank (Ullah et al. 2021).

3.14.2 Scanning electron microscopy (SEM) and Energy dispersive x-ray (EDX)

A thin layer of dried powder of SeNPs nanoparticles was placed on copper stubs and coated with gold using a high vacuum evaporator. It was then analyzed by SEM coupled with EDX using Quanta FEG 250 (Samant et al., 2016).

3.14.3 X-ray diffraction analysis (XRD)

X-ray diffraction pattern for biosynthesized SeNPs was obtained by scanning the dried powder of biogenic SeNPs. This was further used to make a film on a glass slide for XRD analysis using Bruker D8 Advance X-ray diffractometer (Samant et al., 2016).

3.15 BIOMEDICAL APPLICATIONS OF BIOSYNTHEZED SELENIUM NANOPARTICLES

3.15.1 Antimicrobial activity SeNPs

The agar well diffusion method was employed to determine the antimicrobial action of synthesized SeNPs against different clinical isolates namely *Staphylococcus aureus*, *Escherichia coli*, *Salmonella* sp. and *Bacillus* sp. A stock solution of 50 mg/mL of SeNPs in methanol was prepared and 100 μ L of previously grown pathogenic cultures were spread-plated on Muller-Hinton agar plates. Sterile tips of 0.8 mm were used to bore wells in the plates after half an hour of standing time. Different concentrations (25, 50, 75 and 100 μ g/mL) of suspended SeNPs (100 μ L) were loaded onto the wells keeping appropriate controls (Chloroform: Methanol (2:1)). This was followed by incubating plates at 37 °C for 24 h and zone of inhibition was determined which was the measure of antimicrobial activity. The activity was carried out in triplicates and the standard deviation was determined (Sumithra et al., 2023).

3.15.2 Antibiofilm Potential of SeNPs

The anti-biofilm activity of biogenic SeNPs against potential human pathogens was studied using a modified crystal violet assay in a 96-well sterile polystyrene microtiter plate as described previously (Baygar and Ugur, 2017). Initially, 2 mL of nutrient broth was added into a sterile polystyrene microtiter plate to which 12 h old pathogenic bacterial cultures viz. *Staphylococcus aureus*, *Escherichia coli*, *Salmonella* sp. and *Bacillus* sp. were inoculated separately along with four different concentrations of biogenic SeNPs (25, 50, 75 and 100 μ g/mL). Un-inoculated nutrient broth and pathogens grown in nutrient broth without NPs were maintained as controls. The microtiter plate was incubated at 37 °C for 48 h under static conditions. Subsequently,

the microtiter plate was drained and washed gently with sterile 0.1M PBS and distilled water to remove unbound cells, followed by drying for 30 min. Crystal violet (0.2 % w/v) was added (2 mL) to each well and was further incubated at 28 °C for 30 min. The excess dye was gently washed with sterile distilled water. Methanol (2 mL) was added to the dried wells and absorbance was measured at 600 nm keeping methanol as a blank. The anti-biofilm effect was estimated using the following formula:

$$\% \text{ Anti-biofilm activity} = \left[\frac{\text{Absorbance of control} - \text{absorbance of the sample}}{\text{absorbance of control}} \right] \times 100$$

The absorbance of control corresponds to the bacterial cells grown in nutrient broth without NPs. The anti-biofilm assay was carried out in triplicate and the standard deviation was determined.

3.15.3 Free-radical scavenging activity of biogenic SeNPs

DPPH (1, 1-diphenyl-2-picrylhydrazyl) radical scavenging activity of biogenic SeNPs was investigated using the method described by Turlo et al. (2012) with minor modifications. In the presence of the antioxidant purple DPPH changes into a yellow stable compound and the hydrogen donating capacity of the antioxidant determines the extent of the reaction (Niki et al., 2010). Different concentrations of biogenic SeNPs (25, 50, 75 and 100 µg/mL) were mixed with 1 mL of freshly prepared 0.2 mM DPPH. The tubes were mixed and incubated in the dark for 30 min followed by measuring the absorbance at 570 nm using ascorbic acid as standard and methanol as blank. The percent of free radical scavenging activity was determined by the formula:

$$\% \text{ Inhibition} = \left[\frac{\text{Control OD} - \text{Sample OD}}{\text{Control OD}} \right] \times 100.$$

3.16 AGRICULTURAL APPLICATIONS

3.16.1 Production of EPS

3.16.1.a Alcian blue staining for EPS-producing bacterial isolate

Alcian stain is used to stain acidic polysaccharides. Extracellular polysaccharides or extra polymeric substances (EPS) produced by the bacterial isolate PMChW₂ were visualized and stained with alcian blue dye. The culture was grown in nutrient broth (NB) with a sugar substrate (1% of glucose) for 24 h at room temperature (28 °C ± 2). The culture was centrifuged at 4500 rpm for 20 minutes. A thin smear of the supernatant was made on a clean grease-free glass slide. The slides were stained with alcian blue dye for 15 minutes followed by washing with distilled water. The cells were observed for the presence of EPS under a microscope at 40X objective (Sohm et al., 2011).

3.16.1.b Extracellular polymeric substance (EPS) production

The selected isolate PMChW₂ was grown in NB along with 1% of the glucose and incubated at 28 °C ± 2 for 48 h. Then, the broth was centrifuged at 4500 rpm for 20 min. The supernatant was mixed with anhydrous ethanol (1:3). Then, the mixture was stored at 4 °C for 48 h and checked for EPS precipitate formation (Z. Wang et al. 2023).

3.16.1.c EPS extraction

The selected isolate PMChW₂ was grown in NB along with 1% of the glucose and incubated at 28 °C ± 2 for 48 h. Then, the broth was centrifuged at 4500 rpm for 20 min. The supernatant was mixed with anhydrous ethanol in ratio (1:3). Then, the mixture was stored at 4 °C for 48 h. The EPS precipitate formed was centrifuged at

4000 rpm for 40 min and then dissolved in distilled water. The EPS solution was freeze-dried at -20 °C for 48 h by using a deep freezer (RQV-400 PLUS) (Z. Wang et al. 2023).

3.16.1.d Preparation of EPS composite SeNPs

To study the effect of EPS composite SeNPs, a stock solution of 25 mg/mL of EPS solution in distilled water (DW) was prepared and a SeNPs solution (2.5 mL) was added to this EPS solution. (Z. Wang et al. 2023).

3.16.2 Effect of EPS composite SeNPs on the plant using seed priming

The seed priming technology was employed to study the effect of EPS composite SeNPs on rice crop var. *Jaya* and mung bean *Vigna radiata* L. Before seed priming, an equal number of seeds (10) were surface sterilized using 0.1 % sodium hypochlorite solution for 1 min followed by washing with distilled water. The seeds were then dried and treated with various treatments of SeNPs, Na₂SeO₃, EPS composite SeNPs (25 and 75 µg/mL) and distilled water for 24 h (Table 1). Treated seeds were then transferred to sterilized petri plates containing sterile absorbent cotton, incubated for up to 10 days under aseptic conditions and a regular amount of water was added every day. After the fifth and tenth days of incubation, the seedlings were used to measure germination index, root length, shoot length and wet biomass (Vaigankar. 2020).

Table 3.1: Various treatments used for rice and mung seeds

Sr.no	Treatments
1.	S + Distilled water (Control)
2.	S + SeNPs (25 µg/mL)
3.	S + SeNPs (50 µg/mL)
4.	S + SeNPs (75 µg/mL)
5.	S + SeNPs (100 µg/mL)
6.	S + Na ₂ SeO ₃ (1 mg/mL)
7.	S + EPS (1 mg/mL)
8.	S + SeNPs-EPS (25 µg/mL)
9.	S + SeNPs-EPS (75 µg/mL)

Key: S: - seed

3.16.2.a Determination of final germination percentage, root and shoot length, and seedling wet biomass

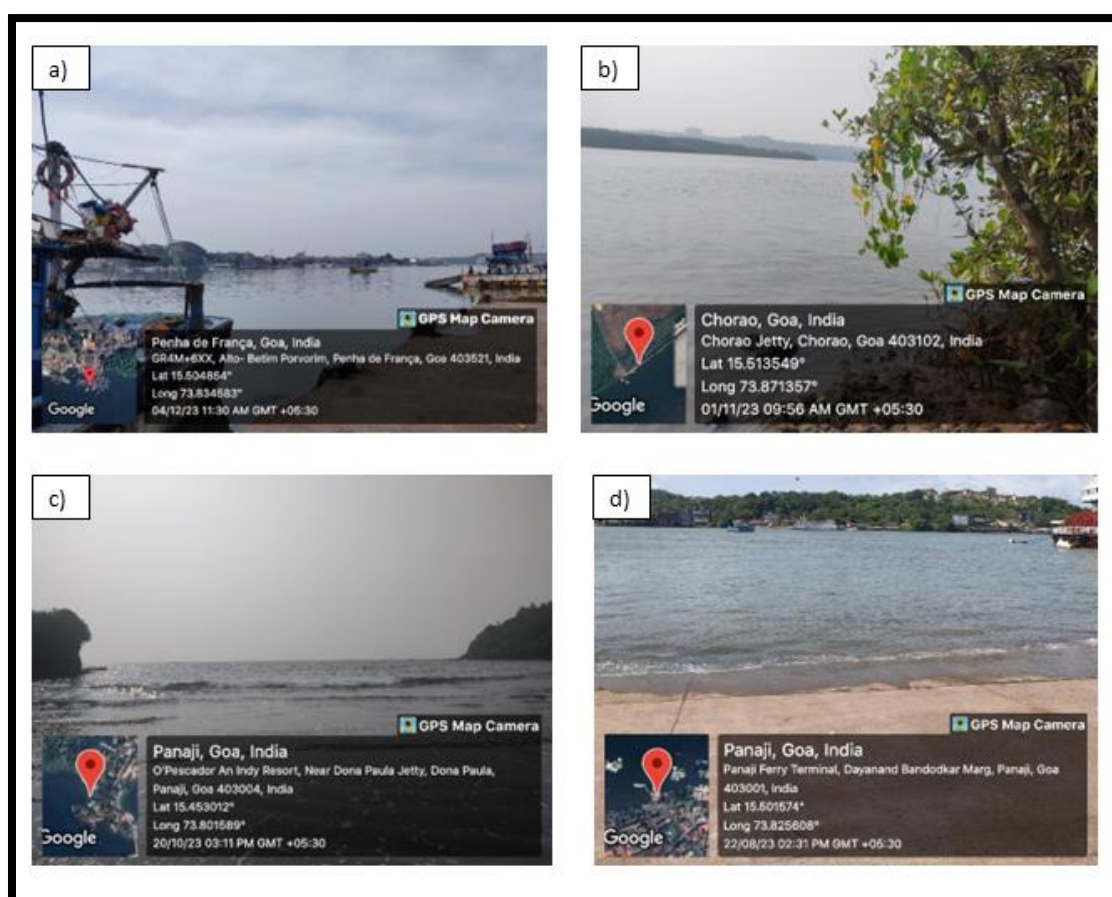
The seedlings were kept on a clean glass plate and root length and shoot length were measured using the scale. The germination percent was measured using a formula (Ellis and Robert, 1981). The wet biomass of the seedlings was also measured using a weighing balance.

CHAPTER 4

RESULTS

4.1. SAMPLE COLLECTION

Water and sediment samples were collected from the different marine and estuarine ecosystems in Goa, India in low tide, with respective codes (Fig.4.1) and checked for various physiochemical parameters (Table 4.1). A total of 9 sampling sites were selected from which 9 water samples and six sediment samples were collected. The pH of water and sediment samples were almost neutral except in Campal waters which showed alkaline while the temperature ranged from 28 to 30 °C.



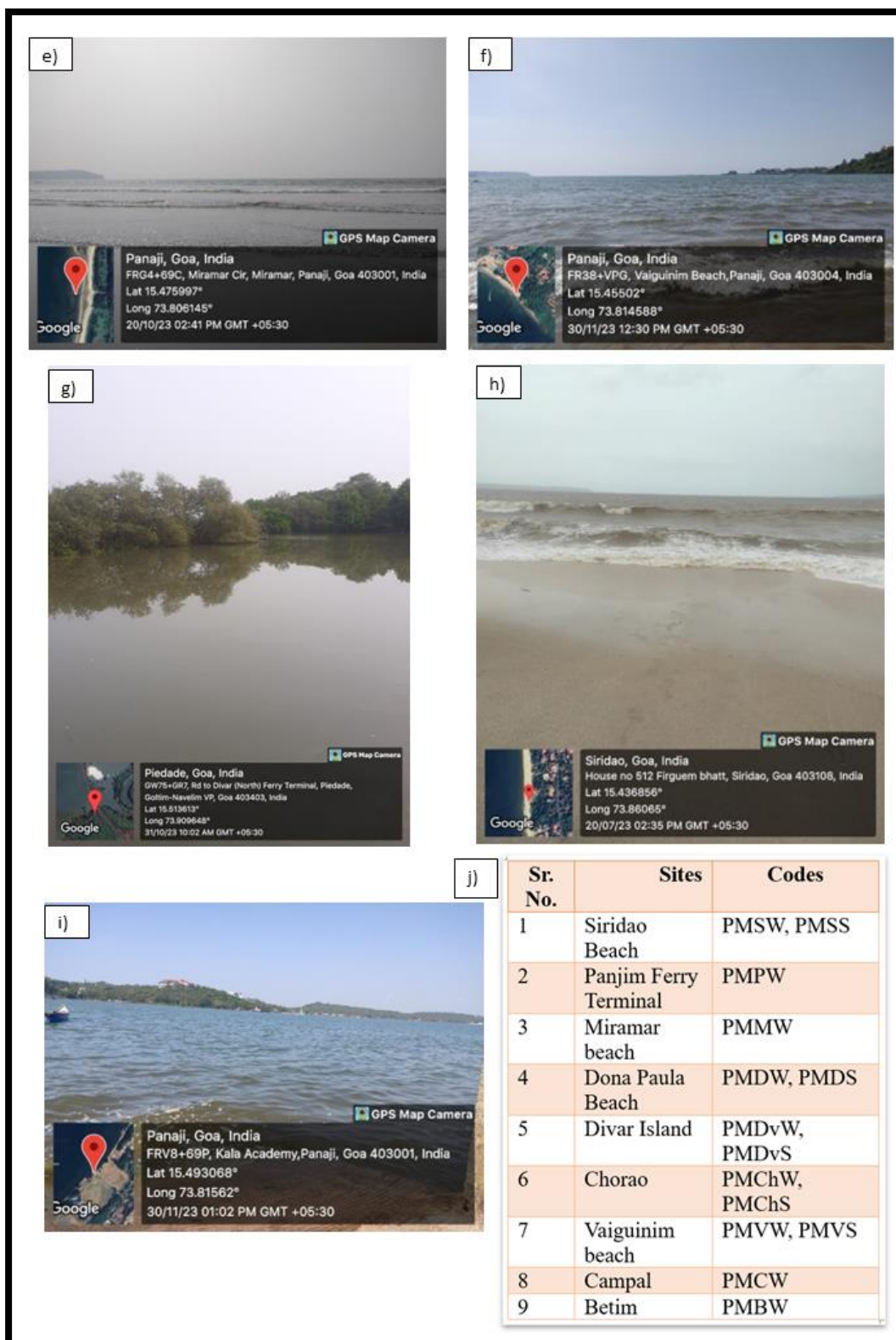


Fig. 4.1: (a) to (i) Sampling sites used for isolation of selenite-reducing marine bacterial isolates and (j) codes used against the respective sites.

Table 4.1 Physicochemical parameters of various samples

Sr. No.	Sampling sites	Sample	Temperature (°C)	pH	Latitude	Longitude
1	Siridao Beach	Water	27	7.3	15.436856	73.86065
		Sediment	27	7.3		
2	Panjim Ferry Terminal	Water	28	7.5	15.501574	73.825608
3	Miramar beach	Water	33	7.6	15.475997	73.806145
		Sediment	33	7.5		
4	Dona Paula Beach	Water	33	7.5	15.453012	73.801589
		Sediment	33	7.6		
5	Divar Island	Water	30	7.5	15.513613	73.909648
		Sediment	30	7.4		
6	Chorao	Water	29	7.6	15.513549	73.871357
		Sediment	29	7.6		
7	Vaigunim beach	Water	31	7.8	15.45502	73.814588
		Sediment	31	7.8		
8	Campal	Water	31	8	15.493068	73.81562
9	Betim	Water	30	7.3	15.504854	73.834583

4.2 ENRICHMENT, ISOLATION and SCREENING OF SELENITE-RESISTANT MARINE BACTERIA

Brick red coloration was observed in enriched flasks treated with 2 mM of Na_2SeO_3 . (Fig. 4.2). Discrete brick red-colored bacterial colonies were obtained after plating the enriched samples on ZMA with 2 mM Na_2SeO_3 while in control (0 mM) no such coloration was seen (Fig. 4.3). Morphologically 25 dissimilar bacterial colonies were selected and sub-cultured on ZMA plates with 2 mM of Na_2SeO_3 and without Na_2SeO_3 (Fig. 4.4).

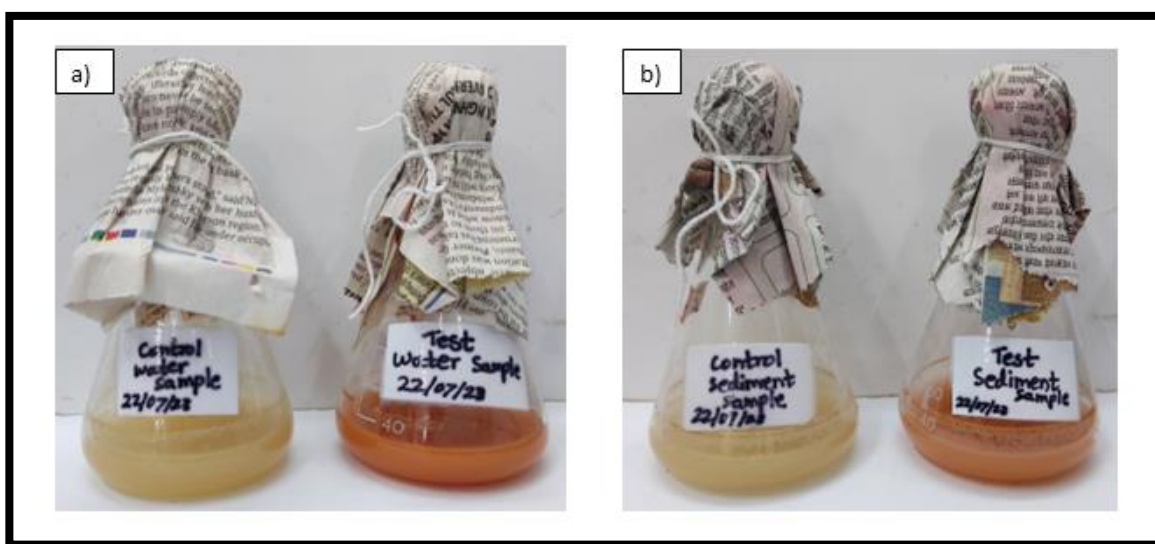


Fig. 4.2: Enriched flasks: (a) water sample with and without Na_2SeO_3 and (b) sediment sample with and without Na_2SeO_3 after 48 h of incubation.

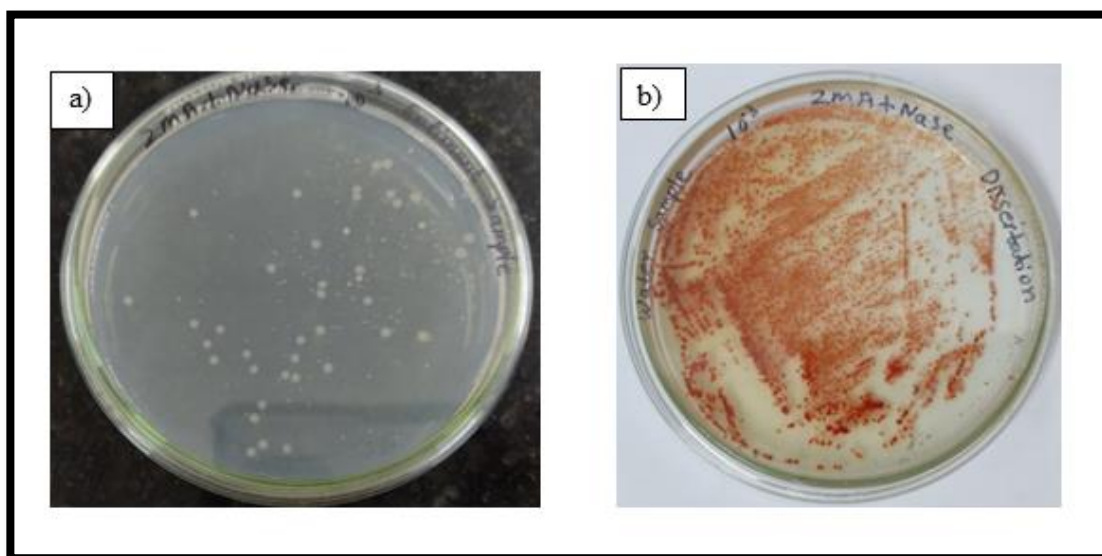


Fig. 4.3: ZMA plates: (a) without Na_2SeO_3 , (b) with (2 mM) Na_2SeO_3 showing brick red colonies.

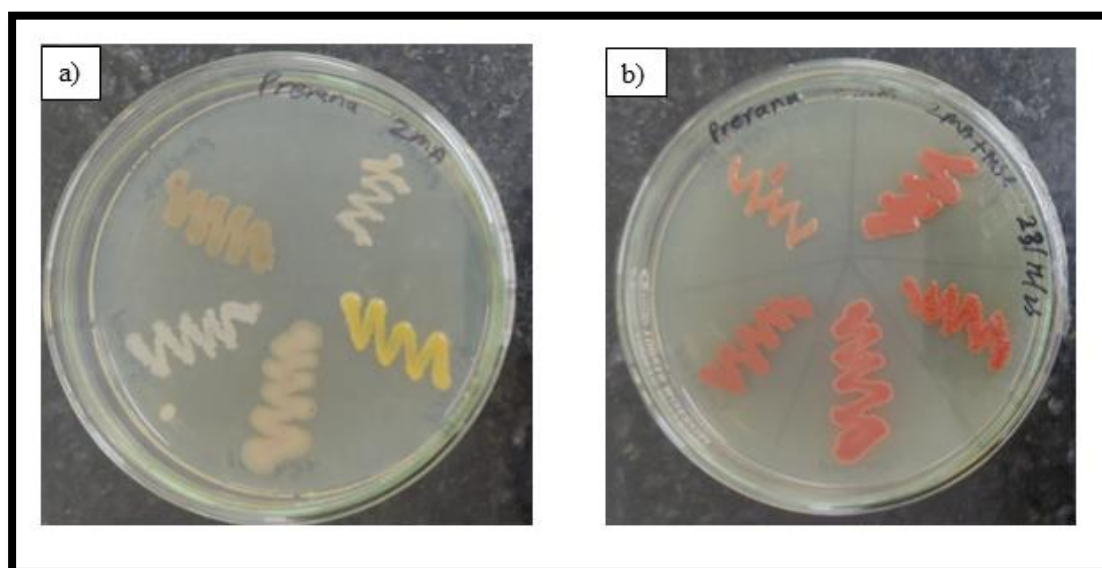


Fig. 4.4: ZMA plates - (a) without Na_2SeO_3 , (b) with 2 mM Na_2SeO_3 showing brick red colonies.

4.3 GROWTH and MAINTENANCE CONDITIONS



Fig. 4.5: ZMA Slants containing isolated bacterial strains

4.3.1 Colony characteristics of the selected colonies

Morphologically 25 dissimilar bacterial colonies were considered for further studies (Table 4.2).

Table 4.2: List of the twenty-five selected bacterial isolates

Isolate number	Name
1	PMSW ₁
2	PMSW ₂
3	PMSS ₁
4	PMSS ₂
5	PMPW ₁
6	PMMW ₁
7	PMDW ₁
8	PMDW ₂
9	PMDS ₁
10	PMDS ₂
11	PMDvS ₁

12	PMDvS ₂
13	PMChW ₁
14	PMChW ₂
15	PMChS ₁
16	PMChS ₂
17	PMVW ₁
18	PMVW ₂
19	PMVW ₃
20	PMVS ₁
21	PMCW ₁
22	PMCW ₂
23	PMBW ₁
24	PMBW ₂
25	PMBW ₃

Table 4.3 Colony characteristics of selected isolated bacterial

Sampling site	Isolate name	Size (mm)	Shape	Color	Elevation	Margin	Opacity	consistency
Siridao Beach	PMSW ₁	1	Circular	White	Flat	Entire	Opaque	Butyrous
	PMSW ₂	1	Circular	Cream	Flat	Entire	Opaque	Butyrous
	PMSS ₁	4	Circular	White	Raised	Entire	Opaque	Butyrous
	PMSS ₂	1	Circular	Yellow	Raised	Entire	Opaque	Butyrous
Panjim Ferry Terminal	PMPW ₁	2	Circular	White	Flat	Entire	Opaque	Dry

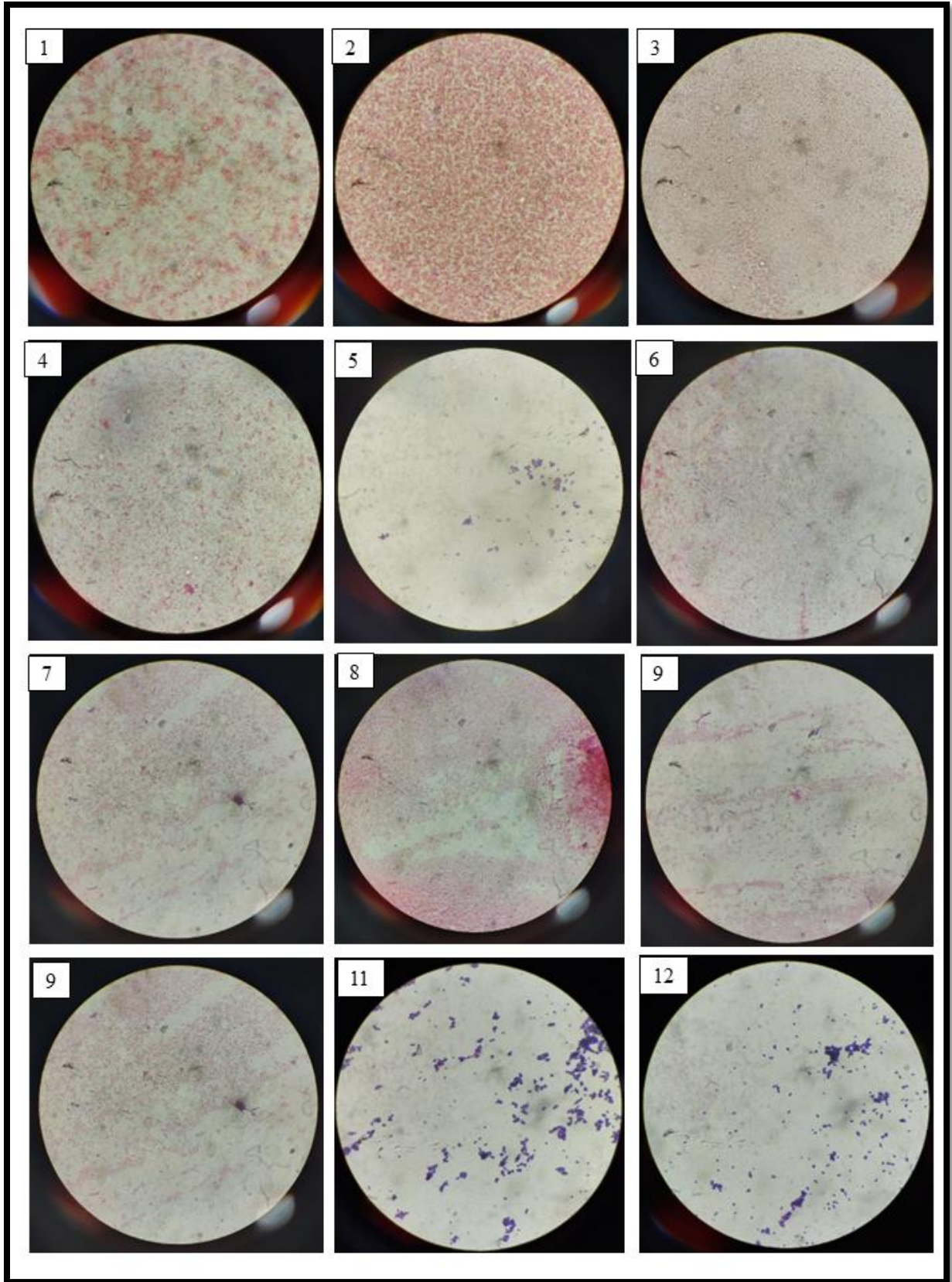
Miramar beach	PMMW ₁	3	Irregular	White	Flat	Entire	Opaque	Butyrous
Dona Paula Beach	PMDW ₁	2	Circular	Cream	Raised	Entire	Opaque	Butyrous
	PMDW ₂	4	Circular	White	Flat	Entire	Opaque	Butyrous
	PMDS ₁	2	Circular	White	Raised	Entire	Opaque	Butyrous
	PMDS ₂	3	Circular	Cream	Raised	Entire	Opaque	Butyrous
Divar Island	PMDvS ₁	1	Circular	White	Flat	Entire	Opaque	Butyrous
	PMDvS ₂	1	Irregular	Yellow	Flat	Entire	Opaque	Butyrous
Chorao Island	PMChW ₁	2	Circular	White	Flat	Entire	Opaque	Butyrous
	PMChW ₂	2	Circular	Brown	Flat	Entire	Opaque	Butyrous
	PMChS ₁	1	Irregular	White	Flat	Entire	Opaque	Butyrous
	PMChS ₂	< 1	Circular	Cream	Flat	Entire	Opaque	Butyrous
Vaigunim beach	PMVW ₁	2	Circular	White	Raised	Entire	Opaque	Butyrous
	PMVW ₂	4	Circular	Cream	Flat	Entire	Opaque	Butyrous
	PMVW ₃	2	Circular	Yellow	Raised	Entire	Opaque	Butyrous
	PMVS ₁	3	Circular	White	Raised	Entire	Opaque	Butyrous
Campal	PMCW ₁	1	Circular	Yellow	Flat	Entire	Opaque	Butyrous
	PMCW ₂	< 1	Circular	Whitish Cream	Flat	Entire	Opaque	Butyrous
Betim	PMBW ₁	1	Circular	White	Flat	Entire	Opaque	Butyrous
	PMBW ₂	3	Circular	Yellow	Raised	Entire	Opaque	Butyrous
	PMBW ₃	1	Circular	Whitish Cream	Flat	Entire	Opaque	Butyrous

4.3.2 Gram staining

Twenty of the isolates were found to be Gram-negative and five were Gram-positive. Most of them showed rod-shaped morphology (table 4.4).

Table 4.4 Gram character of selected isolates

Sampling site	Isolate name	Gram nature	Shape
Siridao Beach	PMSW ₁	Gram-negative	Rods
	PMSW ₂	Gram-negative	Rods
	PMSS ₁	Gram-negative	Rods
	PMSS ₂	Gram-negative	Rods
Panjim Ferry Terminal	PMPW ₁	Gram-positive	Cocci in clusters
Miramar beach	PMMW ₁	Gram-negative	Rods
Dona Paula Beach	PMDW ₁	Gram-negative	Rods
	PMDW ₂	Gram-negative	Rods
	PMDS ₁	Gram-negative	Rods
	PMDS ₂	Gram-negative	Rods
Divar Island	PMDvS ₁	Gram positive	Cocci
	PMDvS ₂	Gram positive	Cocci
Chorao Island	PMChW ₁	Gram-negative	Rods
	PMChW ₂	Gram-negative	Rods
	PMChS ₁	Gram-positive	Rods
	PMChS ₂	Gram-positive	Rods
Vaiguinim beach	PMVW ₁	Gram-negative	Rods
	PMVW ₂	Gram-negative	Rods
	PMVW ₃	Gram-negative	Rods
	PMVS ₁	Gram-negative	Rods
Campal	PMCW ₁	Gram-negative	Rods
	PMCW ₂	Gram-negative	Rods
Betim	PMBW ₁	Gram-negative	Rods
	PMBW ₂	Gram-negative	Rods
	PMBW ₃	Gram-negative	Rods



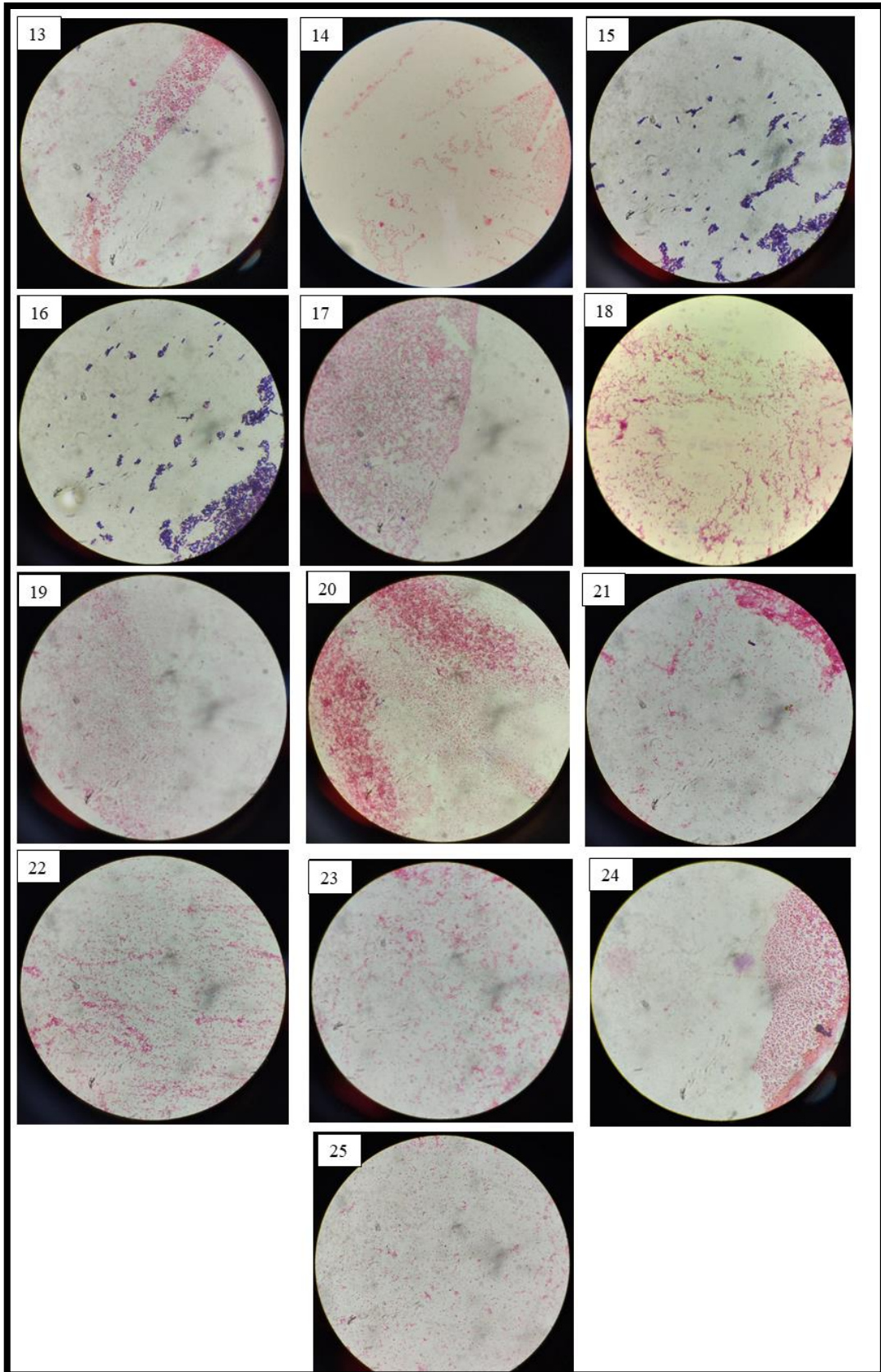


Fig. 4.6: Gram staining of selected bacteria under a microscope.

4.4 Determination of MTC (Maximum Tolerance Concentration) and Minimum Inhibitory Concentration (MIC) of selenite

Out of twenty-five selenite-reducing bacterial isolates, five strains exhibiting MTC higher than 360 mM on ZMA were selected for further studies (Fig. 4.7 to 4.11). Among all the estuarine bacterial isolates the strain designated as PMVW₃ showed an MTC of 360 mM to Na₂SeO₃, in solid medium and MIC of 380 mM in liquid medium (Fig. 4.12 to 4.17).

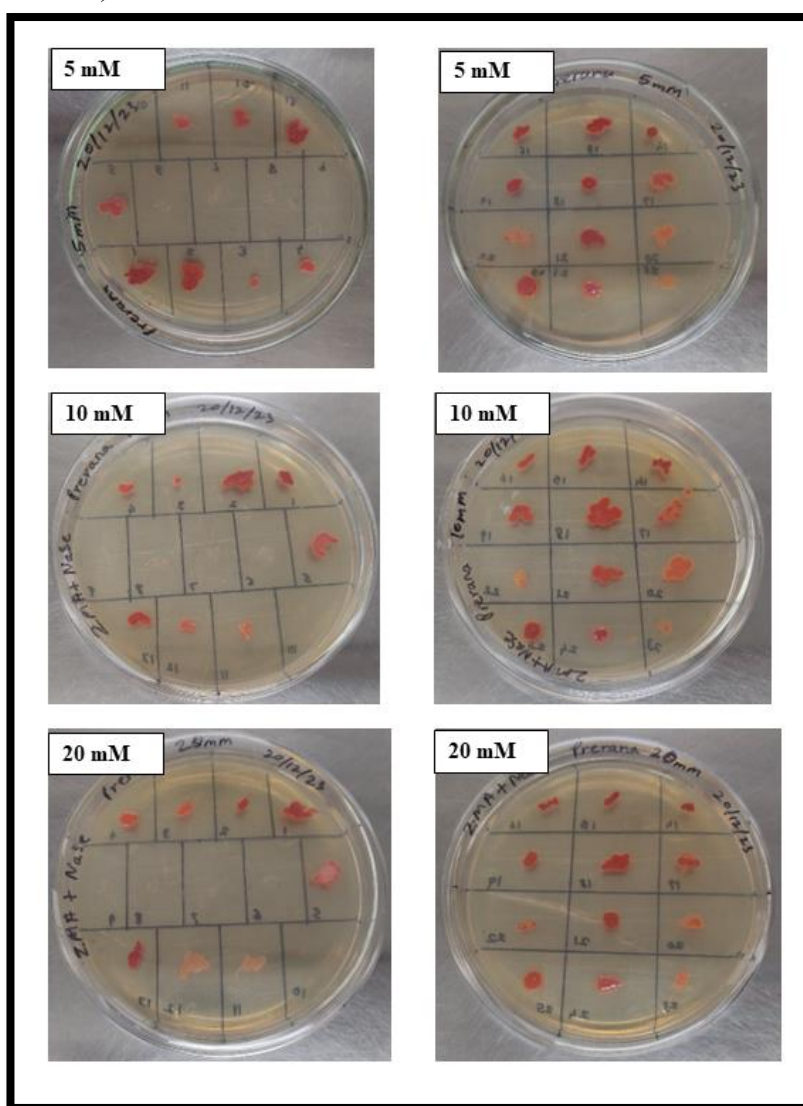


Fig. 4.7: Growth of selected bacterial isolates on ZMA with increasing concentrations of Na₂SeO₃ (5,10 and 20 mM).

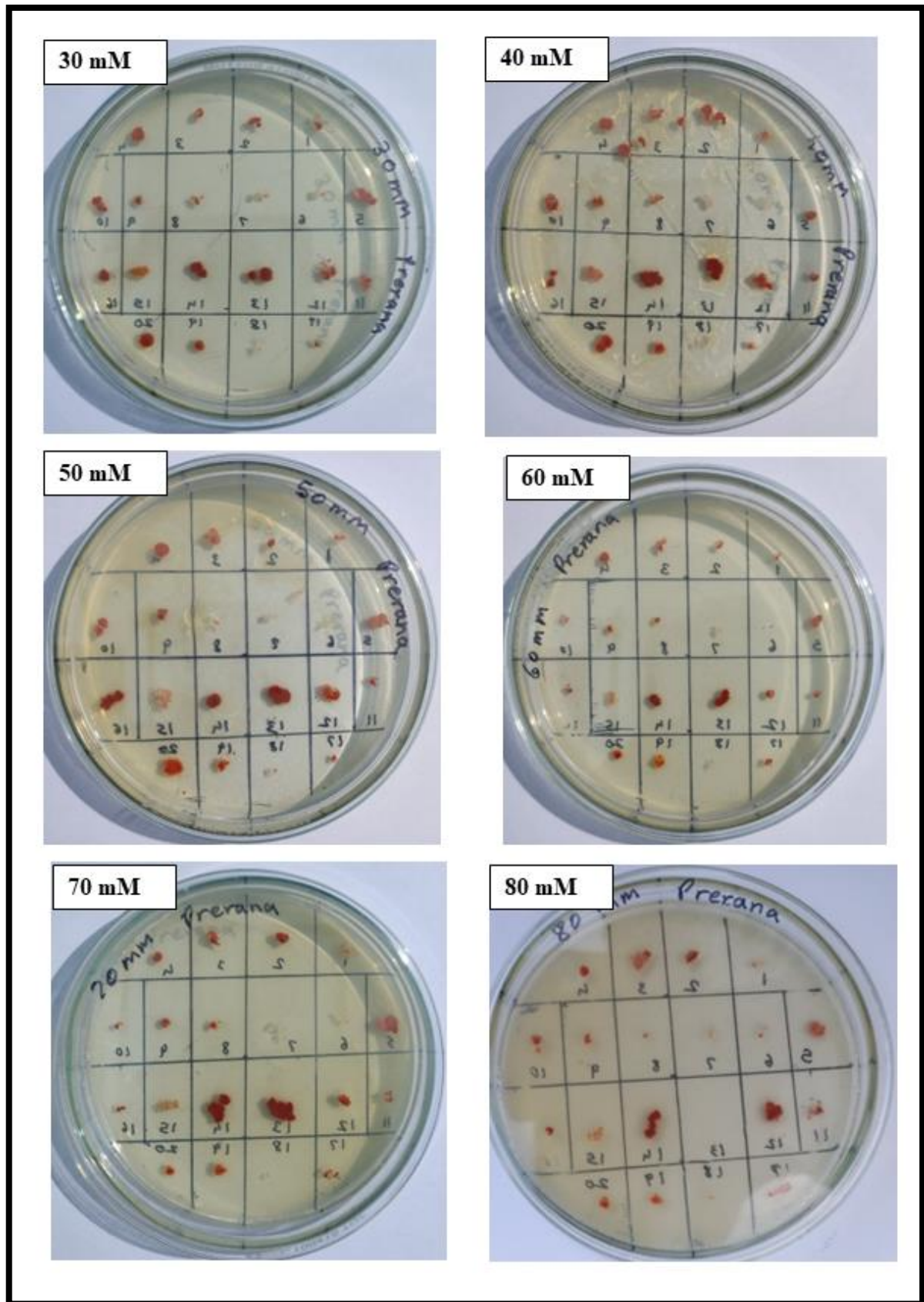


Fig. 4.8: Growth of selected bacterial isolates on ZMA with increasing concentrations of Na_2SeO_3 (30-80 mM).

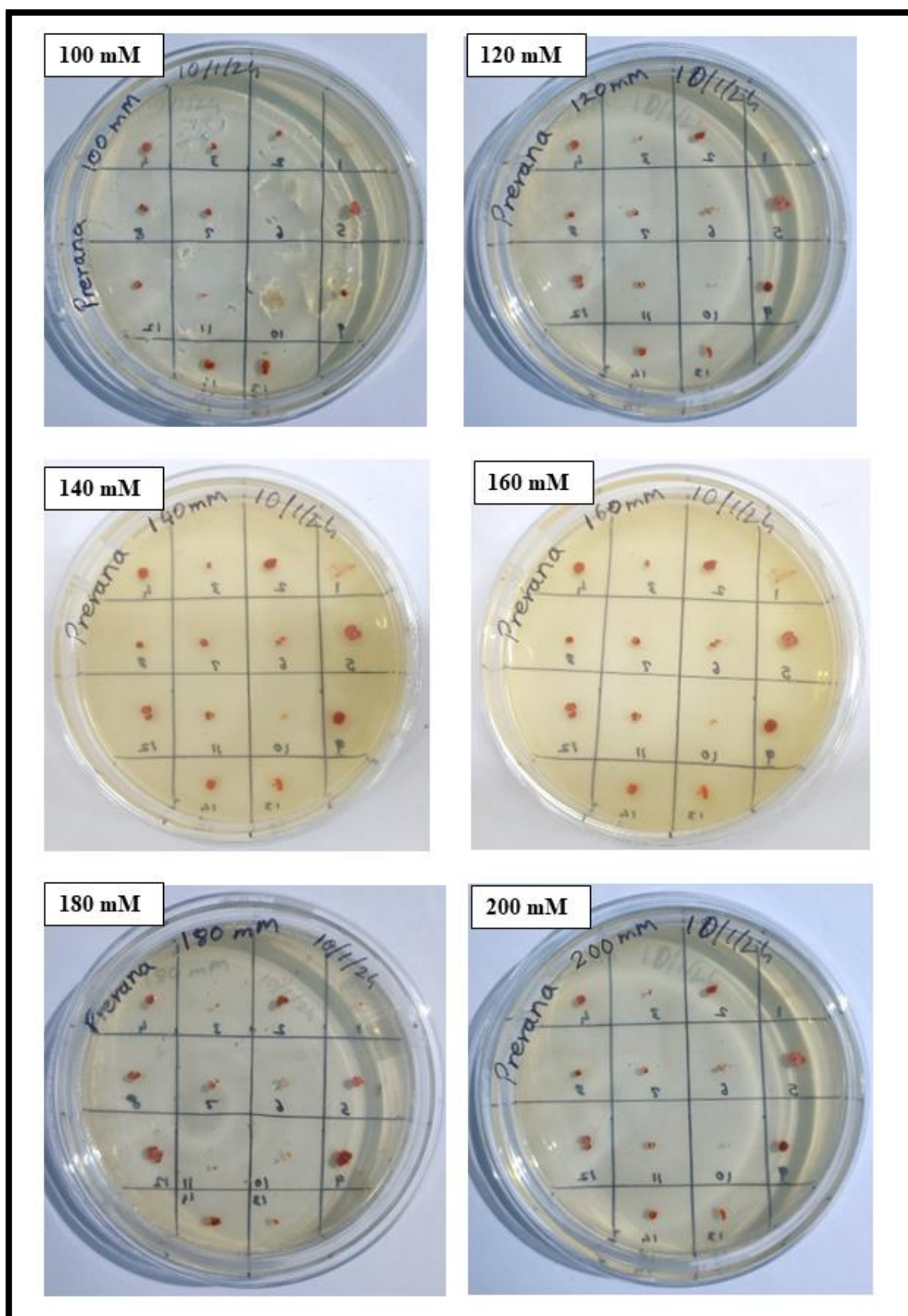


Fig. 4.9: Growth of 14 bacterial isolates on ZMA with increasing concentrations of Na_2SeO_3 (100-200 mM).

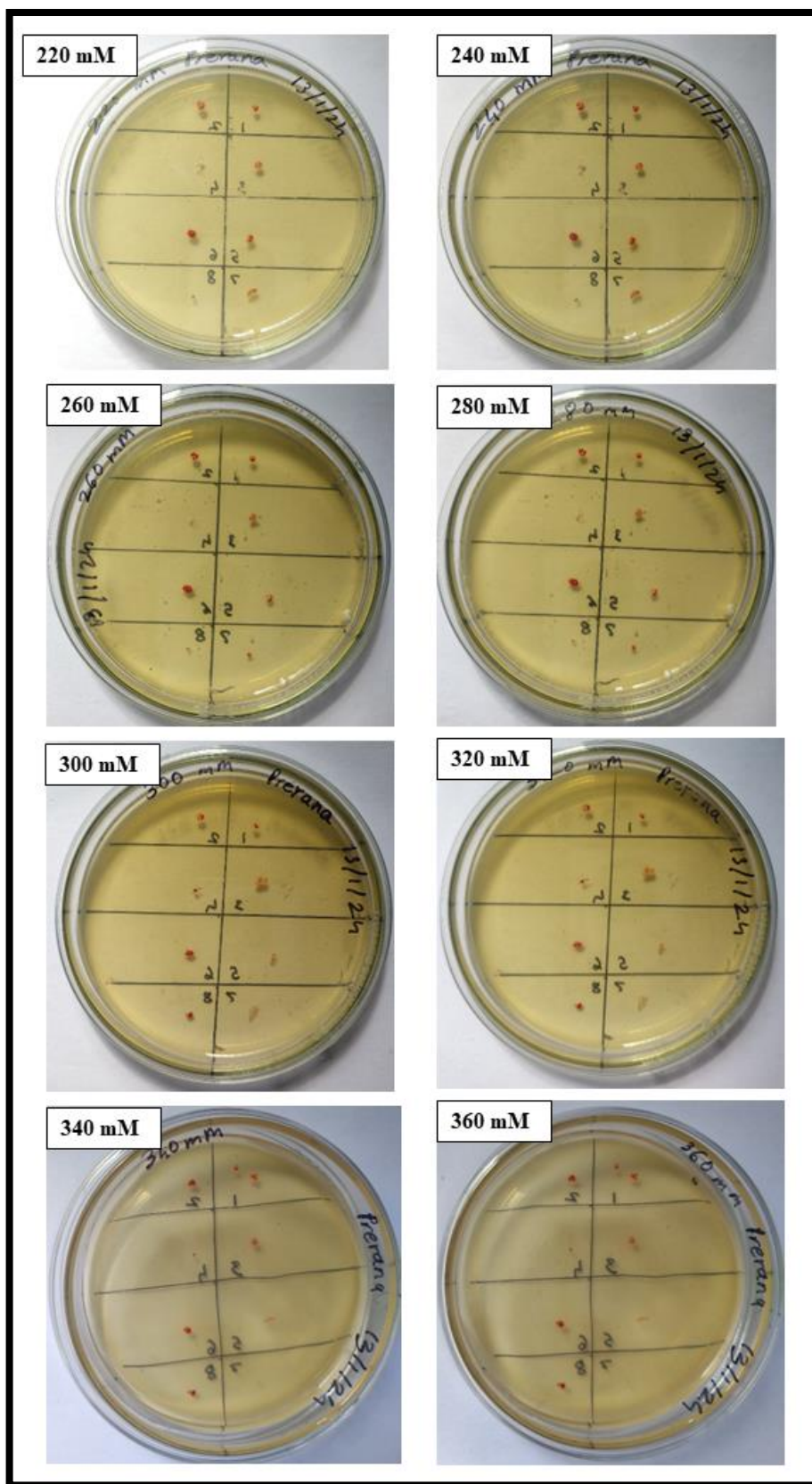


Fig. 4.10: Growth of 8 bacterial isolates on ZMA with increasing concentrations of Na_2SeO_3 (220-360 mM).

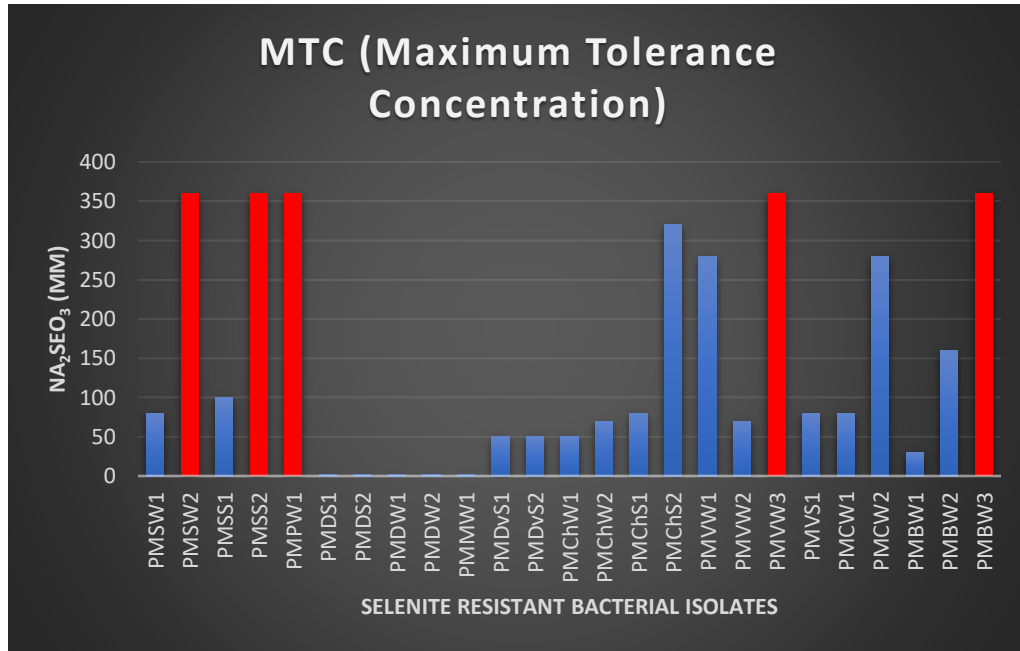


Fig. 4.11: MTC of selected potential selenite-reducing bacterial isolates

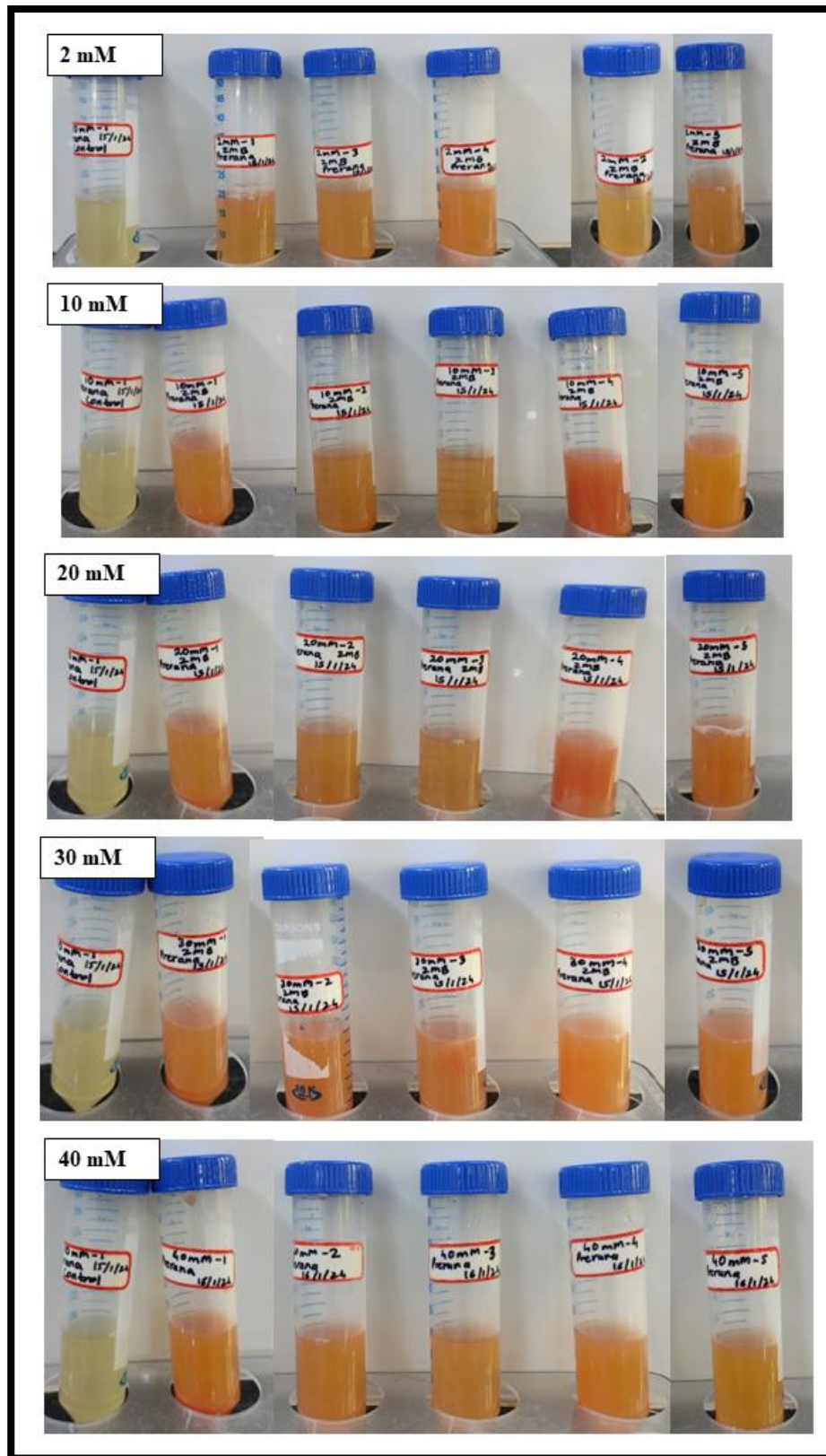


Fig. 4.12: Isolates grown in ZMB with increasing concentrations of Na_2SeO_3 . (2-40 mM).

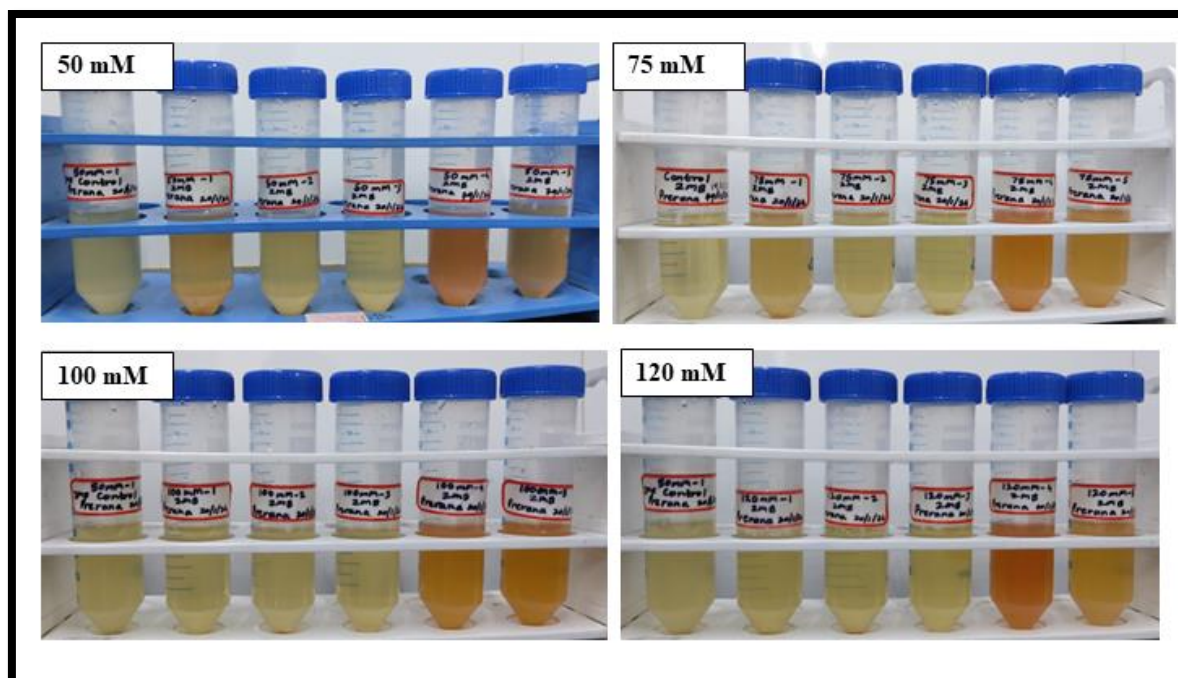


Fig. 4.13: Isolates grown in the presence of 50-120 mM Na_2SeO_3 .

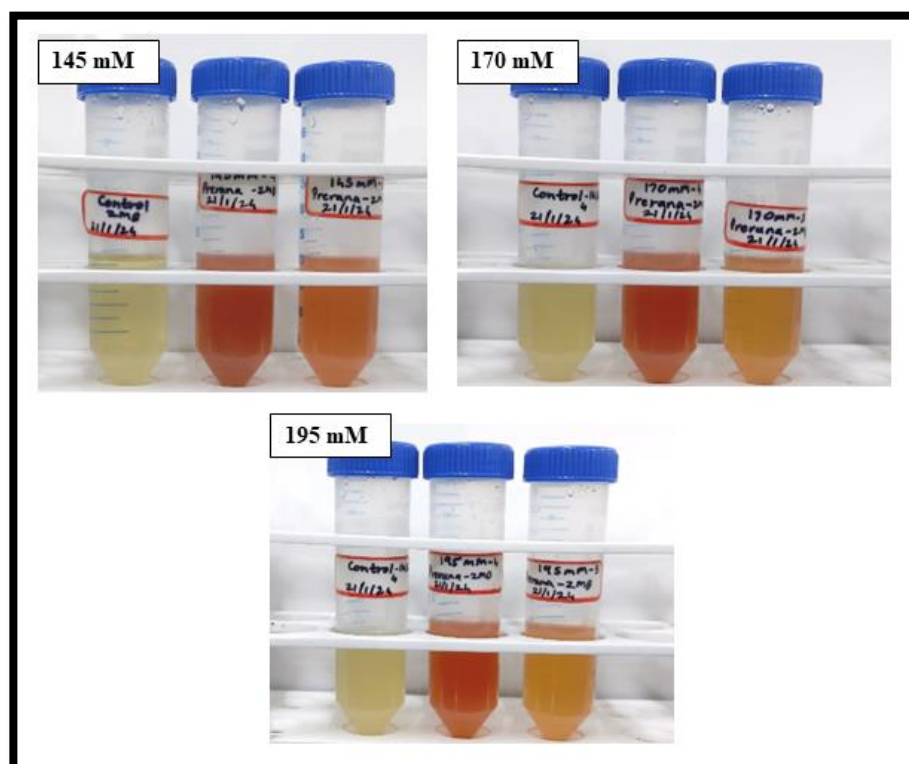


Fig. 4.14: Isolates grown in the presence of 145-195 mM Na_2SeO_3 .

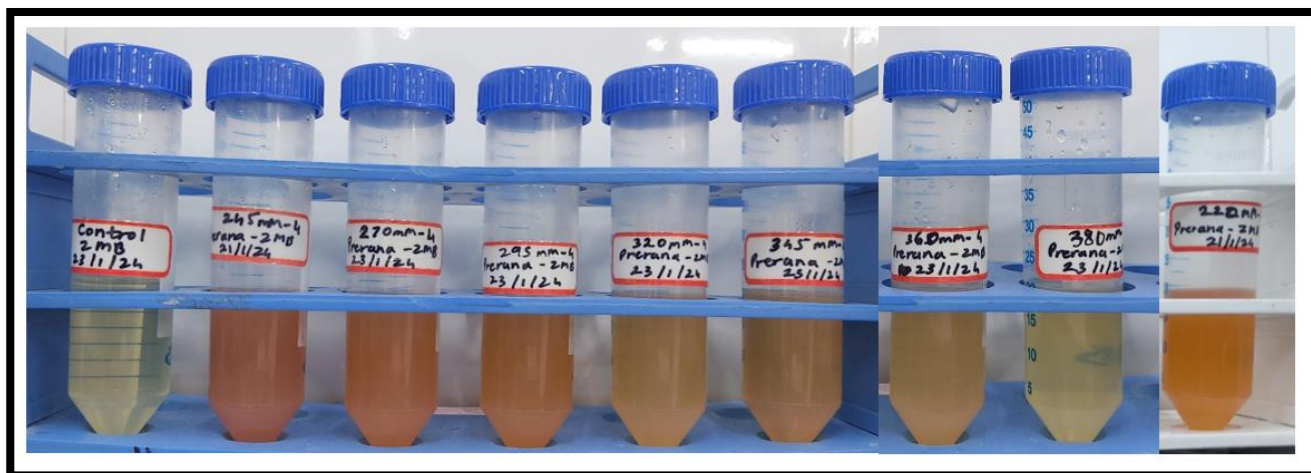


Fig. 4.15: Bacterial isolate PMV₃ grown in the presence of 220-380 mM concentrations of Na₂SeO₃.

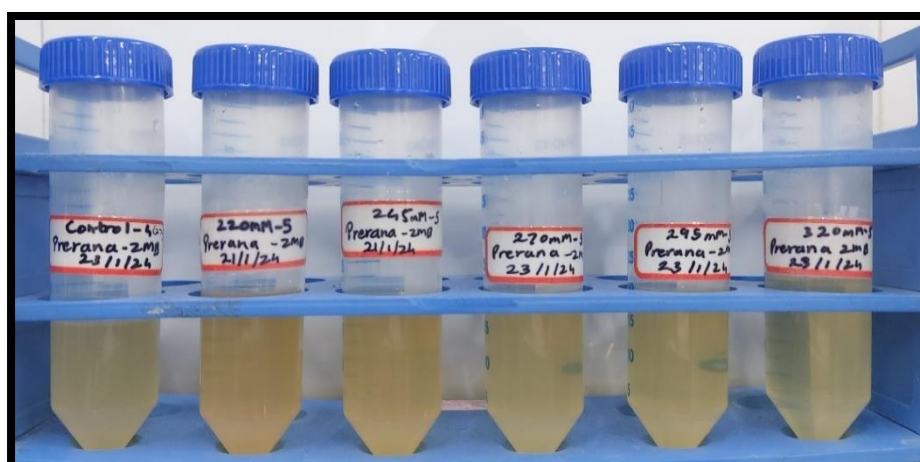


Fig. 4.16: Bacterial isolate PMBW₃ grown in the presence of 220-320mM Na₂SeO₃.

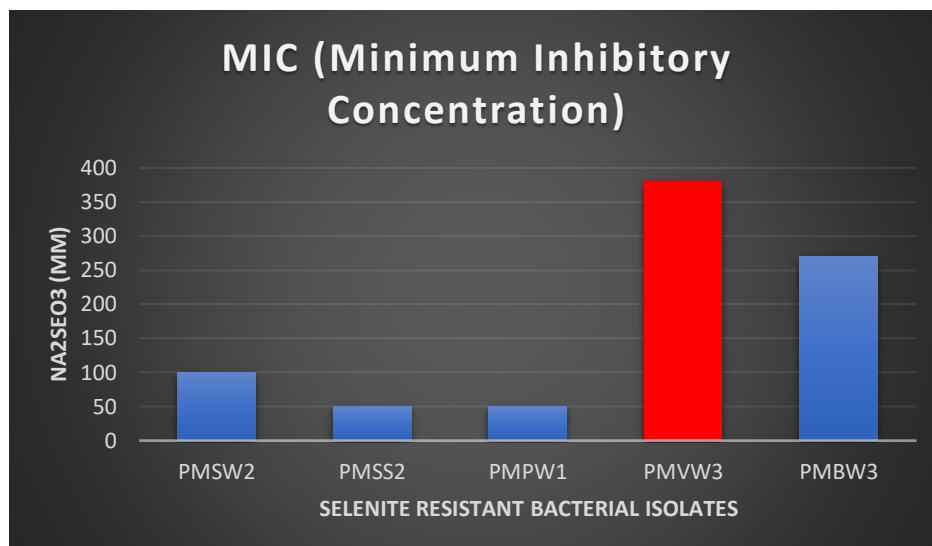


Fig. 4.17: MIC of selected potential selenite-reducing bacterial isolates.

4.5 EPS PRODUCTION

Among all the bacterial isolates, PMChW2 was the exclusive strain demonstrating EPS production, with a Minimum Tolerable Concentration (MTC) of 70 mM towards Na_2SeO_3 . Given the connection between EPS and the synthesis of SeNPs as indicated by previous research (Sheng et al., 2010; Wang et al., 2023), albeit limited, this particular culture was selected for further investigation (Fig. 4.18).

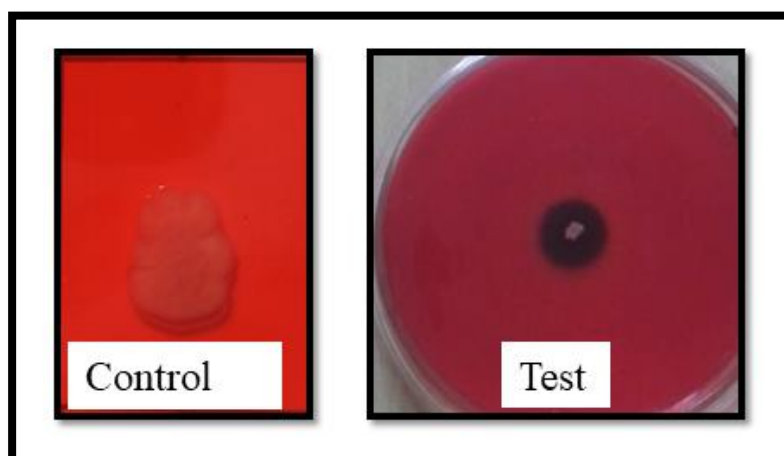


Fig. 4.18: Congo red staining of the *Shewanella* sp. indicating EPS production

4.6 BIOCHEMICAL CHARACTERIZATION OF THE BACTERIAL ISOLATES

Biochemical tests revealed that the isolate PMVW₃ is oxidase positive and showed the presence of enzymes such as catalase and nitrate reductase on the other hand, bacterial isolate PMChW₂ also showed the presence of enzymes such as catalase and nitrate reductase. Indole, VP, and methyl red tests were found to be negative, however, it was able to utilize citrate. Evidence of glucose fermentation was also seen. Additionally, the TSIA test revealed the formation of H₂S gas and revealed oxidase and EPS positive (Fig: 4.19 and table 4.5)).

Table: 4.5. Biochemical characteristics of selenite-resistant marine bacterial isolates

Sr.No.	Biochemical media	PMVW ₃	PMChW ₂
1	Morphology	Rods (short)	Rods (long)
2	Gram character	Gram-negative	Gram-negative
3	Pigmentation	White	Brown
4	EPS	-	+
5	Motility	+	+
6	Oxidase	+	+
7	Facultative anaerobe	-	-
8	Catalase	+	+

10	Nitrate reduction	+	+
11	Phenylalanine deamination	-	-
	IMVIC Test		
13	Indole	-	-
14	Methyl red	-	-
15	Voges Proskauer	-	-
16	Citrate	-	+
	TSIA		
17	Slant	-	+
18	Butt	-	+
19	H ₂ S production	-	+
20	Gas production	-	+
	Sugar fermentation tests		
21	D-Glucose	-	+
22	Lactose	-	-

Key: + Positive; - Negative

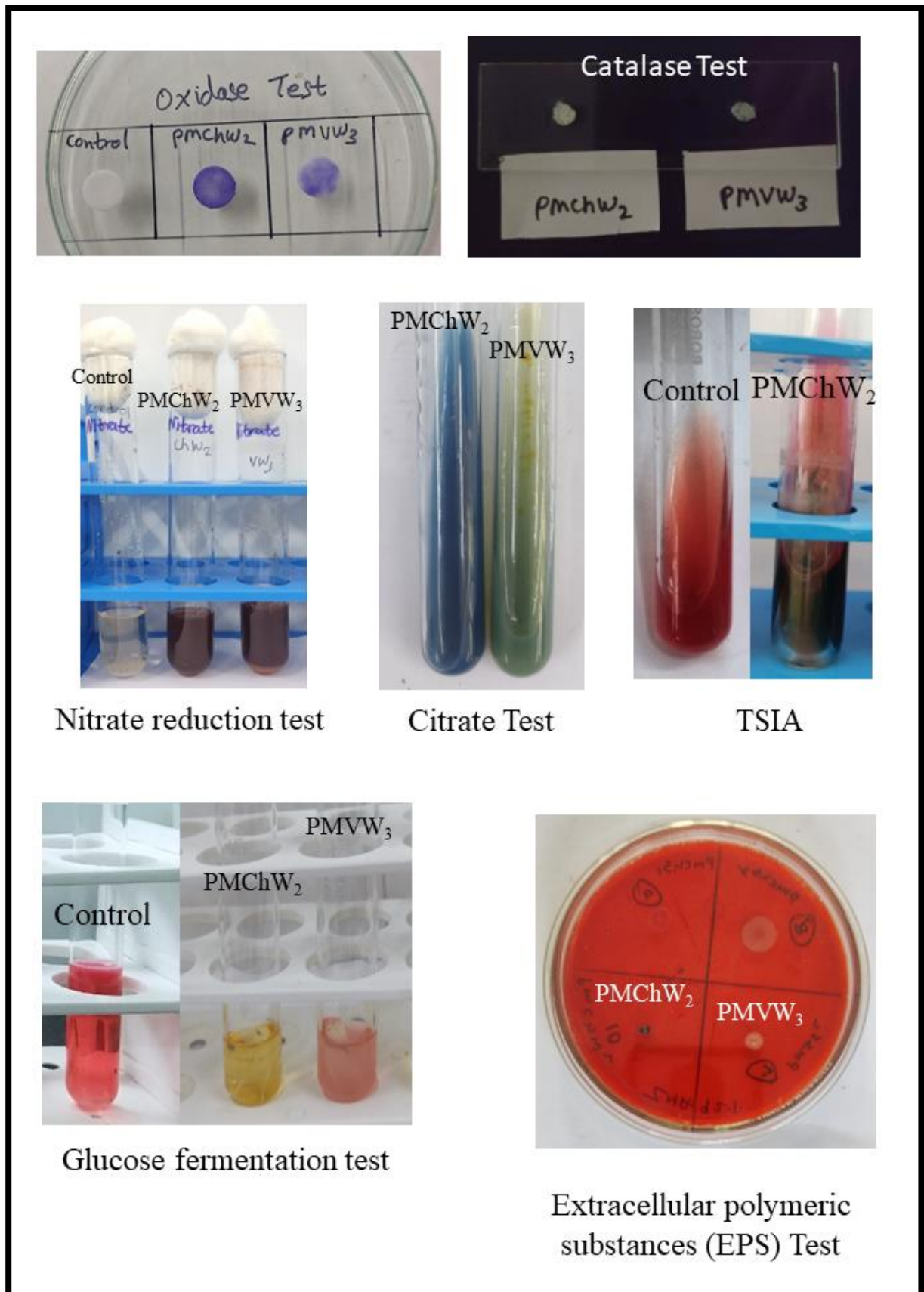


Fig. 4.19: Biochemical tests of selected bacterial isolates for PMVW₃ and PMChW₂.

4.7 ANTIBIOTIC SUSCEPTIBILITY OF SELECTED BACTERIA

The sensitivity of selected selenite-resistant bacterial isolates PMVW₃ and PMChW₂ was tested in the presence of antibiotics using sterile HiMedia antibiotic disks (Fig. 4.20) and the results obtained are given in the following table (Table no. 4.6). It was interesting to note that both the isolates were sensitive to all four antibiotics used namely Streptomycin (10µg), Penicillin - G (10 units), Chloramphenicol(30µg) and Tetracycline (30µg). (refer to Appendix V and Fig. 4.21).

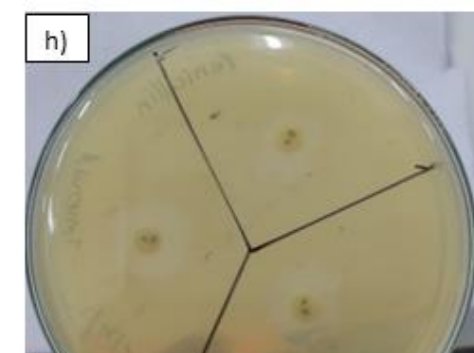
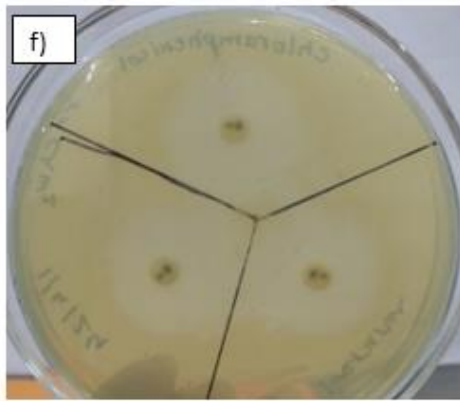
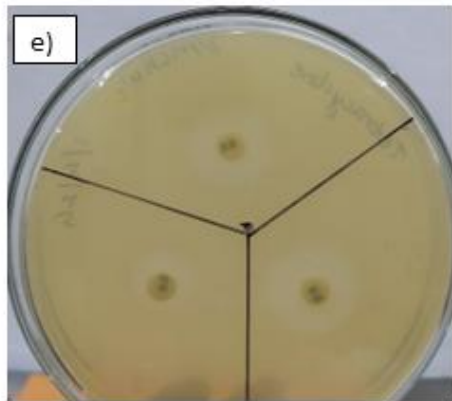
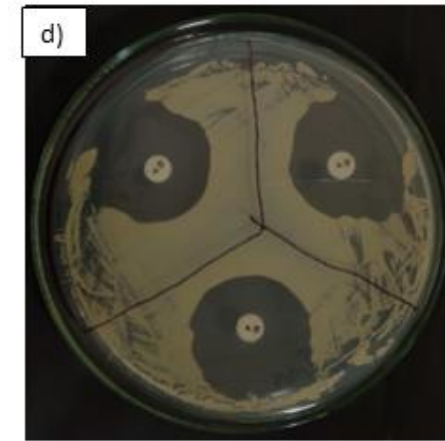
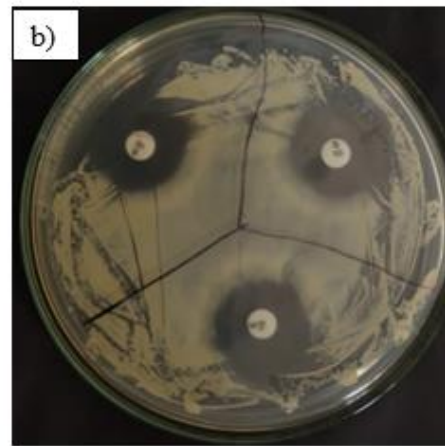
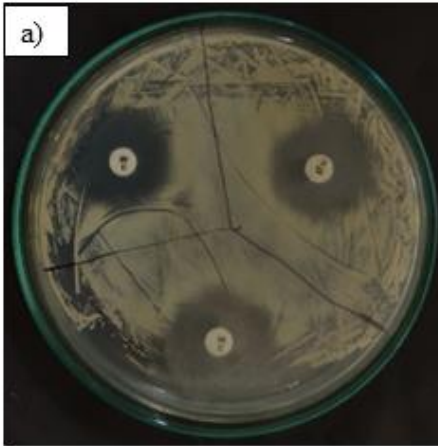
Table no: 4.6 Antibiotic susceptibility of selected bacterial isolates.

Antibiotics discs	Concentration (per disc)	Response of isolates			
		PMVW ₃	Zone of inhibition(mm)	PMChW ₂	Zone of inhibition(mm)
Streptomycin	10µg	S	20	S	20
Penicillin - G	10 units	S	26	S	15
Chloramphenicol	30µg	S	23	S	26
Tetracycline	30µg	S	25	S	17

Key: Sensitive (S); Resistant(R)



Fig. 4.20: Antibiotic disks used to carry out antibiotic sensitivity testing of the bacterial isolates.



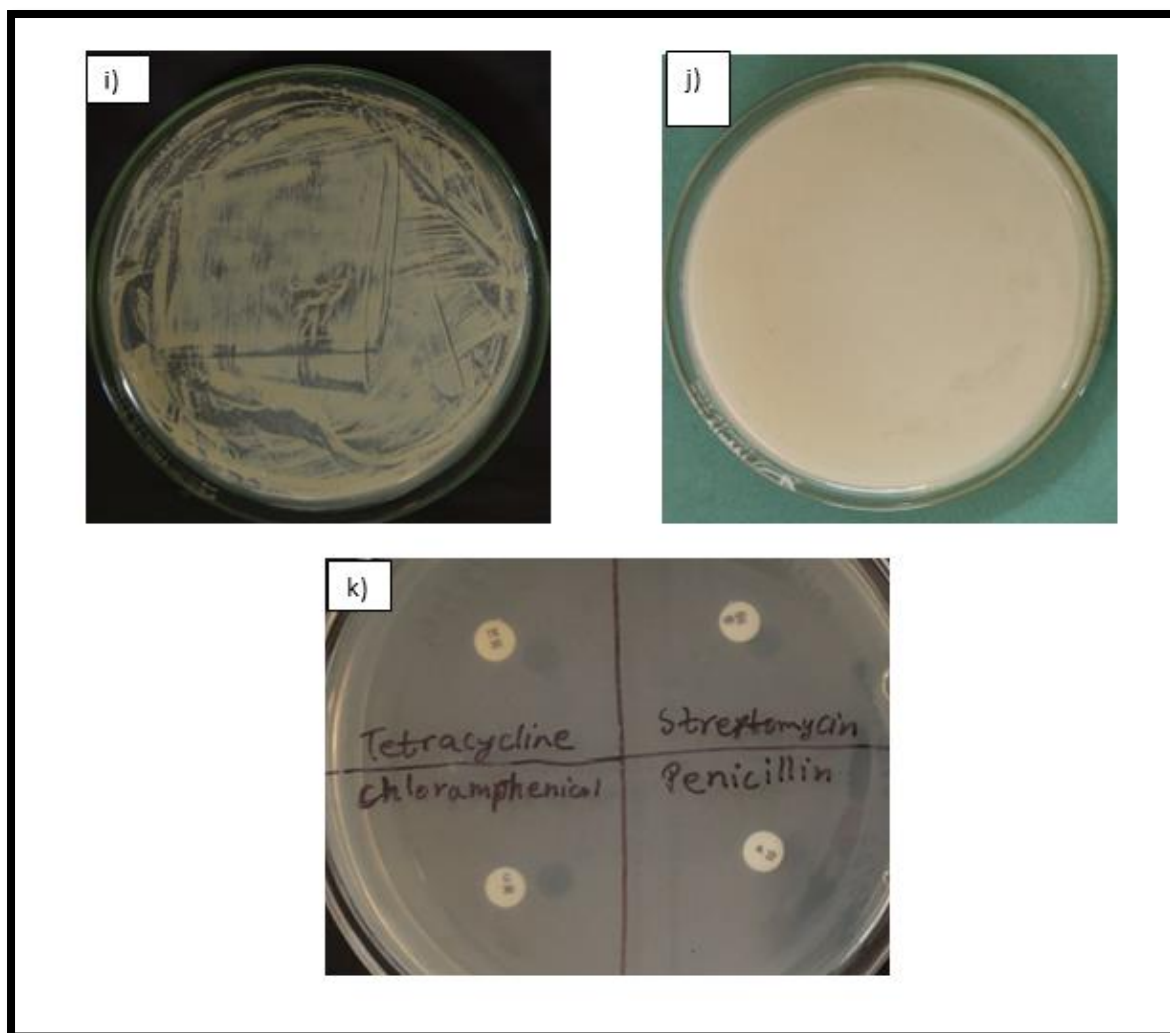


Fig. 4.21: Bacterial cultures showing zone of inhibition against respective antibiotics; (a-d) antibiotic susceptibility against isolate PMVW₃; (e-h) antibiotic susceptibility against PMChW₂; (i and j) negative control and (k) positive control.

4.8 SEM-EDX ANALYSIS OF SELECTED BACTERIAL STRAINS

4.8.1 SEM analysis of selected bacterial strains

The cells of strain PMVW₃ and PMChW₂ showed unique alteration patterns in the cell morphology due to selenite exposure. In the presence of 2 mM sodium selenite, the cells tend to aggregate and elongation of cells was prominent in all the fields for both the cultures. (Fig. 4.22).

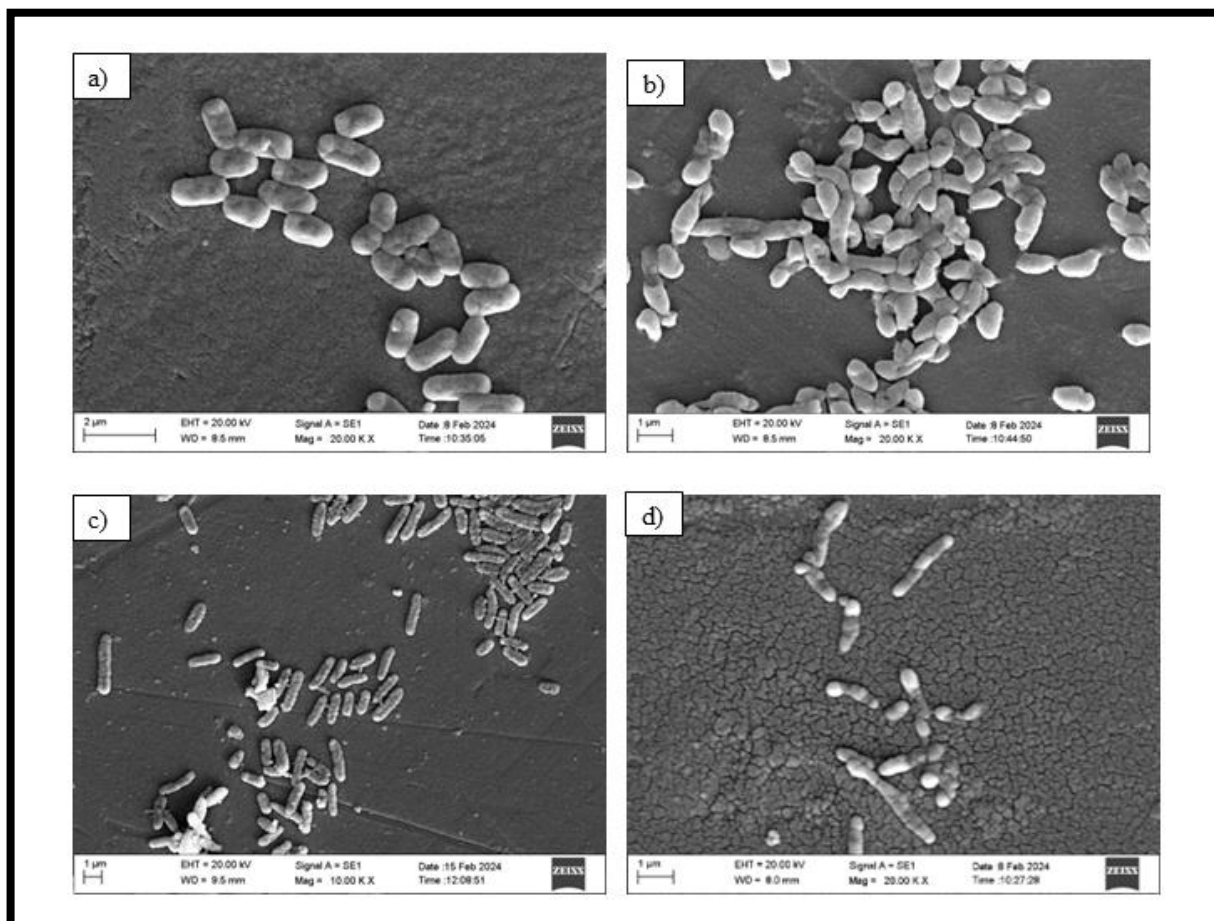


Fig. 4.22: Scanning electron micrographs (SEM) of strain PMVW₃ and PMChW₂; (a) Bacterial cells of PMVW₃ without Na_2SeO_3 exposure, (b) Bacterial cells with 2 mM Na_2SeO_3 exposure, (c) Bacterial cells of PMChW₂ without Na_2SeO_3 exposure and (d) Bacterial cells with 2 mM Na_2SeO_3 exposure.

4.8.2 Scanning electron microscopy (SEM) and Energy dispersive X-ray (EDX) of the bacterial pellet

The selected bacterial strains PMVW₃ and PMChW₂ cells grown in the presence and absence of sodium selenite when subjected to EDX showed a peak attributed to Se while in control no such peak was observed (Fig. 4.23).

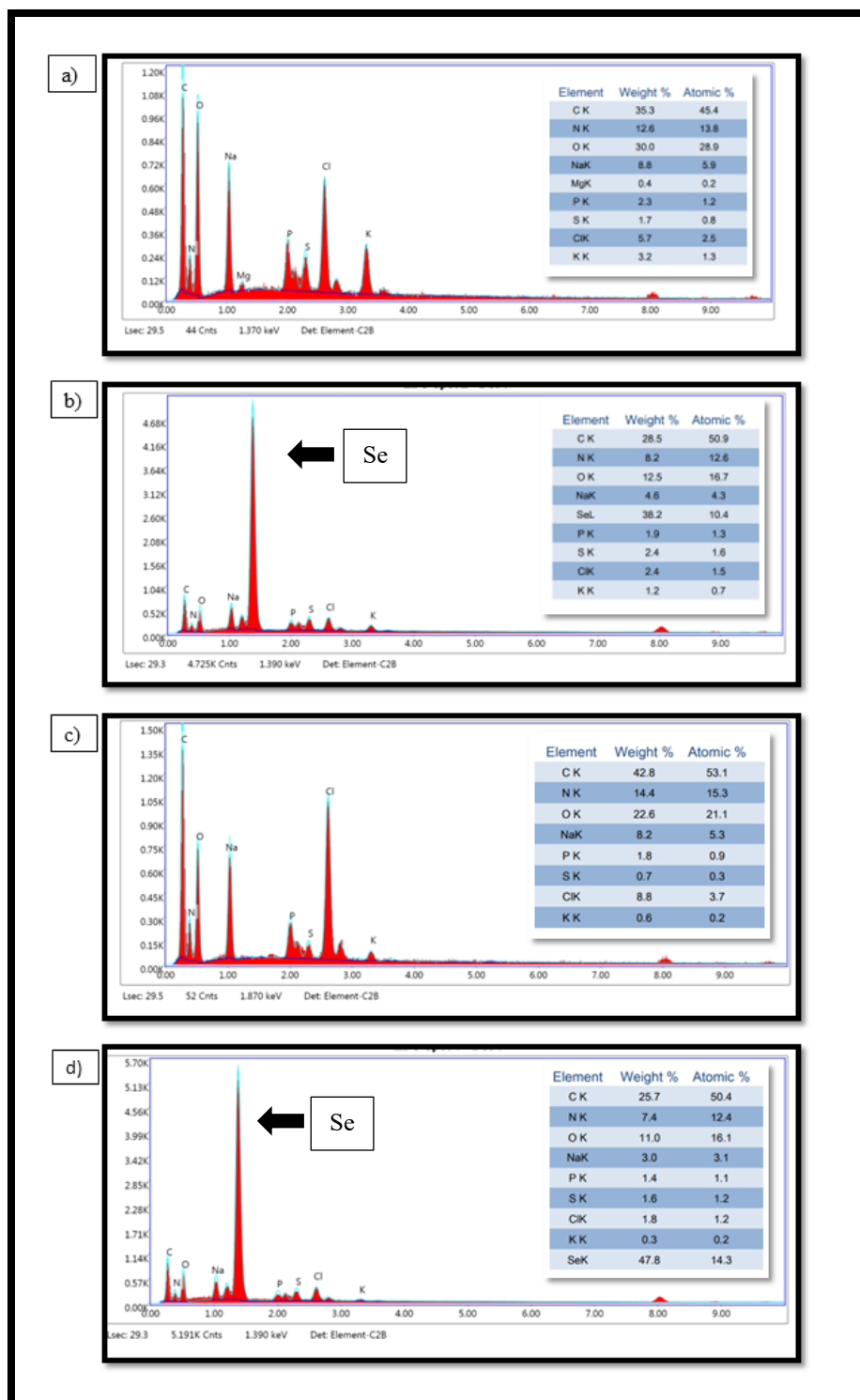


Fig. 4.23: Electron dispersive X-ray (EDX) spectrum of strain PMVW₃ and PMChW₂; (a) PMVW₃ cell without Na₂SeO₃ exposure, (b) Bacterial cells with 2 mM Na₂SeO₃ exposure, (c) Bacterial cells of PMChW₂ without Na₂SeO₃ exposure and (d) Bacterial cells with 2 mM Na₂SeO₃ exposure (arrow indicating Se peak).

4.9 Extraction of genomic DNA

Distinct genomic DNA bands of strains PMVW₃ and PMChW₂ without RNA contamination were obtained (Fig. 4.24). A distinct band of PCR amplicons (approx. 1.5 kb) was observed on 1 % agarose gel (Fig. 4.25). In the 16S rRNA gene sequencing and sequence comparison against the GenBank database using NCBI-BLAST search, the strain PMVW₃ showed the closest match (99.78 %) to *Pseudoalteromonas carrageenovora*. The sequence has been deposited in Genbank as *Pseudoalteromonas* sp. strain PMVW₃ with an accession number 24C110_519_2. The dendrogram analysis also clearly revealed phylogenetic relatedness with other species of *Pseudoalteromonas* (Fig. 4.26).

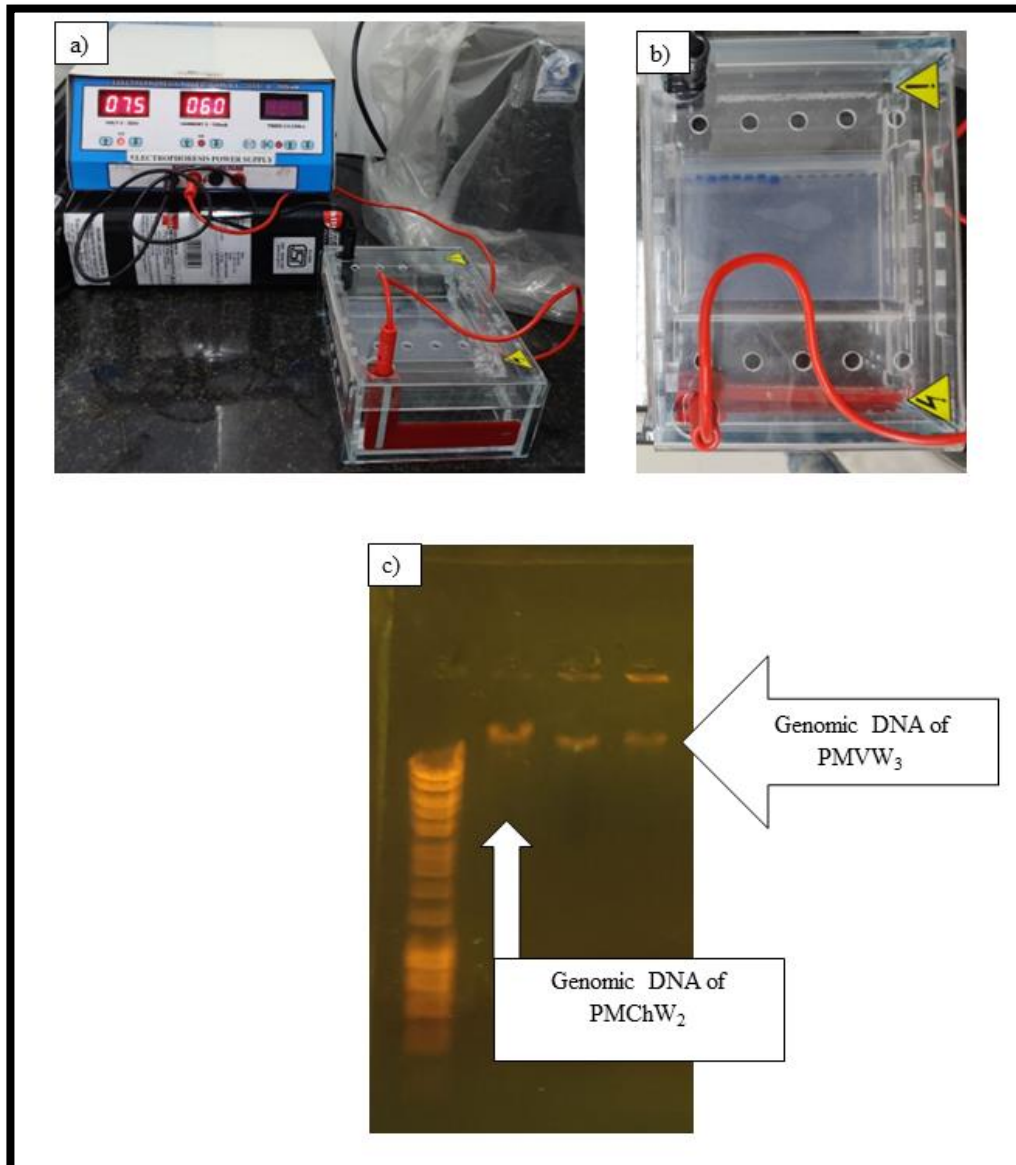


Fig. 4.24: (a) Electrophoresis unit, (b) Agarose gel and (c) Genomic DNA isolation of PMVW₃ and PMChW₂

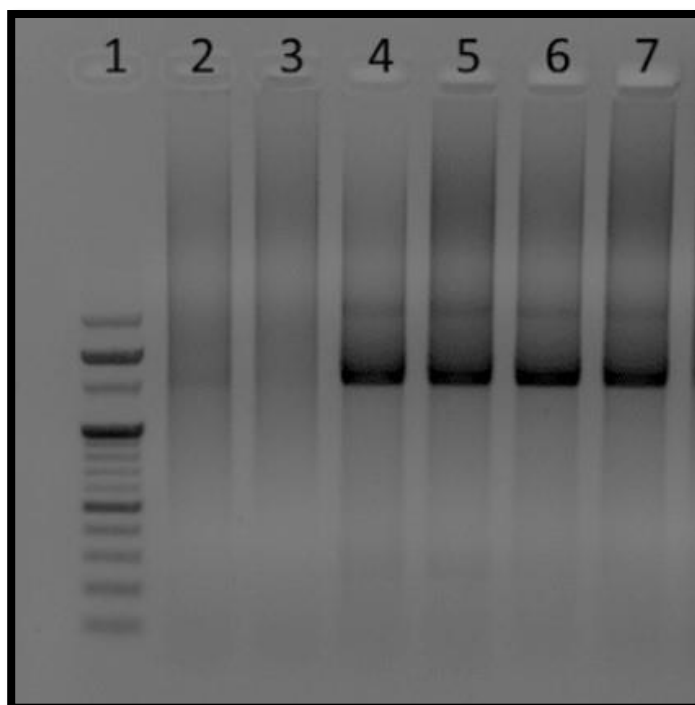


Fig. 4.25: 16S rRNA gene amplicon of PMVW₃ and PMChW₂

Lane 1: 100 bp DNA ladder; Lane 4-5: PMVW₃; Lane 6-7: PMChW₂

Similarly, BLAST analysis of the 16S rDNA sequence of PMChW₂ showed a match (99.71 %) to *Shewanella algae* and the sequence is now publicly available in Genbank with an accession number 24C110_520_3. The dendrogram analysis has revealed the phylogenetic relatedness with other species of *Shewanella* (Fig. 4.27).

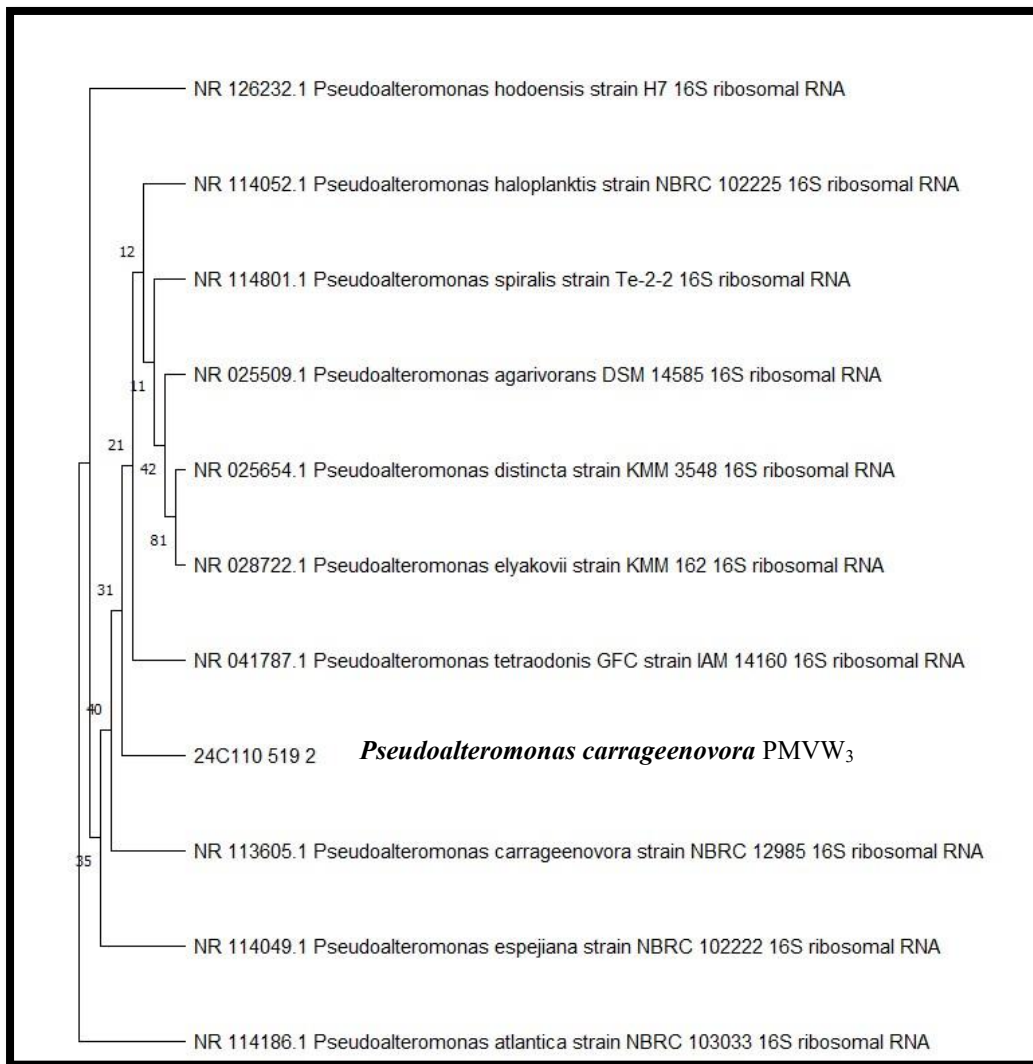


Fig. 4.26: Phylogenetic tree showing relatedness of *Pseudoalteromonas* sp. strain PMVW₃ (accession number: 24C110_519_2) with other strains of *Pseudoalteromonas*, constructed using neighbor-joining method (Tamura et al., 2013).

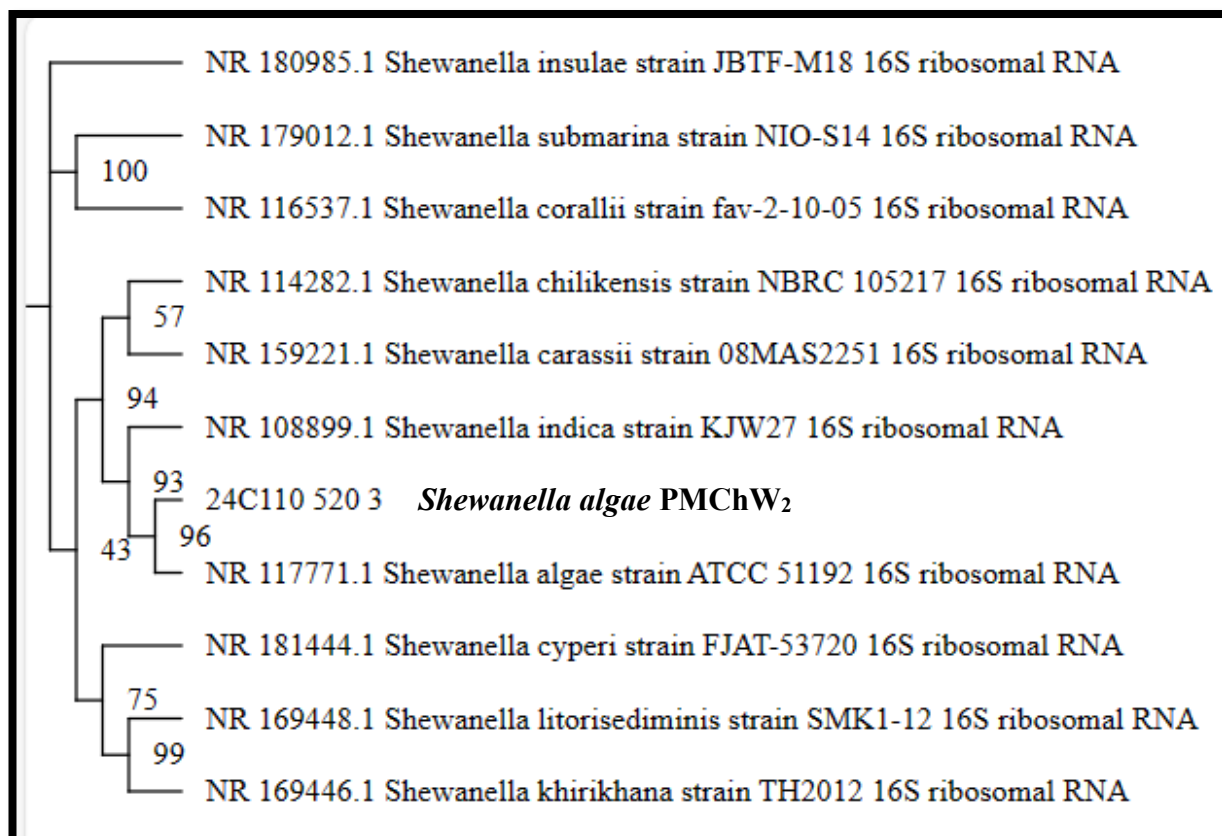


Fig. 4.27: Phylogenetic tree showing relatedness of *Shewanella* sp. strain PMChW₂ (accession number: 24C110_520_3) with other strains of *Shewanella*, constructed using neighbor-joining method (Tamura et al., 2013).

4.10 BIOSYNTHESIS OF SELENIUM NANOPARTICLES

4.10.1 To determine the ability of PMVW₃ and PMChW₂ strain to biosynthesize SeNPs during its growth phase and using cell-free culture supernatant

Selenite reduction to elemental Se using strains PMVW₃ and PMChW₂ was evident by the color change in the medium from yellow to brick red in a flask supplemented with 2 mM Na₂SeO₃. Whereas, the control flask without Na₂SeO₃ did not

show any brick red coloration (Fig. 4.28). The culture supernatant did not show any color change after 48 h of incubation thus indicating intracellular biosynthesis of SeNP. (Fig. 4.29).

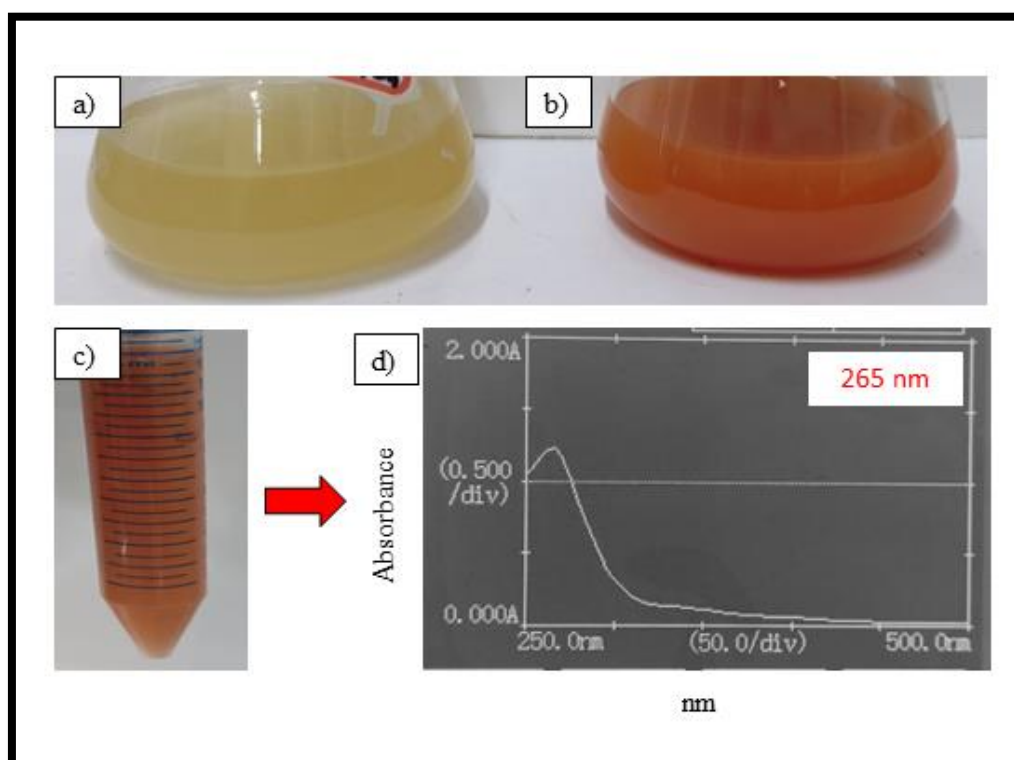


Fig. 4.28: Flasks showing (left to right) strain PMVW₃ grown in ZMB culture (a) containing 0 mM Na₂SeO₃ (b) with 2 mM Na₂SeO₃; (c) harvested SeNPs suspension (d) characteristic absorbance maxima of biogenic SeNPs using UV-Vis spectrophotometry.

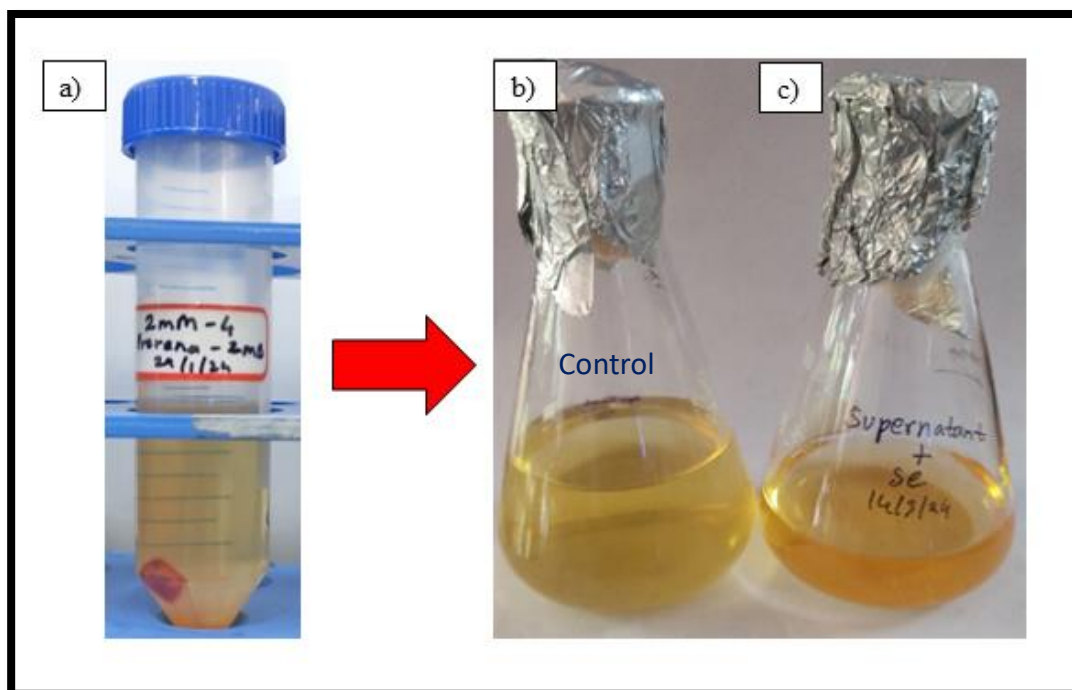


Fig. 4.29: (a) Colourless culture supernatant; Flasks showing (left to right) culture supernatant of PMVW₃ (b) containing 0 mM Na₂SeO₃ (c) with 2 mM Na₂SeO₃.

4.11 OPTIMIZATION OF PARAMETERS FOR OBTAINING (SeNPs)

Optimization of both the bacterial strains PMVW₃ and PMChW₂ in ZMB flasks with varying pH, Na₂SeO₃ concentration and temperature were studied. Bacterial strain PMChW₂ showed highest NP production at pH 7 (Fig. 4.30). Whereas bacterial strain PMVW₃ showed optimum pH, Na₂SeO₃ concentration and temperature for SeNPs biosynthesis was at pH 7, 2 mM Na₂SeO₃ concentration and 28 °C (temperature) respectively (Fig. 4.31 to 4.39).



Fig. 4.30: Bacterial strain PMChW₂ grown in ZMB flasks with varying pH 5-10.



Fig. 4.31: Bacterial strain PMVW₃ grown in ZMB flasks with varying pH 5-10

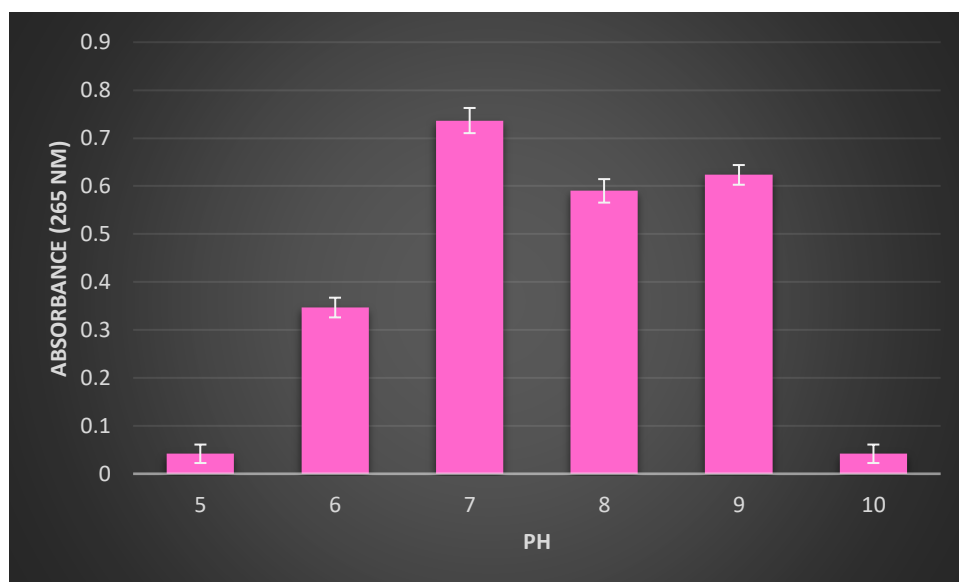


Fig. 4.32: Effect of SeNPs at different pH.

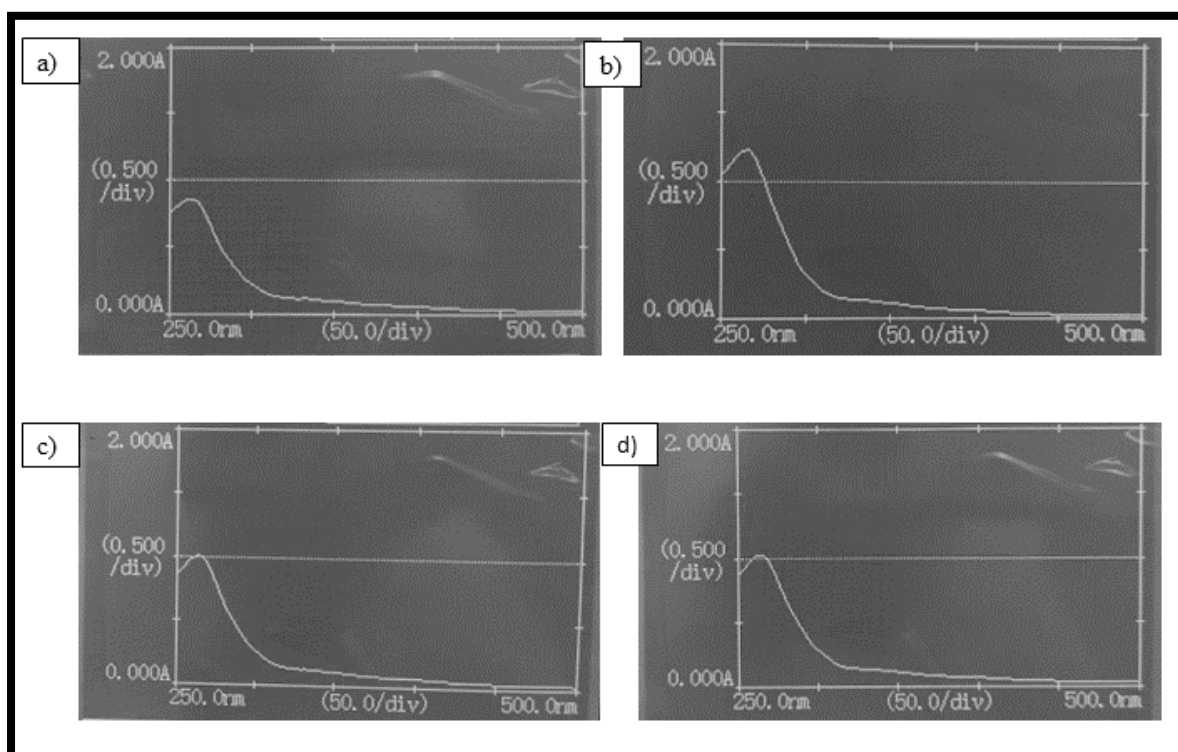


Fig. 4.33: UV-Vis absorption spectra of biosynthesized SeNPs at varying pH (a) 6, (b) 7, (c) 8 and (d) 9.



Fig. 4.34: Bacterial strain PMVW₃ grown in ZMB flasks with varying Na₂SeO₃ concentrations (1-6 mM)

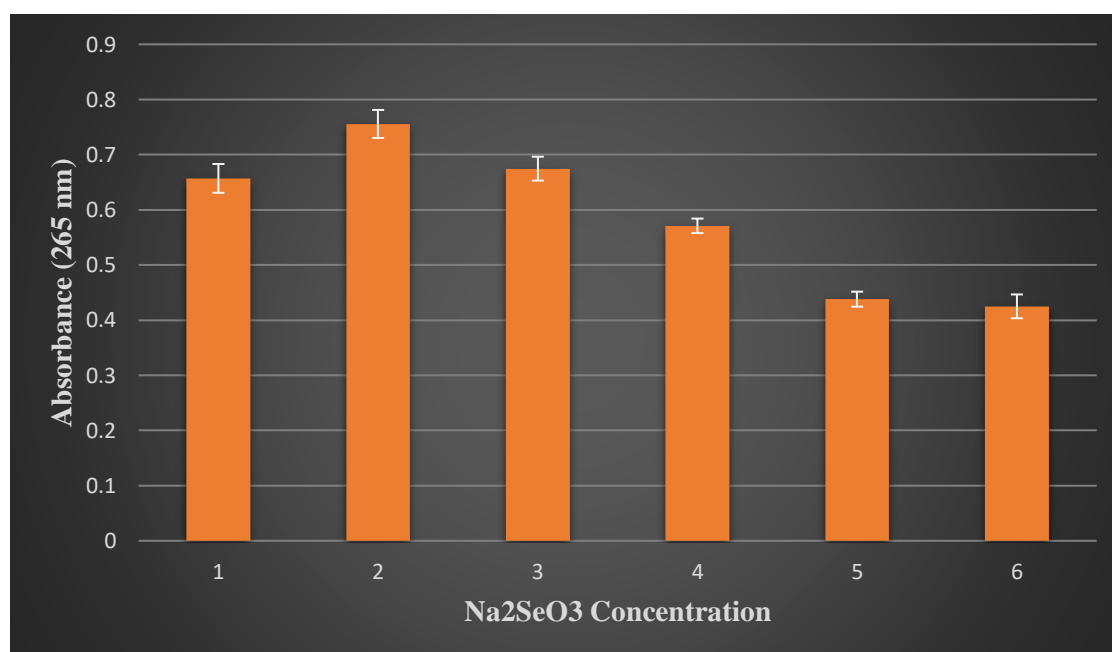


Fig. 4.35: Effect of SeNPs at different Na₂SeO₃ concentrations

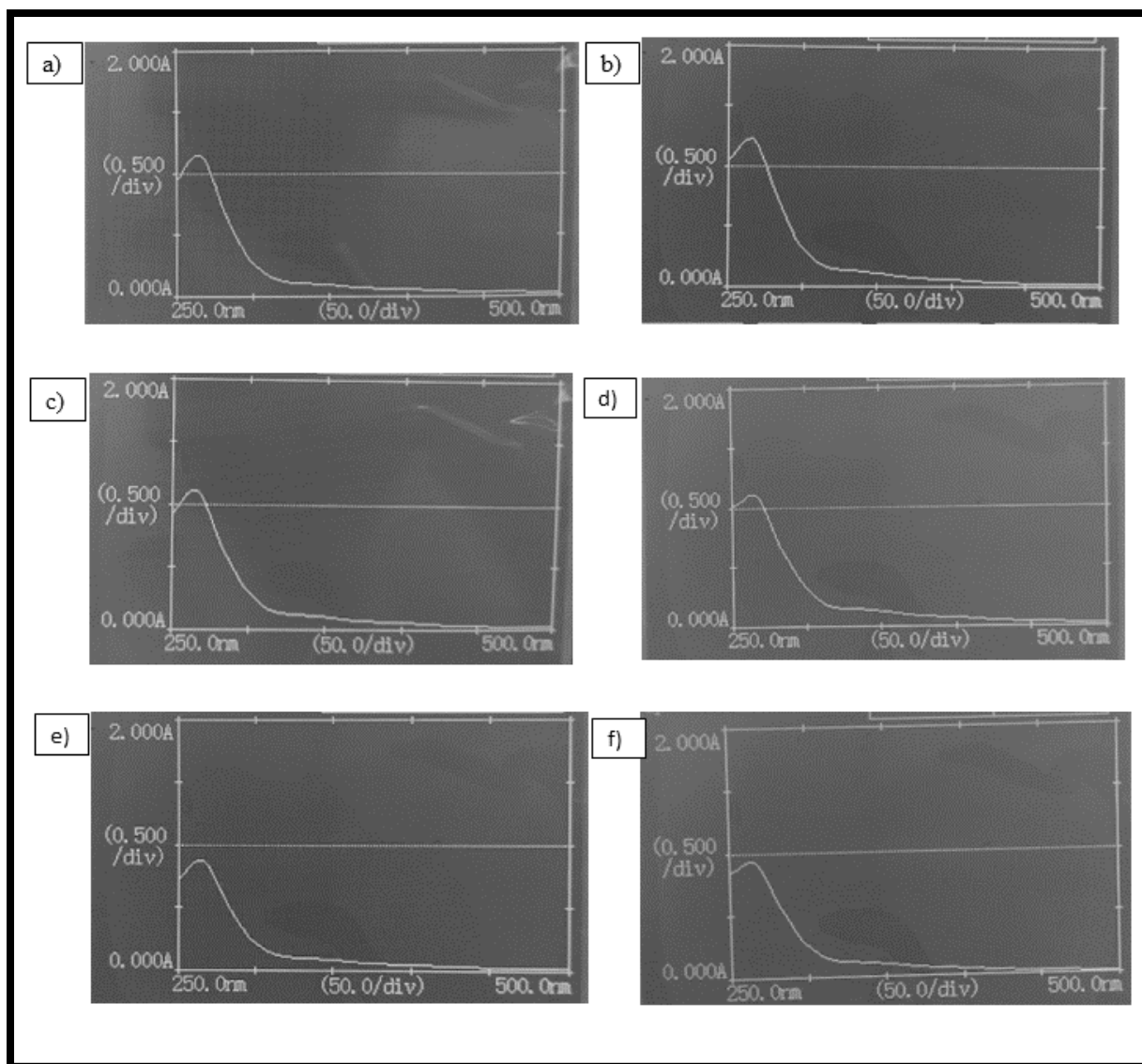


Fig. 4.36: UV-Vis absorption spectra of biosynthesized SeNPs in varying Na_2SeO_3 concentrations: (a) 1mM (b) 2mM, (c) 3mM, (d) 4mM, (e) 5mM and (f) 6mM



Fig. 4.37: Bacterial strain PMVW₃ grown in ZMB flasks with pH 7, 2 mM concentration and at different temperatures (28°C, 32°C and 37°C).

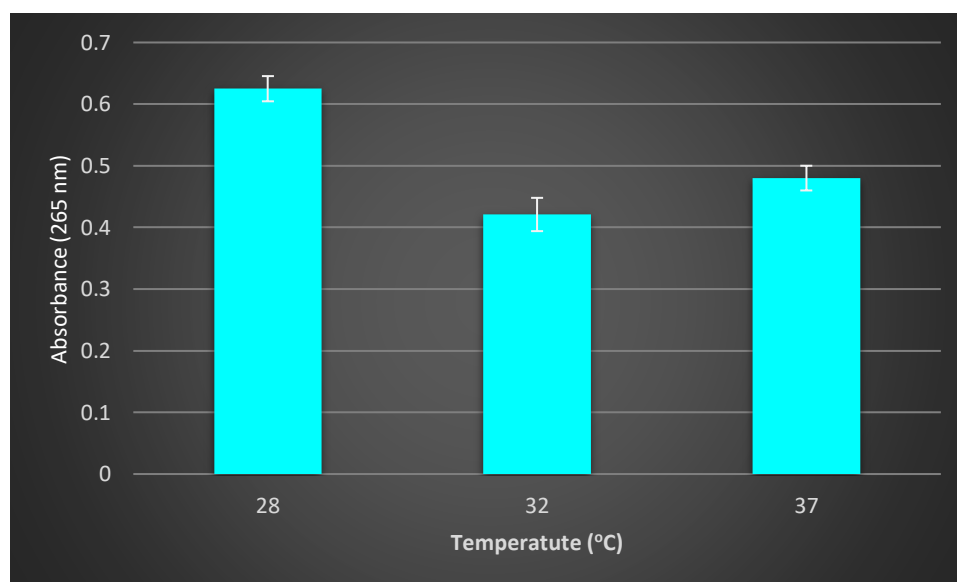


Fig. 4.38: Effect of SeNPs at different temperatures.

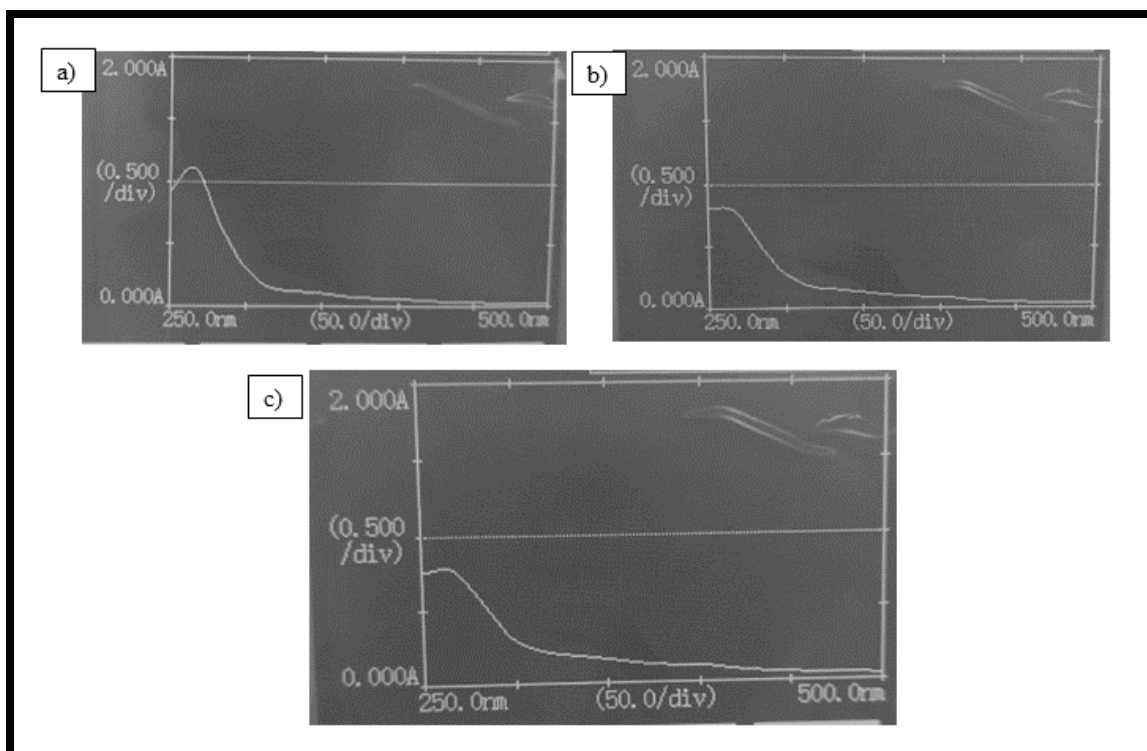


Fig. 4.39: UV-Vis absorption spectra of biosynthesized SeNPs grown at varying temperatures: (a) 28 °C (b) 32 °C and (c) 37 °C.

4.12 GROWTH BEHAVIOUR OF STRAIN PMVW₃ IN PRESENCE OF SeNPs

Time course study of SeNPs revealed that the biosynthesis was initiated during the early bacterial log phase (24 h) which was evident from the color change in the media and a distinct peak at 265 nm (Fig. 4.40). The lag phase was extended from zero to four hours followed by the log phase from four to 40th hours of bacterial growth. Following the stationary phase from forty to forty-four hours, a deceleration in growth became apparent. Subsequently, the onset of decline commenced after the forty-fourth hour of growth.

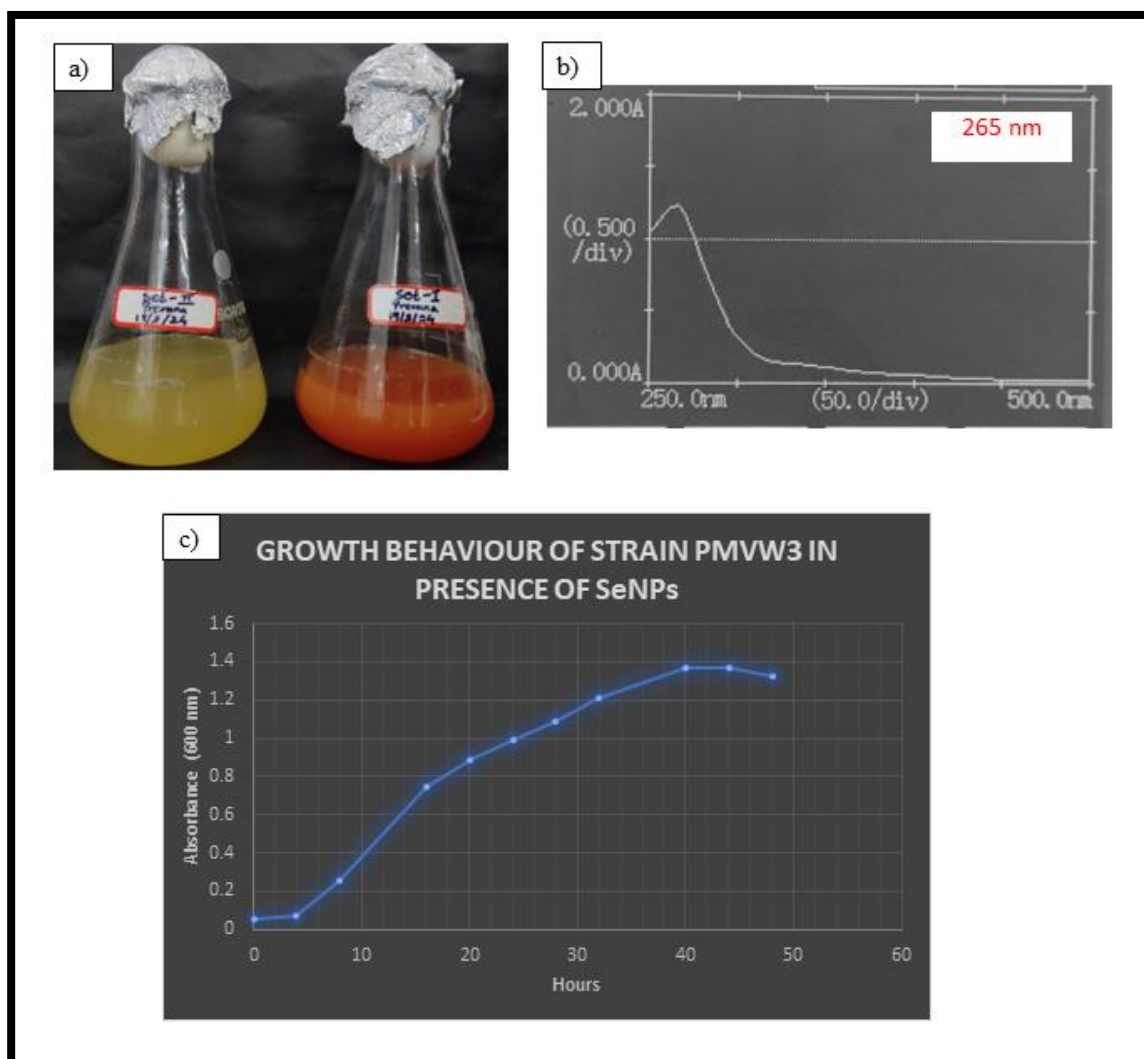


Fig. 4.40: Time course study of SeNPs biosynthesis under optimized conditions; (a) flask with strain PMVW₃ grown in ZMB with all optimized conditions, (b) UV-Vis absorption spectra acquired after 48 h and (c) Growth behavior of strain PMVW₃ in the presence of selenite.

4.13 HARVESTING OF BIOSYNTHEZED SENPs

The SeNPs were harvested from the bacterial strain PMVW₃ partially purified and made into powder using mortar and pestle and stored until used (Fig. 4.41).



Fig. 4.41: Harvested SeNP powder.

4.14 CHARACTERIZATION OF BIOGENIC SENPs

4.14.1 UV-Vis spectroscopic analysis

An absorbance peak at 265 nm was obtained from the brick red colloidal solution indicating the presence of SeNPs (Fig. 4.42).

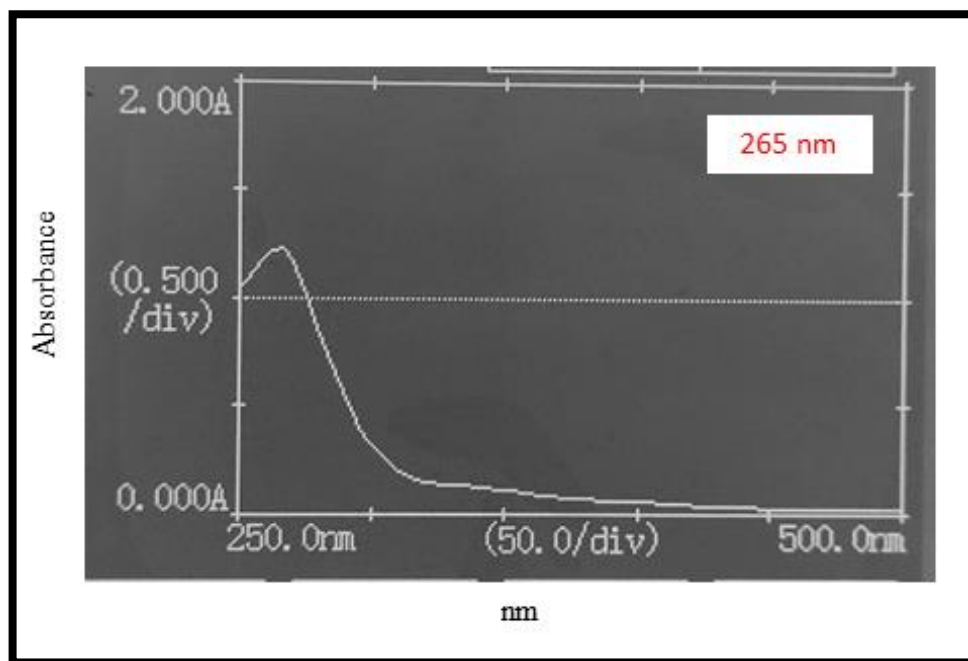


Fig. 4.42: Absorbance maxima for biosynthesized SeNPs at 265 nm.

4.14.2 Scanning electron microscopy (SEM) and Energy dispersive spectroscopy (EDX)

Interestingly SEM analysis SeNPs synthesized by *Shewanella* sp. strain PMChW₂ showed two morphotypes namely Spherical nanopshers and rod-shaped NPs were seen in many fields (Fig. 4.44). These were further assured with EDX that confirmed the presence of Se thus further strengthening the studies on SeNPs biosynthesis (Shirsat et al., 2015). In the case of *Pseudoalteromonas* sp. strain PMVW₃ presence of needle-shaped SeNPs was observed throughout and EDX analysis further affirmed SeNPs biosynthesis (Fig. 4.43).

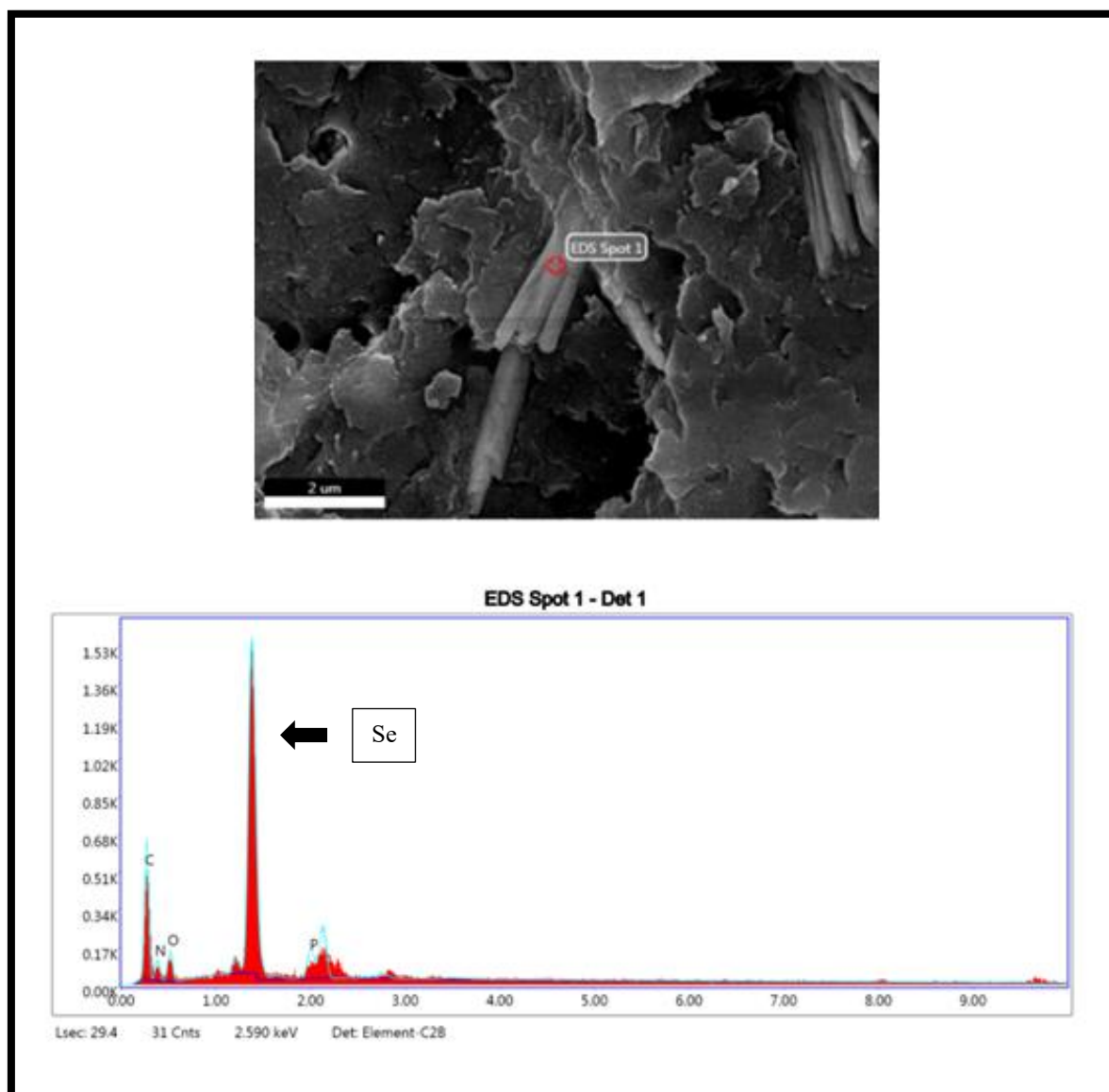


Fig. 4.43: SEM-EDX profile of biogenic SeNPs from strain PMVW₃.

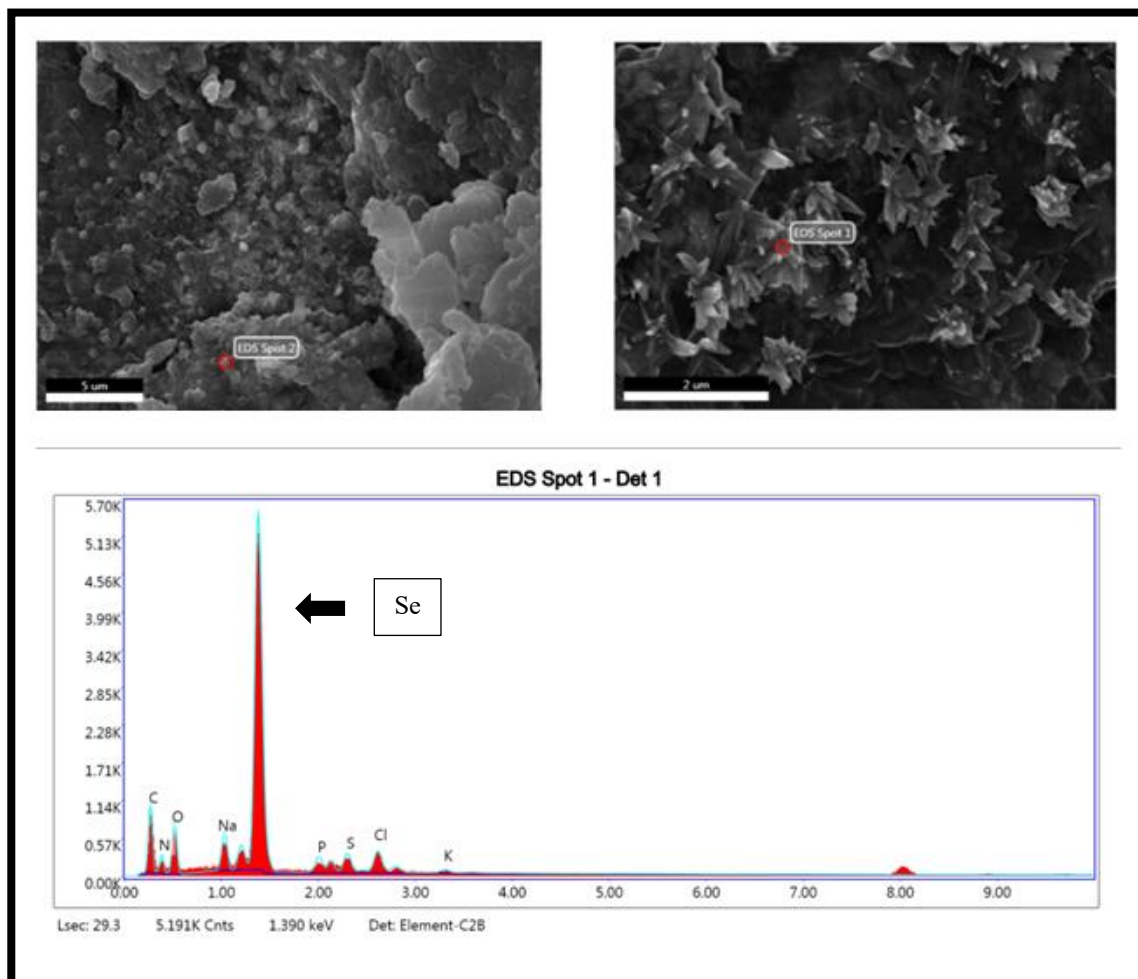


Fig. 4.44: SEM-EDX profile of biogenic SeNPS from strain PMChW₂

4.14.3 X-ray diffraction analysis (XRD)

X-ray data analysis using Origin 8 software showed certain peaks exclusively in the sample exposed to sodium selenite (Fig. 4.45). The peaks corresponding to the 2θ value for the bacterial cells exposed to selenite were 23.57, 29.77, and 43.75 which indicated the presence of elemental selenium. This further confirmed that selenite is being biotransformed to elemental selenium by the cells of *Pseudoalteromonas* sp. strain PMVW₃.

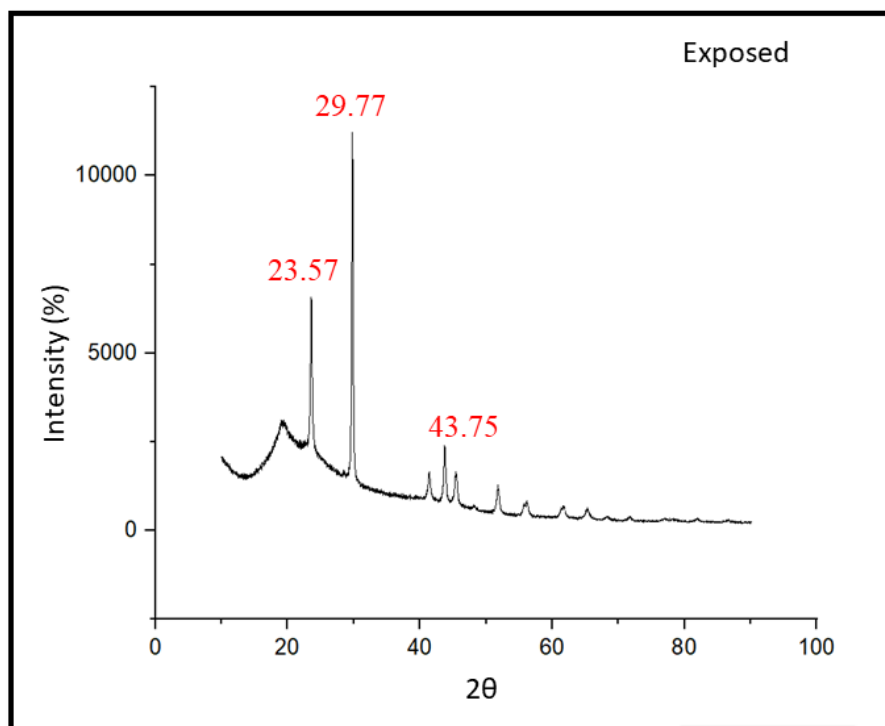


Fig. 4.45: X-ray diffraction profile of SeNPs

4.15 BIOMEDICAL APPLICATIONS OF BIOSYNTHEZED SELENIUM NANOPARTICLES

4.15.1 Antimicrobial activity SeNPs

The antimicrobial activity of biogenic SeNPs against *Staphylococcus aureus* (*S.aureus*), *Escherichia coli* (*E.coli*), *Salmonella* sp. and *Bacillus* sp. was studied by agar well diffusion method. No zone of inhibition with increasing concentrations of SeNPs was observed (Fig. 4.46), however, a zone of inhibition was observed in positive control (Ampicillin). (Fig. 4.47).

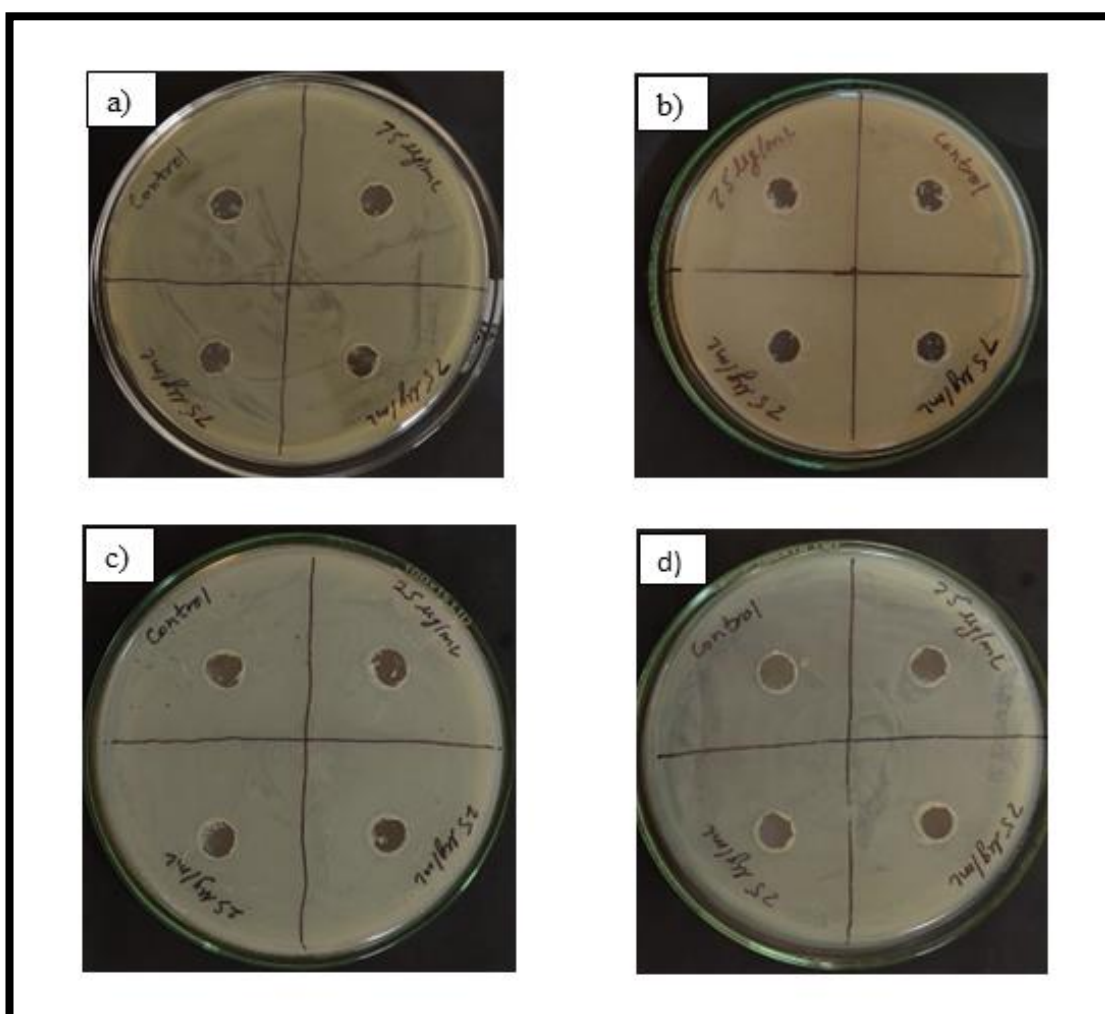


Fig. 4.46: The antimicrobial activity of biogenic SeNPs against (a) *E.coli*, (b) *Salmonella* sp., (c) *Bacillus* sp. and (d) *S.aureus* (with negative control).

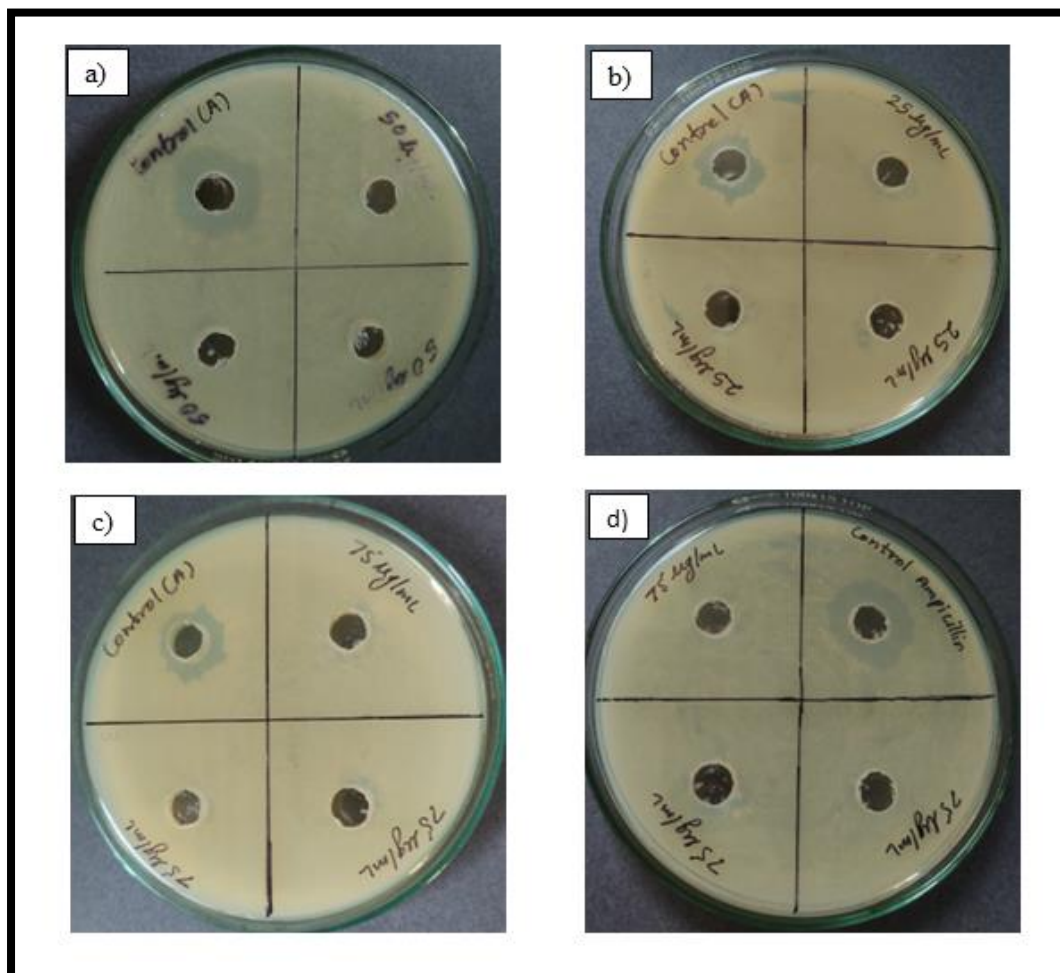


Fig. 4.47: The antimicrobial activity of biogenic SeNPs against (a) *E.coli*, (b) *Salmonella* sp., (c) *Bacillus* sp. and (d) *S.aureus* (with positive control).

4.15.2 Anti-biofilm potential of SeNPs

SeNPs demonstrated dose-dependent antibiofilm activity against Gram-positive and Gram-negative pathogens (Fig. 4.48 and 4.49). The highest antibiofilm activity was recorded against *E. coli* at 25 (18.69 %), 50 (71.58 %) and 75 (75.14 %) $\mu\text{g/mL}$. This was followed by *S.aureus* in which 30.78, 46.72 and 61.16% inhibition of biofilm was observed at 25, 50 and 75 $\mu\text{g/mL}$ of SeNPs. In *Bacillus* sp. 8.69, 16.05 and 27.86 % inhibition were observed and in *Salmonella* sp. inhibition recorded were 9.03, 15.77 and 20.22% at 25, 50 and 75 $\mu\text{g/mL}$ of SeNPs respectively.

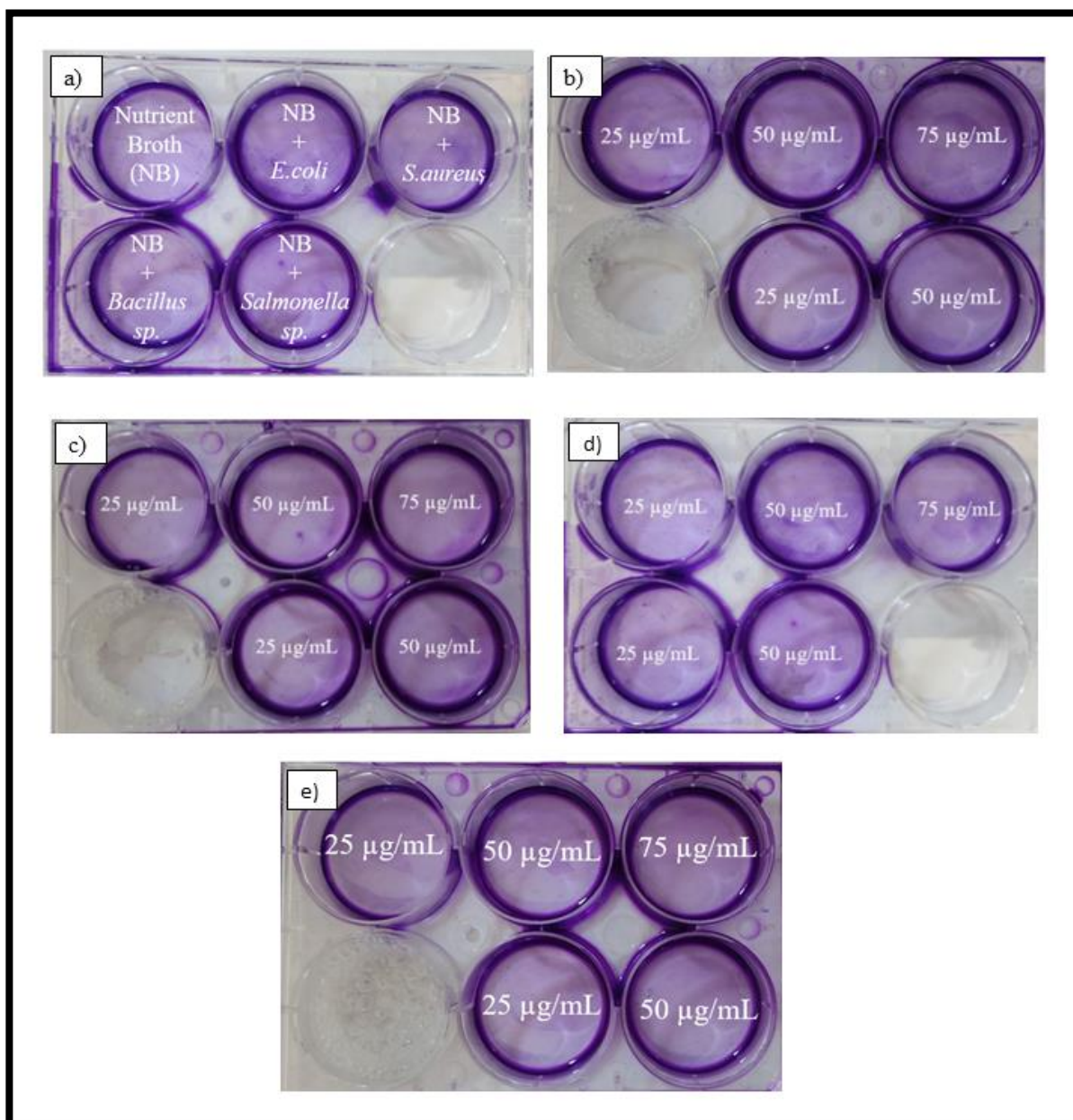


Fig. 4.48: Antibiofilm activity against human pathogens with increasing SeNPs concentrations; (a) control plate, (b) *E. coli*, (c) *S. aureus*, (d) *Bacillus sp.* and (e) *Salmonella sp.*

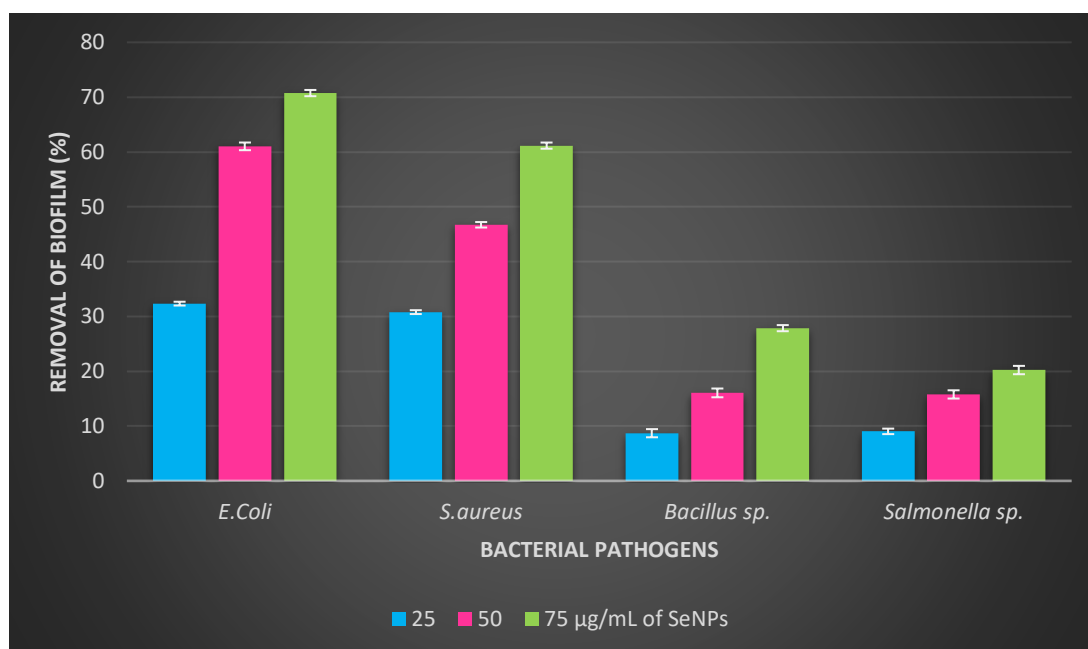


Fig. 4.49: Antibiofilm activity of the different SeNP concentrations against human pathogens.

4.15.3 Free-radical scavenging activity of SeNPs

Biogenic SeNPs exhibited excellent dose-dependent antioxidant potential. An increasing % radical scavenging activity with increasing concentrations of SeNPs was recorded. For instance, the percent scavenging activity at 25 µg/mL of biogenic SeNPs was found to be 60%, at 50 µg/mL showed 74%, 75 µg/mL showed 83%, while 92% was recorded at 100 µg/mL (Fig. 4.50).

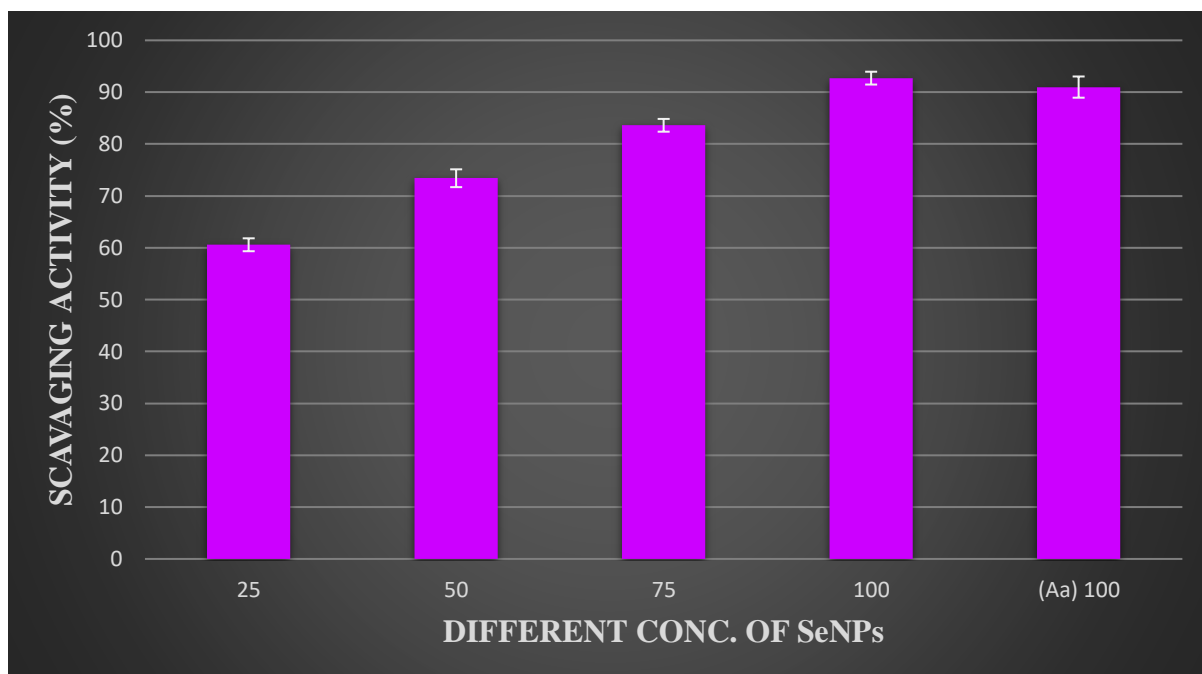


Fig. 4.50: Free radical scavenging activity of biogenic SeNPs (Ascorbic acid (Aa) served as a standard).

4.16 AGRICULTURAL APPLICATIONS

Since production of EPS by bacterial isolate PMChW₂ was confirmed by biochemical test. Therefore, a further in-depth study of EPS was performed (Fig 4.18).

4.16.1 Production of EPS

4.16.1.a Alcian blue staining for EPS-producing bacterial isolate

The secretion of an extracellular polymeric substance (EPS) was confirmed by performing the alcian blue staining for the bacterial isolate PMChW₂. Fig. 4.51 shows the generation of EPS which is stained by alcian blue dye. To confirm the same PMChW₂ EPS negative culture was stained and observed which did not show such results.

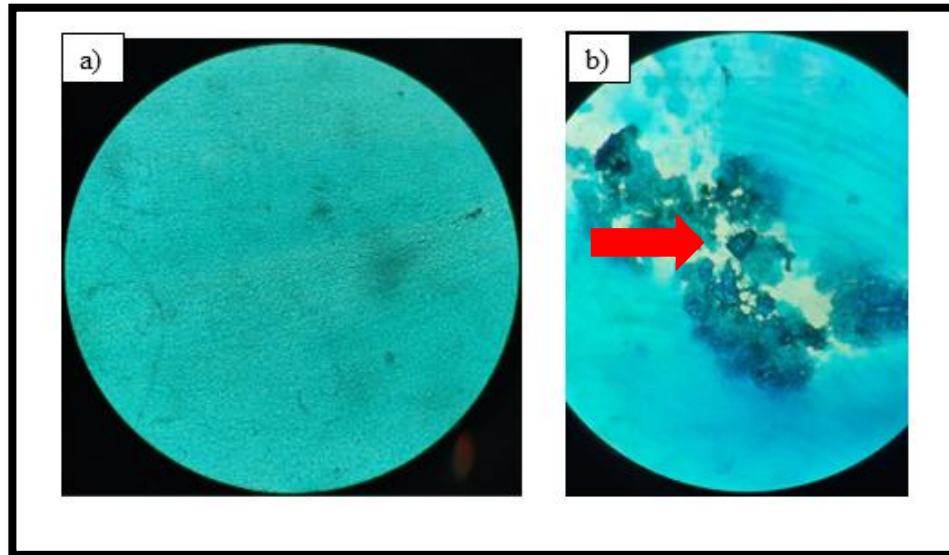


Fig. 4.51: Bacterial cells stained with alcian blue dye; (a) Control, (b) and showing EPS (arrows indicating EPS).

4.16.1.b Extracellular polymeric substance (EPS) production

The selected bacterial isolate PMChW₂ showed the formation of EPS precipitate, whereas no EPS was observed under control conditions (Fig. 4.52).

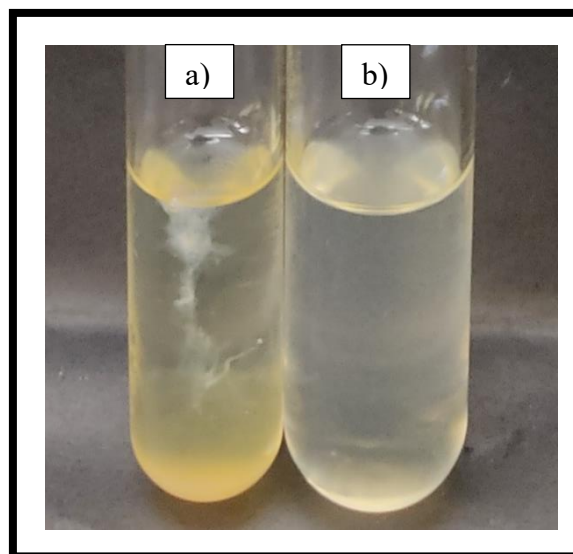


Fig 4.52: (a) Showing the formation of EPS precipitate and (b) Control

4.16.1.c EPS extraction

The EPS was extracted from the selected isolate PMChW₂ and the precipitate was dried and stored until used (Fig. 4.53). EPS-SeNPs solution was prepared (Fig. 4.54).

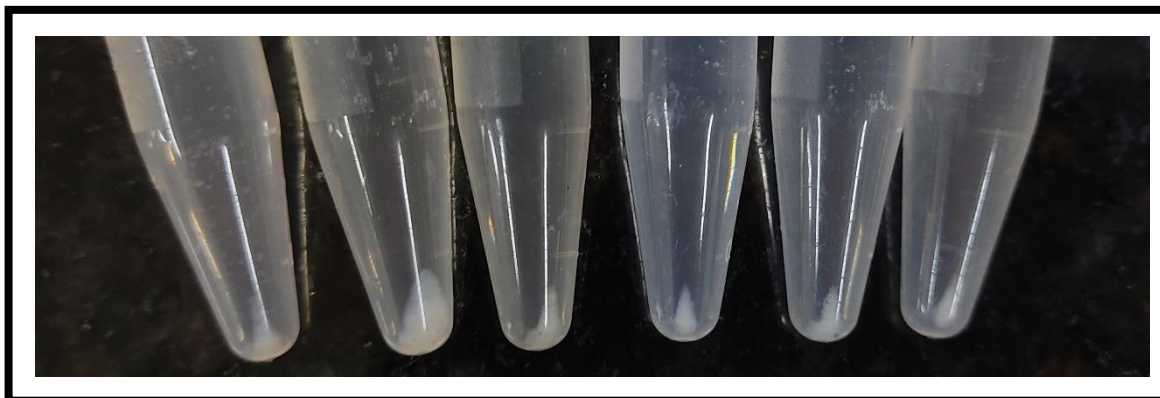


Fig. 4.53: Eppendorf tubes containing dried EPS precipitate.



Fig. 4.54: EPS-SeNPs solution.

4.16.2 Effect of SeNPs and SeNPs-EPS on seed priming

4.16.2.a Determination of final germination percentage, root and shoot length, and seedling wet biomass

The % germination was found to be 90% for all the treatments. SeNPs supplemented seeds (var. *Jaya* and *Vigna radiata* L.) via priming alone, enhanced the root lengths, shoot length and biomass accumulation.

For var. *Jaya*

In the case of root lengths of var. *Jaya*, in the presence of (25, 50, 75 and 100 $\mu\text{g/mL}$) of SeNPs alone, the root lengths were recorded to be 1.7, 1.8, 2.1 and 1 cm respectively after the 10th day of incubation (Fig. 4.55). Whereas, in control (seeds with DW) the root length was found to be 2.1 cm. The root lengths of the seeds under EPS-SeNPs (25 and 75 $\mu\text{g/mL}$) were 3 and 3.2 cm respectively. Selenite (1 mg/L) primed seeds also showed root length (1.2 cm) as compared to control (2.1 cm). Additionally, seeds primed with EPS (1 mg/L) showed an increase of 2.3 cm but were not as effective as compared to the seeds treated with SeNPs alone. Figure 4.58 depicts the comparative growth of rice seedlings under various treatments.

In the case of shoot lengths, a similar pattern was observed such as in the presence of (25, 50, 75 and 100 $\mu\text{g/mL}$) of SeNPs alone, the shoot lengths were recorded to be 3, 3.1, 3.5 and 4 cm respectively after 10th day of incubation (Fig. 4.56). Whereas, in control (seeds with DW) the shoot length was found to be 3.4 cm. In the presence of 1 mg/L Selenite, the shoot length was 3 cm. While seeds treated with EPS-SeNPs (25 and 75 $\mu\text{g/mL}$) exhibited shoot lengths of 4.5 and 5 cm respectively. Additionally, seeds

primed with EPS (1 mg/L) showed an increase of 4.2 cm but were not as effective as SeNPs. Figure 4.58 depicts the comparative growth of rice seedlings under various treatments.

Similar observations were also recorded in the case of wet biomass where 52.1 mg was recorded in case of control seeds while SeNPs primed of (25, 50, 75 and 100 $\mu\text{g}/\text{mL}$) seeds showed 45.5, 46.3, 56.2 and 60.3 mg of biomass respectively after 10th day of incubation (Fig. 4.57). While biomass in EPS-SeNPs seeds (25 and 75 $\mu\text{g}/\text{mL}$) was found to be 58.7 and 62.1 mg. Selenite (1 mg/L) primed seeds also showed a biomass of 43.3 mg. Additionally, seeds primed with EPS (1 mg/L) showed a biomass of 50.2 mg.

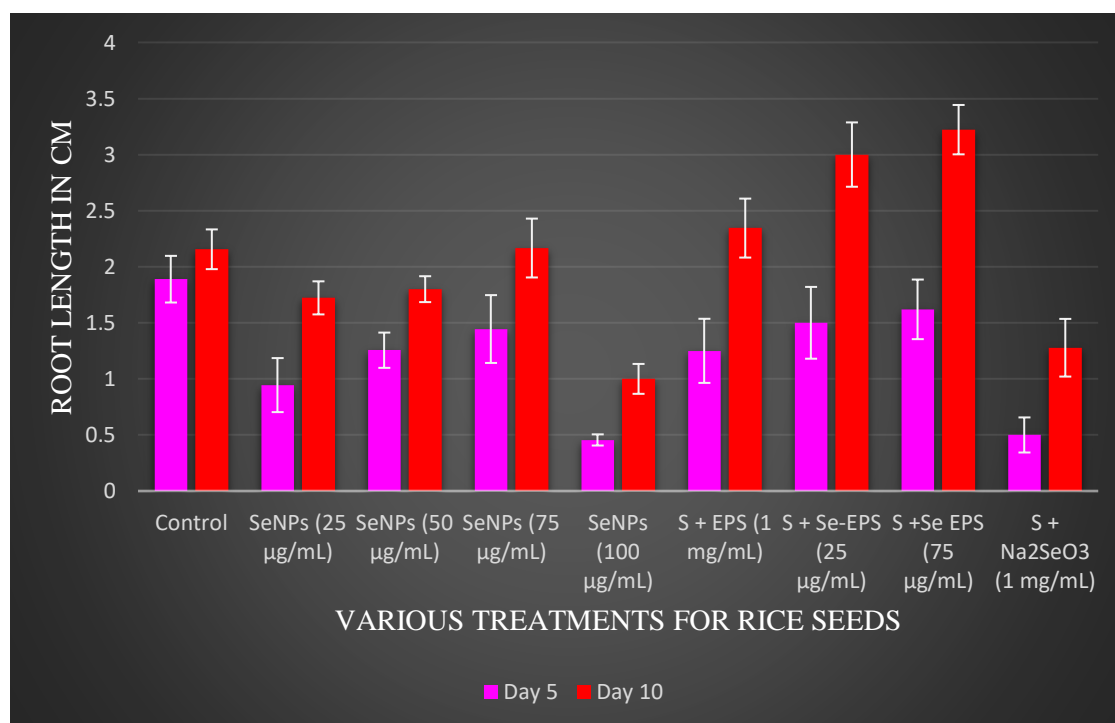


Fig. 4.55: Root length under various treatments after 5 and 10 days of germination.

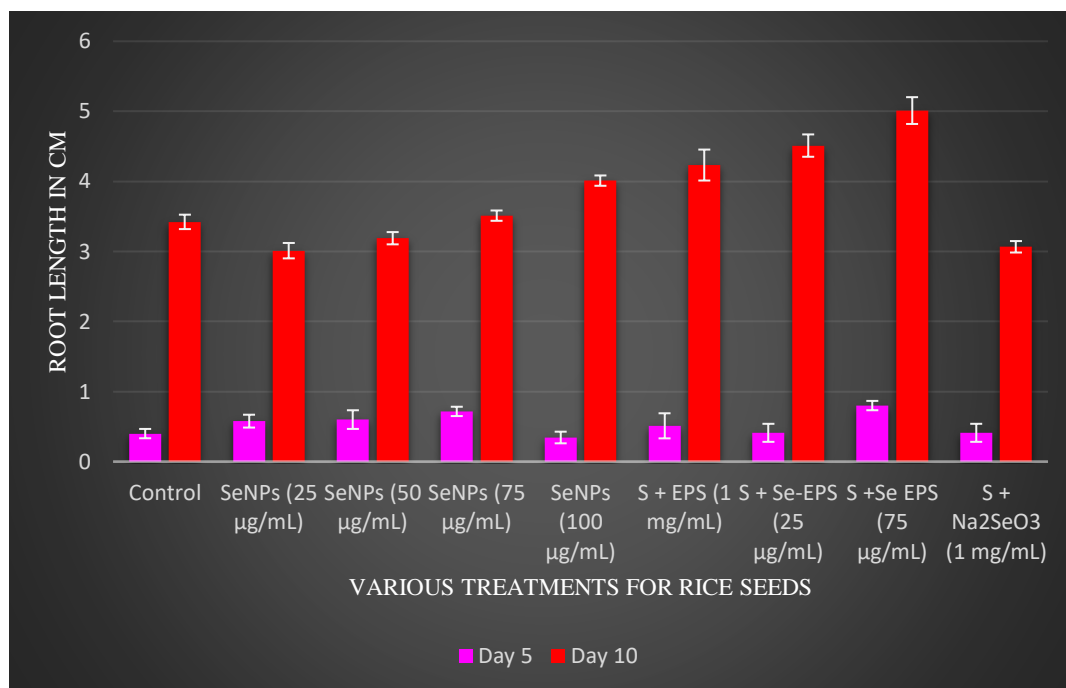


Fig. 4.56: Shoot length under various treatments after 5 and 10 days of germination.

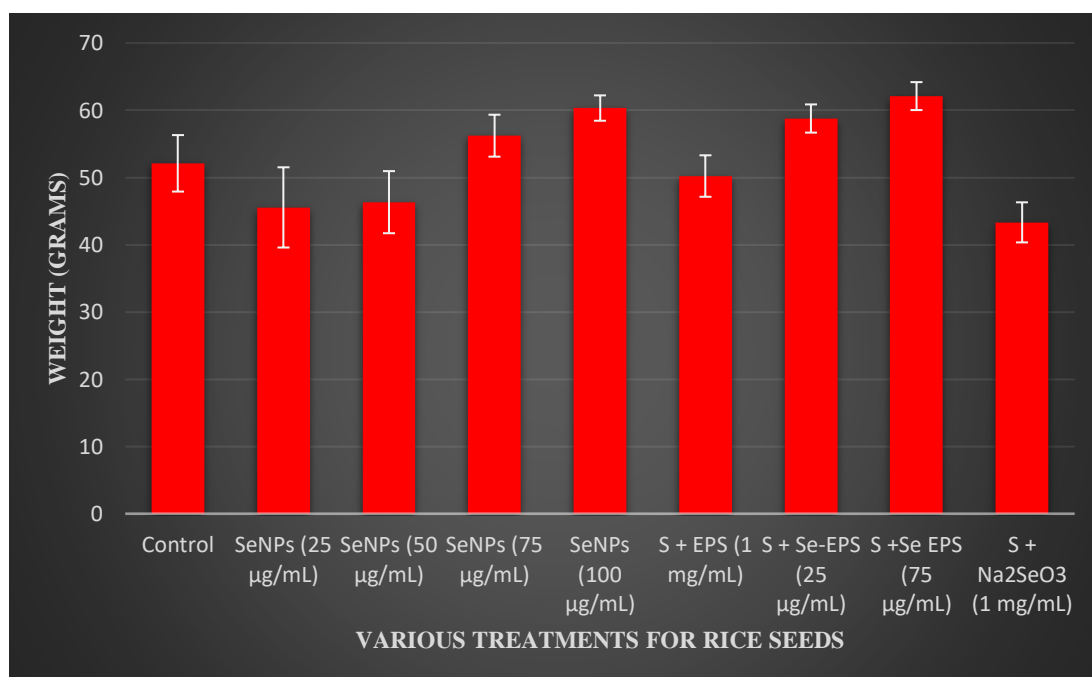


Fig. 4.57: Wet weight under various treatments after 10 days of germination.



Fig. 4.58: Rice seeds under various treatments after (a) 5th and (b) 10th day of germination.

For *Vigna radiata* L.

The root lengths of *Vigna radiata* L., in the presence of SeNPs (25, 50, 75 and 100 µg/mL) alone, were found to be 3, 2, 2.5 and 1 cm respectively after the 10th day of incubation (Fig. 4.59). Whereas, in control (seeds with distilled water) the root length was found to be 2.5 cm. The root lengths of the seeds under EPS-SeNPs (25 and 75 µg/mL) were found to be 5 and 4 cm respectively. Selenite (1 mg/L) primed seeds exhibited a root length of (1 cm). Additionally, the root length recorded for seeds primed with EPS (1 mg/L) was 1.5 cm. Figure 4.62 depicts the comparative growth of rice seedlings under various treatments.

In the case of shoot lengths, a similar pattern was observed for instance, in the presence of (25, 50, 75 and 100 µg/mL) of SeNPs alone, the shoot lengths recorded

were 6, 6.5, 8 and 1 cm respectively after 10th day of incubation (Fig. 4.60). Whereas, in control (seeds with DW) the shoot length was found to be 5 cm. In the presence of 1 mg/L Selenite, the shoot length was e 5 cm. While the shoot lengths of the seeds under EPS-SeNPs (25 and 75 µg/mL) were found to be 6 and 7 cm. Additionally, seeds primed with EPS (1 mg/L) showed an increase of 5 cm. Figure 4.62 depicts the comparative growth of rice seedlings under various treatments.

Similar observations were also recorded for wet biomass where 102 mg was recorded in control seeds while SeNPs primed (25, 50, 75 and 100 µg/mL) seeds showed 134, 142, 181 and 60 mg of biomass respectively (Fig. 4.61). Biomass of seeds treated with EPS-SeNPs (25 and 75 µg/mL) was found to be 145 and 178 mg respectively. Selenite (1 mg/L) primed seeds also exhibited a biomass of 134.6 mg. Additionally, seeds primed with EPS (1 mg/L) exhibited a biomass of 134 mg.

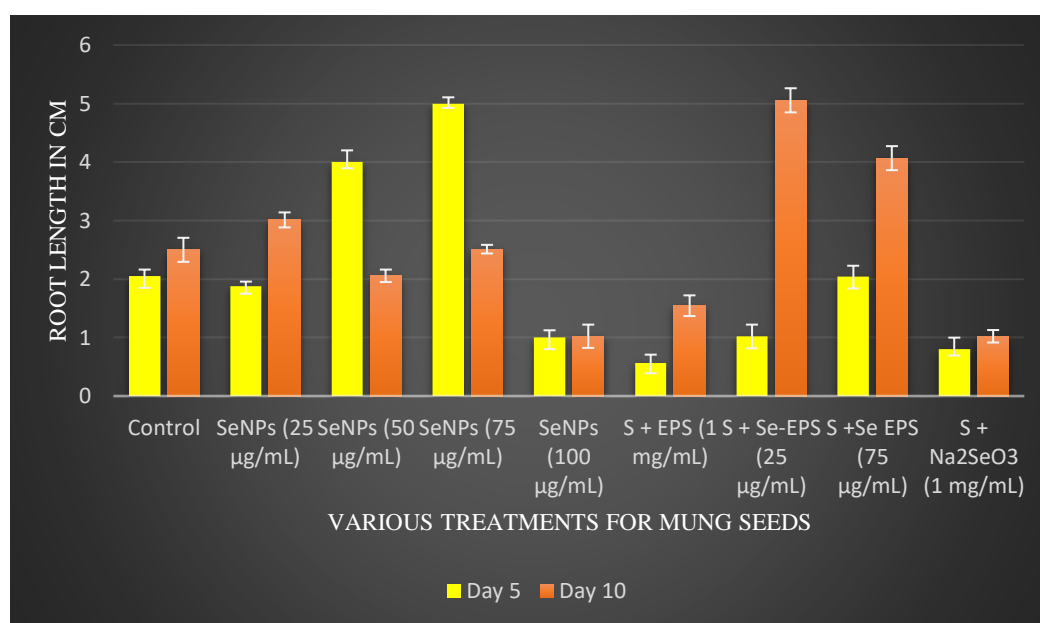


Fig. 4.59: Root length under various treatments after 5 and 10 days of germination.

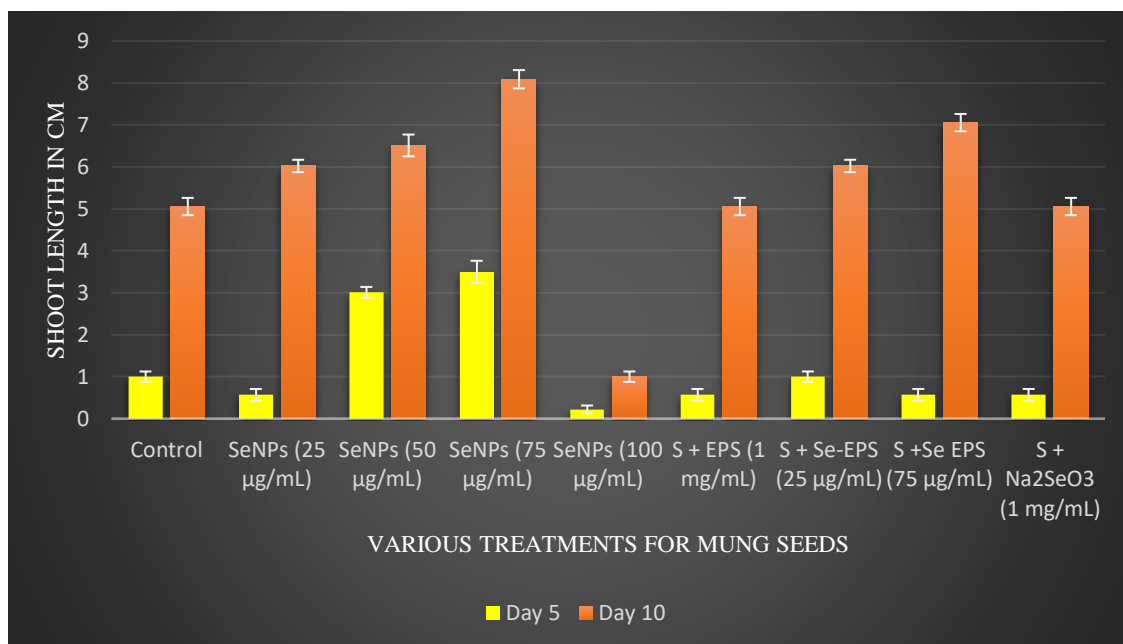


Fig. 4.60: Shoot length under various treatments after 5 and 10 days of germination.

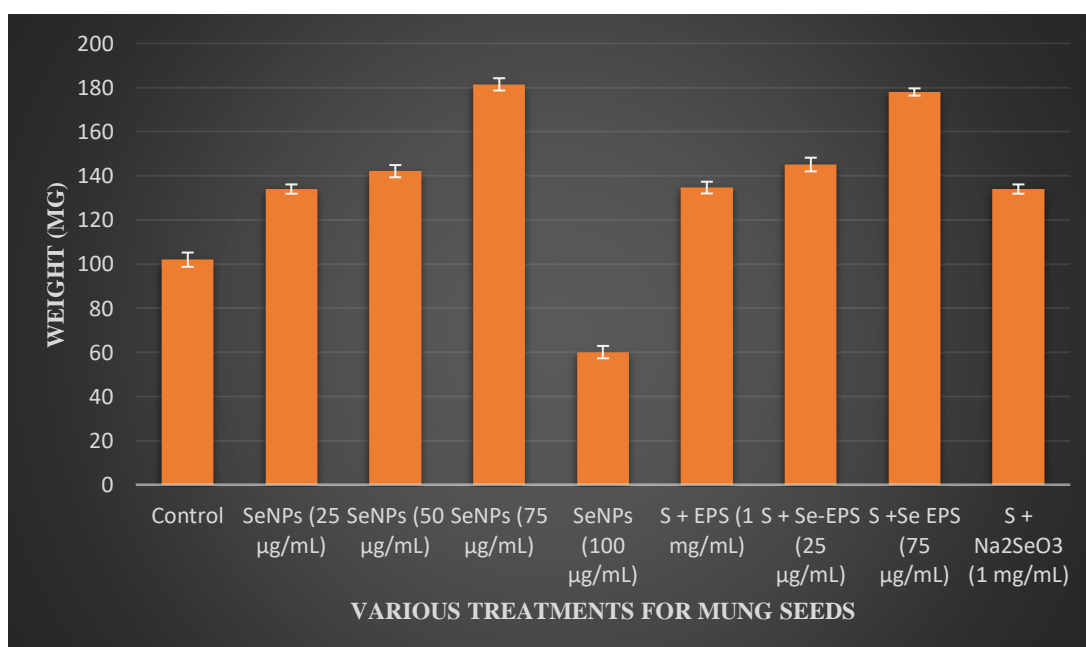


Fig. 4.61: Wet weight under various treatments after 10 days of germination.

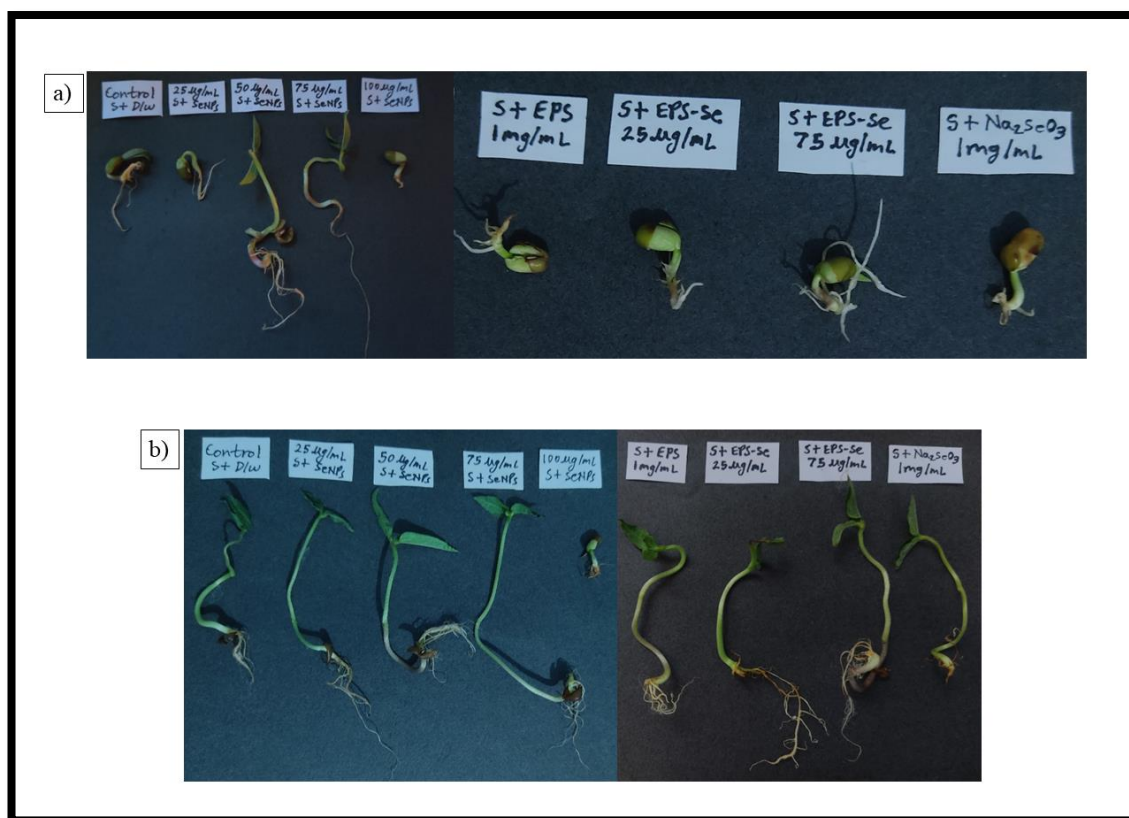


Fig. 4.62: Mung beans under various treatments after (a) the 5th and (b) 10th day of germination

CHAPTER 5

DISCUSSION

AND

CONCLUSION

5.1: DISCUSSION

The marine environment is a unique habitat characterized by extreme conditions and possesses a rich microbial diversity. However, these marine sites are also considered to be heavily contaminated with various metals and metalloids (Ansari et al., 2004). The coastal part of Goa viz. (Chorao Island and Vaguinim beach) and especially Mandovi and Zuary estuaries are mainly flanked by various electronic and other industries. Due to heavy anthropogenic activities, these habitats are polluted by contaminants that are disseminated and deposited in the water and sediments. Moreover, selenite is used in various agro, electrical and electronics industries (Kumar and Prasad 2021). Extensive shipping and other transport activities in marine habitats have led to widespread metal or metalloid pollution (Mishra et al., 2023). A total of 9 sampling sites were selected for the collection of water and sediment samples from different marine and estuarine ecosystems in Goa, India based on earlier reports (Samant et al., 2018; Mujawar et al., 2018; Vaigankar et al., 2022).

Marine microorganisms have developed unique adaptive mechanisms to reduce selenite/selenate into its elemental Se form (Ike et al., 2000; Li et al., 2014). The appearance of a reddish color in enrichment broth after 48 h indicated the conversion of soluble selenite (Na_2SeO_3) into red-colored elemental selenium (Se^0) when compared to the control flask which failed to show a color change when incubated under the same conditions. Morphologically 25 dissimilar selenite-reducing bacterial isolates did not show any brick-red pigmentation upon streaking on ZMA plates without incorporation of Na_2SeO_3 which confirmed that the brick-red coloration was not due to bacterial pigment production but due to selenite reduction and hence selected for further study.

Selenite is a toxic compound, that can be tolerated by microorganisms like bacteria at high concentrations without causing any adverse effects on their cellular metabolism (Chen,

2012; Morris and Crane, 2013). Out of 25 selenite-reducing bacterial isolates, 5 bacterial isolates showed the highest MTC (360 mM) in Zobell Marine Agar (ZMA), whereas, the bacterial strain isolated from Vaiguinim beach designated as PMVW₃ exhibited a MIC of 380 mM thus, was selected for further studies. This study reported a MIC that is highest as compared to previous studies on selenite-resistant marine bacterial isolates although there are very few reports available. For instance, *Citrobacter freundii* isolated from the Mandovi estuary in Goa, India showed MIC of 60 mM for selenite which is 6.3 times lower than the present study (Samant et al., 2016). Moreover, *Halomonas* sp. isolated from the Mandovi estuary of Goa showed MIC of 101 mM to Na₂SeO₃ in a liquid medium with MTC of 100 mM which is 3.8 times lower than the present study (Vaigankar. 2020). Additionally, strain PMChW₂ with MIC 70 mM was also selected since it could form EPS. Studies in the past have already been carried out on the importance of EPS in aiding SeNPs synthesis thus, opening a new arena from an application point of view. The above findings are highly substantial since the bacterial strains PMVW₃ and PMChW₂ could be ideal candidates for bioremediation of selenite-contaminated sites.

Biochemical tests are used to identify bacterial species by differentiating them based on biochemical activities. The study identified two marine bacterial isolates, PMVW₃ and PMChW₂, which were found to be selenite-resistant and EPS-producing, respectively. PMVW₃ was oxidase positive and had catalase nitrate reductase enzymes, while PMChW₂ was long rods and fermentative.

A true antibiotic is an antimicrobial chemical produced by microorganisms against other microorganisms (Kirby-Bauer). The antibiotic sensitivity of selected selenite-resistant bacterial isolates PMVW₃ and PMChW₂ showed that both isolates were susceptible to all the antibiotics tested namely Streptomycin (10µg), Penicillin - G (10 units), Chloramphenicol(30µg) and Tetracycline (30µg). It has been reported that the genes of

antibiotic resistance and metal/metalloid resistance are closely located. It's a widely recognized fact that bacteria often carry genes for resistance to heavy metals, metalloids, and various antibiotics, either on their chromosomes or plasmids (Silver and Phung, 1996; Lupo et al., 2012). This phenomenon was also observed in *Escherichia coli* Cont-1, which exhibited resistance to multiple antibiotics as well as heavy metals and metalloids (Mohapatra and Sar, 2018).

The analysis of the 16S rRNA gene sequence of the selected bacterial strains revealed that the strain PMVW₃ belongs to *Pseudoalteromonas carrageenovora* and strain PMChW₂ belongs to *Shewanella algae*. Till now only two reports on selenite reduction by the genus *Pseudoalteromonas* have been reported. Moreover, this is the first detailed report on selenite reduction by *Pseudoalteromonas* sp. isolated from the Vaiguinim Beach or marine habitats of Goa, India showing the highest level of selenite resistance. Thus, making it a remarkable candidate for selenite bioremediation in varying habitats from estuaries to saline lakes and oceans. Bacteria belonging to the genus *Shewanella* sp. are capable of anaerobic respiration using several electron acceptors. A study by Li et al., (2014) reported selenite reduction to Se⁰ carried out through fumarate reductase (FccA) by *Shewanella oneidensis* and this process is carried out in periplasm.

SEM analysis revealed that the cells of strain PMVW₃ and PMChW₂ are well isolated. However, upon exposure to 2 mM selenite, the cells displayed a tendency to aggregate, forming clusters likely as a defence mechanism against the metalloids' toxicity. Additionally, elongation of cells was also prominent in exposed cells. This aggregation and elongation potentially reduces the total surface area of the cells relative to their volume, serving as an effective strategy for mitigating the toxic effects. This phenomenon of bacteria responding to elevated concentrations of toxic metals and metalloids to alleviate toxicity is well-documented (Sharma

et al., 2017; Mujawar et al., 2019). Interestingly, EDX analysis revealed the absence of any adsorption peak of selenium on the bacterial cell surface indicating internalization (Fig 4.22).

The appearance of a brick-red coloration stands as a robust indication of selenium nanoparticles (SeNPs) synthesis, attributed to the surface plasmon resonance effect (Srivastava and Mukhopadhyay, 2013). Additionally, the culture supernatant did not show any color change after 48 h of incubation thus indicating intracellular biosynthesis of SeNPs. This report is one of its kind demonstrating the intracellular biosynthesis of SeNPs by *Pseudoalteromonas sp.* and *Shewanella sp.*

Bacterial cell pellets of both the cells grown in the presence and absence of selenite when analysed through EDX analysis revealed a distinct peak of Se which was absent in the control cell's pellet. This strongly indicates the biotransformation of selenite within strains PMVW₃ and PMChW₂ into elemental selenium.

Minute SeNPs undergo subsequent growth through particle aggregation, facilitated by the Ostwald ripening phenomenon (Huang et al., 2007). Hence, optimization of the biosynthesis protocol is imperative to attain optimal yields. The optimum pH, temperature and Na₂SeO₃ for SeNPs biosynthesis by *Pseudoalteromonas sp.* strain PMVW₃ was found to be 7, 25 °C, and 4 mM respectively. The color intensity of SeNPs increased with increasing Na₂SeO₃. It was interesting to note that the estuarine strain PMVW₃ could synthesize SeNPs at broad temperatures (28 to 37 °C) and pH (6 to 9). Although MIC for the strain PMVW₃ was recorded to be 380 the nanoparticle synthesis was not carried at such a high concentration since it is a well-known fact that nanoparticles at high salt concentrations tend to aggregate forming particles with larger diameters which is undesirable (Shrestha et al., 2020). These reaction conditions including various experimental factors viz. pH, temperature and metalloid

concentrations of the culture medium improve the chemical composition, shape, size distribution of NPs and allow maximum fabrication (Klaus et al., 1999).

An absorbance peak at 265 nm due to surface plasmon resonance was obtained from the brick red colloidal solution indicating the presence of SeNPs. Similar findings conferring the biosynthesis of SeNPs have been published previously (Fesharaki et al., 2010; Srivastava et al., 2015; Vaigankar. 2020). Time course study of SeNPs by *Pseudoalteromonas sp.* strain PMVW₃ revealed that the biosynthesis was initiated during the early bacterial log phase (24 h) which was evident from the color change in the media and a distinct peak at 265 nm. A similar synthesis pattern was also reported in *Bacillus sp.* synthesized SeNPs after 14 h of incubation (Forootanfar et al., 2015). Additionally, in another study by Vaigankar et al., (2022) time course study of SeNPs revealed that the biosynthesis was initiated during the early bacterial log phase (4 h). Furthermore, a study by Keskin et al., (2020) reported that *Lysinibacillus sp.* synthesized SeNPs after 24 h of incubation same as my strain PMVW₃. It was noticed that *Shewanella sp.* strain PMChW₂ synthesized SeNPs at pH 7 and 2 mM of selenite.

The EDX analysis of biogenic SeNPs harvested by *Pseudoalteromonas sp.* strain PMVW₃ and *Shewanella sp.* strain PMChW₂ depicted the presence of elemental Se. It is worth mentioning that SeNPs synthesized by *Shewanella sp.* strain PMChW₂ showed the presence of spherical and rod-shaped NPs (Fig. 4.43) using FESEM analysis. Similar studies reporting the presence of two morphotypes by a single strain are well documented. For instance, in recent studies involving *Haloferax volcanii* BBK2 and *Haloarcula japonica* BS2, haloarchaea reported formations of nanospheres and rosette-like nanoneedle (Nagar et al., 2022). Also, another study by Shirsat et al. (2015) involving *Bacillus substilis* reported to change in their crystalline structure from monoclinic to trigonal selenium over time.

The peaks at 2Q (23.57, 29.77, and 43.75) have been already reported for the synthesis of SeNPs (Vaigankar et al., 2022). Thus, confirming the biotransformative ability of *Pseudoalteromonas sp.* strain PMVW₃ to crystalline elemental selenium.

The antimicrobial activity of biogenic SeNPs against human pathogens showed no zone of inhibition with increasing concentrations of SeNPs suggesting further optimization of the SeNPs concentrations.

SeNPs, with their unique physicochemical properties and biocompatibility, offer a novel approach to disrupt biofilm formation and eradicate established biofilms (Gomez-Gomez et al., 2019). The antibiofilm activity of SeNPs against *Pseudoalteromonas sp.* strain PMVW₃ was found to be the highest against *E. coli* at 25 (18.69 %), 50 (71.58 %) and 75 (75.14 %) µg/mL. After the addition of different concentrations of SeNPs, biofilm formation began to decrease and by increasing the SeNPs concentration, bacteria were changed to be a weak-biofilm producer. Antibiotics are unable to cross the EPS layer due to factors like overproduction of efflux pumps, enzymatic modification of antimicrobial compounds, membrane lipid changes, and persists in dormant cells. These factors make biofilms multidrug-resistant, making antibiotic treatment ineffective for chronic infections. Therefore, antibiotics are not effective in treating these biofilms (Singh 2017; Yu et al., 2020). SeNPs by *Streptomyces sp.* showed inhibitory effects on biofilm formation by *Pseudomonas aeruginosa* at concentrations higher than 25 µg/ml by Sumithra et al., in 2023. Biogenic SeNPs by *Halomonas venusta* exhibited excellent dose-dependent antioxidant potential at 50 µg/mL as studied by Vaigankar et al., (2022).

An increasing % radical scavenging activity with increasing concentrations of SeNPs was recorded. Previous findings on antioxidant activity by biogenic SeNPs also showed a similar dose-dependent trend but at higher concentrations i.e. 100 to 1000 µg/mL (Ramya et

al., 2015). Where, the percent scavenging activity at 100 µg/mL was 80 % while, at 1000 µg/mL the activity was found to be 100%. However, the current study exhibits around 92% was recorded at 100 µg/mL SeNPs which is highly significant. In a study by Ullah et al., (2021) SeNPs exhibited good antioxidant activity in terms of DPPH and ABST scavenging action at a concentration of 150 µg/mL, with no significant differences between the 24 and 48-hour incubation periods.

SeNPs scavenge reactive oxygen species (ROS), such as 1,1- diphenyl-2-picrylhydrazyl (DPPH), superoxide anion ($O_2 \bullet^-$), singlet oxygen (1O_2), and carbon-centered free radicals (Forootanfara et al., 2013; Torres et al., 2012). This activity of nanoparticles is size-dependent where smaller SeNPs possess higher free radical scavenging potential (Torres et al., 2012).

Since production of EPS by *Shewanella* sp. strain PMChW₂ was confirmed by biochemical test. Therefore, a further in-depth study of EPS was performed by doing the alcian blue stain method which indicated the presence of EPS. The Alcian blue stain is commonly used for staining EPS due to its specificity for acidic polysaccharides, which are abundant in EPS. Alcian blue selectively binds to carboxyl and sulfate groups, which are prevalent in the EPS matrix, allowing for visualization and quantification of EPS in microbial samples.

Seed priming is a process by which seeds are induced into a state of pre-germinative metabolism by controlled rehydration to increase germination rates and germination vigor (Paparella et al., 2015). Seed priming was performed with two types of seeds viz. rice crop var. *Jaya* and mung bean *Vigna radiata* L. It was observed that with increasing concentrations of SeNPs the root, shoot length and wet biomass also increased as compared to the control. Expect in and mung bean *Vigna radiata* L at 100 µg/mL it is possible mainly because a high concentration of SeNPs might have a toxic effect on these beans. A study by Setty et al., (2023)

reported that rice seeds primed with SeNP 20 μM and SeNP 25 μM showed early protrusion of radicles thus enhanced germination compared to hydro-primed control. It also reported that nanoprimed seeds attained germination up to 95% after 48 h of incubation and also showed a significantly higher rate of germination than the selenite-primed seeds alone (Se 10 μM , Se 20 μM). Additionally, another study by Vaigankar et al., (2022) reported that in the presence of SeNPs (0.8 and 1 mg/L) germination and seed growth increased.

Seeds of var. *Jaya* and *Vigna radiata* L. treated with EPS-SeNPs showed an increase in the root, shoot length and wet biomass as compared to control, EPS alone and Na_2SeO_3 . This increase in growth and biomass is due to increased biosynthesis of chlorophyll and carotenoids (Ishtiaq et al., 2023). A study by Ran et al., (2024) reported that the EPS-SeNPs addition significantly alleviated Cadmium (Cd) toxicity, especially at a concentration of 0.05 g/L, and increased the length of shoots and roots compared to Cd stress alone which indicated that exogenous application of EPS-SeNPs might be an efficient strategy for alleviating Cd toxicity and improving rice growth. Keeping the above facts into consideration biogenic SeNPs by starin is more efficient for treating seeds with EPS-SeNPs than SeNPs alone as it showed an increase in the root, shoot length and wet biomass of var. *Jaya* can be used as a micronutrient to enhance plant growth.

Even though Se is a nonessential element for plants, previous studies have reported that Se NPs can help to improve the germination, growth, and stress resilience of different crops (Adhikary et al 2022; Abouelhamd et al., 2023; Ghanbari et al., 2023). Although the exact mechanisms of such improvements with SeNPs are still unknown, it has been proposed that the germination rate of different seeds can increase due to the NPs creating nanopores through their penetration, which consequently increases the imbibition of water by the seeds. Also, the selective permeability of the seed surface pores can help to internalize or restrict the uptake of

NPs (Pereira et al., 2019). SeNPs pass through a cell wall and penetrate the plasma membrane. Only NPs aggregates with diameters smaller than the pore diameter could pass through the cell wall successfully (Wang et al., 2020). The cell wall of the plant acts as a barrier, preventing easy entry of any external influences, including SeNPs, into the plant's cell walls (Carpita et al., 1979).

Extracellular polysaccharides or extracellular polymeric substances (EPS) are secreted by microorganisms. The presence of microbial extracellular polymeric substances (EPS), which are high-molecular-weight biopolymers produced by the secretion or cell lysis of microbes, is observed to be widespread and abundant in natural waters (Bhaskar and Bhosle, 2005; Flemming and Wingender, 2010). EPS plays a crucial role in cell protection, cell aggregation, adhesion, floc formation, cell-cell recognition, biofilm structure, sorption of compounds, enzymatic activities, and polysaccharide interaction with enzymes (Wingender et al., 1999; Tian, Y, 2008). Bacterial EPS (polysaccharides) are known for their antibacterial properties, which help prevent plant diseases by preventing pathogens from causing damage (Kumar et al., 2007; Mohamed et al., 2018). Due to its numerous advantages, the inoculation of Plant growth-promoting bacteria (PGPB) is a highly common and significant practice in agriculture. Minimal changes in water potential promote nutrient absorption and enhance plant growth. Thus, these bacteria can aid the plant in a variety of ways, and their separated EPS can address production issues and soil aggregation. The use of Se composite EPS would potentially enhance the effect of plant growth. To the best of my knowledge, no study has focused on EPS-SeNPs production by marine bacteria but studies from waste cane molasses by Wang et al., in 2023 and from soil by Qurashi and Sabri, (2012) have been reported. Additionally, a study by Kim, (2010) reported the synthesis of chitosan-based selenium nanoparticles using an environmentally friendly and cost-effective method using EPS. The study demonstrated that the resulting nanoparticles exhibited excellent stability and biocompatibility, making them

suitable for agricultural applications. Considering all the facts use of EPS composite SeNPs would be an ideal alternative for agricultural applications. Improving the germination quality can result in a more efficient nutrient and water uptake of seedlings, enhancing their resilience to biotic and abiotic stress (Eevera et al. 2023).

5.2 CONCLUSION

Selenite-reducing *Pseudoalteromonas* sp. bacterial strain PMVW₃ was isolated from Vaiguinim Beach and tolerated up to 360 mM for Na₂SeO₃ in ZMA with a MIC of 380 mM for Na₂SeO₃ in ZMB. Additionally, *Shewanella* sp. strain PMCH₂ tolerating 70 mM selenite showing EPS formation was also used for the studies. A prominent peak of selenium due to surface plasmon resonance at 265 nm assured the presence of SeNPs. *Pseudoalteromonas* sp. and *Shewanella* sp. were found to be sensitive against antibiotics tested such as Streptomycin, Penicillin – G, Chloramphenicol and Tetracycline. The optimum pH, temperature, and Na₂SeO₃ for SeNPs biosynthesis were found to be 7, 28 °C, and 2 mM respectively. SEM analysis showed well-isolated strain PMVW₃ and PMChW₂ cells in control, but upon exposure to 2 mM selenite, they aggregated, with elongations. EDX analysis further confirmed the formation of elemental Selenium. SeNPs synthesized by *Shewanella* sp. strain PMChW₂ showed the presence of spherical and rod-shaped NPs whereas, *Pseudoalteromonas* sp. showed rod-shaped NPs. SeNPs by *Pseudoalteromonas* sp. strain PMVW₃ demonstrated the highest antibiofilm activity against *E. coli*. Free radical scavenging activity exhibits around 92% was recorded at 100 µg/mL SeNPs which is highly significant. This is the first report of selenium biosynthesis by *Pseudoalteromonas* sp. and *Shewanella* sp. with the highest MIC of 380 and 71 mM for selenite respectively. Thus, these strains could be exploited for bioremediation of selenite from selenite-polluted sites. Also, SeNPs and EPS-SeNPs can be used as micronutrients with microgram concentrations for enhancing plant growth in the agriculture sector.

REFERENCES

- Abouelhamd, N., Gharib, F. A. E. L., Amin, A. A., and Ahmed, E. Z. (2023). Impact of foliar spray with Se, nano-Se and sodium sulfate on growth, yield and metabolic activities of red kidney bean. *Scientific Reports*. 13(1), 17102.
- Adhikari, B. and Banerjee, A., (2010). Facile synthesis of water-soluble fluorescent silver nanoclusters and HgII sensing. *Chem. Mater*. 22(15), 4364-4371.
- Adhikary, S., Biswas, B., Naskar, M. K., Mukherjee, B., Singh, A. P., and Atta, K. (2022). Remote sensing for agricultural applications. In *Arid Environment- Perspectives, Challenges and Management*. IntechOpen.
- Adschiri, T., Hakuta, Y., Sue, K. and Arai, K. (2001). Hydrothermal synthesis of metal oxide nanoparticles at supercritical conditions. *J. Nanopart. Res.* 3(2-3), 227-235.
- Altschul, S. F., Gish, W., Miller, W., Myers, E. W., and Lipman, D. J. (1990). Basic local alignment search tool. *J. mol. biol.* 215(3), 403-410.
- Amendola, V. and Meneghetti, M. (2009). Laser ablation synthesis in solution and size manipulation of noble metal nanoparticles. *Phys. Chem. Phys.* 11(20): 3805-3821.
- Anil Kumar, S., Abyaneh M.K., Gosavi, S.W., Kulkarni, S.K., Pasricha, R., Ahmad, A. and Khan, M.I. (2007). Nitrate reductase mediated synthesis of silver nanoparticles from AgNO₃. *Biotechnol. Lett.* 29:439-445.
- Ansari, M. I., and Malik, A. (2007). Biosorption of nickel and cadmium by metal-resistant bacterial isolates from agricultural soil irrigated with industrial wastewater. *Bioresource technol.* 98(16), 3149-3153.
- Ashengroph, M., and Hosseini, S. R. (2021). A newly isolated *Bacillus amyloliquefaciens* SRB04 for the synthesis of selenium nanoparticles with potential antibacterial properties. *International Microbiology*. 24(1), 103-114.
- Baesman, S.M., Bullen, T.D., Dewald, J., Zhang, D., Curran, S., Islam, F.S., Beveridge, T.J. and Oremland, R.S. (2007). Formation of tellurium nanocrystals during anaerobic growth of bacteria that use Te oxyanions as respiratory electron acceptors. *Appl. Environ. Microbiol.* 73(7), 2135-2143.
- Bahrulolum, H., Nooraei, S., Javanshir, N., Tarrahimofrad, H., Mirbagheri, V. S., Easton, A. J., and Ahmadian, G. (2021). Green synthesis of metal nanoparticles using microorganisms and their application in the agrifood sector. *J. Nanobiotechnol.* 19, 1-26.

- Baygar, T., and Ugur, A. (2017). In vitro evaluation of antimicrobial and antibiofilm potentials of silver nanoparticles biosynthesised by *Streptomyces griseorubens*. *IET Nanobiotechnol.* 11(6), 677-681.
- Bergey, D. H. (1994). *Bergey's manual of determinative bacteriology*. Lippincott Williams and Wilkins.
- Bharathi, S., Kumaran, S., Suresh, G., Ramesh, M., Thangamani, V., Pugazhvendan, S. R., and Sathiyamurthy, K. (2020). Extracellular synthesis of nanoselenium from fresh water bacteria *Bacillus* sp., and its validation of antibacterial and cytotoxic potential. *ISBAB.* 27, 101655.
- Bhaskar, P. V., Grossart, H. P., Bhosle, N. B., and Simon, M. (2005). Production of macroaggregates from dissolved exopolymeric substances (EPS) of bacterial and diatom origin. *FEMS Microbiol Ecol.* 53(2), 255-264.
- Borah, S. N., Goswami, L., Sen, S., Sachan, D., Sarma, H., Montes, M., ... and Narayan, M. (2021). Selenite bioreduction and biosynthesis of selenium nanoparticles by *Bacillus paramycoides* SP3 isolated from coal mine overburden leachate. *Environ Pollut.* 285, 117-519.
- Boyle, V. J., Fancher, M. E., and Ross Jr, R. W. (1973). Rapid, modified Kirby-Bauer susceptibility test with single, high-concentration antimicrobial disks. *AAC.* 3(3), 418-424.
- Brelle, M., Zhang, J., Nguyen, L. and Mehra, R. (1999). Synthesis and ultrafast study of cysteine and glutathione-capped Ag₂S semiconductor colloidal nanoparticles. *J. Phy Chem.* 103:10194- 10201.
- Cameotra, S. S., and Dhanjal, S. (2010). Environmental nanotechnology: nanoparticles for bioremediation of toxic pollutants. In *Bioremediation technology: recent advances*. 348-374.
- Carpita, N., Sabularse, D., Montezinos, D., and Delmer, D. P. (1979). Determination of the pore size of cell walls of living plant cells. *Science.* 205(4411): 1144-1147.
- Chen, J. (2012). An original discovery: selenium deficiency and Keshan disease (an endemic heart disease). *Asia Pacific journal of clinical nutrition.* 21(3), 320-326.
- Cushen, M., J. Kerry, M. Morris, M. Cruz-Romero, and E. Cummins. (2012). Nanotechnologies in the food industry – Recent developments, risks and regulation. *Trends Food Sci. Technol.* 24 (1), 30–46.

- Devasagayam, T. P. A., Tilak, J. C., Bloor, K. K., Sane, K. S., Ghaskadbi, S. S., and Lele, R. D. (2004). Free radicals and antioxidants in human health: current status and future prospects. *Japi*. 52(794804), 4.
- Douglas, T., Dickson, D.P., Betteridge, S., Charnock, J., Garner, C.D., and Mann, S. (1995). Synthesis and structure of an iron (iii) sulphide-ferritin bioinorganic nanocomposite. *Science*. 269,54- 57
- Dwivedi, S., AlKhedhairi, A.A., Ahamed, M., Musarrat, J. (2013). Biomimetic synthesis of selenium nanospheres by bacterial strain js-11 and its role as a biosensor for nanotoxicity assessment: a novel se-bioassay. *PLoS One*. 8, 57404.
- Ealia S., Saravanakumar MP. (2017) A review on the classification, characterisation, synthesis of nanoparticles and their application. In: *IOP Conference Series: Materials Science and Engineering*. IOP Publishing. 32019.
- El-Basiouny, N. M., Soliman, S., Khalil, N. M., El-Ghany, A., and Mohamed, N. (2024). Green Nano-Composite Film Coating in Food Preservation. *Egypt. J. Bot.*
- El-deeb, B. A., Asem, E., and Mohammed, K. (2023). Biosynthesis and optimization of selenium nanoparticles using *streptomyces* Sp. *Sohag Journal of sciences*, 8(1), 1-6.
- Ellis, R. and Roberts, E., (198)1. The quantification of ageing and survival in orthodox seeds. *Seed Sci. Technol.* 9, 373-409.
- El-Ramady, H., Abdalla, N., Taha, H., Dirk, S., Silvia, H. and El-Henawy, A. (2016). Selenium and nano-selenium in plant nutrition. *Environ. Chem. Lett.* 14, 123–147.
- Estevam, E. C., Griffin, S., Nasim, M. J., Denezhkin, P., Schneider, R., Lilischkis, R., and Jacob, C. (2017). Natural selenium particles from *Staphylococcus carnosus*: Hazards or particles with particular promise? *J haz mat.* 324, 22-30.
- Fedlheim DL, Foss CA. (2001) Metal nanoparticles: synthesis, characterization, and applications. *Boca Raton*.
- Fesharaki, P. J., Nazari, P., Shakibaie, M., Rezaie, S., Banoee, M., Abdollahi, M., and Shahverdi, A. R. (2010). Biosynthesis of selenium nanoparticles using *Klebsiella pneumoniae* and their recovery by a simple sterilization process. *Brazilian J. microbiol.* 41, 461-466.
- Flemming, H. C., and Wingender, J. (2010). The biofilm matrix. *Nature reviews microbiol.* 8(9), 623-633.
- Forootanfar, H., Adeli-Sardou, M., Nikkhoo, M., Mehrabani, M., Amir-Heidari, B., Shahverdi, A. R., and Shakibaie, M. (2014). Antioxidant and cytotoxic effect of

biologically synthesized selenium nanoparticles in comparison to selenium dioxide. *Journal of Trace Elements in Medicine and Biology*, 28(1), 75-79.

- Gericke, M. and Pinches, A., (2006). Biological synthesis of metal nanoparticles. *Hydrometallurgy*. 83(1-4): 132-140.
- Ghanbari, A. A., Gholami, M., and Ahmadi, M. (2023). Evaluation of adaptability and stability of yield of selected PachBaghela lines in spring cultivation (*Phaseolus vulgaris*) in Guilan province. *Iran. J. Field Crops Res.* 54(3), 27-40.
- Gómez-Gómez, B., Arregui, L., Serrano, S., Santos, A., Pérez-Corona, T., and Madrid, Y. (2019). Selenium and tellurium-based nanoparticles as interfering factors in quorum sensing-regulated processes: Violacein production and bacterial biofilm formation. *Metallomics*. 11(6), 1104-1114.
- Gujrati, M., Malamas, A., Shin, T., Jin, E., Sun, Y. and Lu, Z-R. (2014). Multifunctional cationic lipid-based nanoparticles facilitate endosomal escape and reduction-triggered cytosolic siRNA release. *Mol Pharm.* 11(8):2734–44
- Gutteridge, J. M. (1994). Biological origin of free radicals, and mechanisms of antioxidant protection. *Chemico-biological interactions*. 91(2-3), 133-140.
- Haferburg, G., and Kothe, E. (2007). Microbes and metals: interactions in the environment. *Journal of basic microbiology*. 47(6), 453-467.
- Hasani, S., Khare, T., and Oak, U. (2021). Antibiofilm activity of selenium nanorods against multidrug-resistant *staphylococcus aureus*. *MGM Journal of Medical Sciences*. 8(4), 415-421.
- Hasanuzzaman, M., Nahar, K., García-Caparrós, P., Parvin, K., Zulfiqar, F., Ahmed, N., and Fujita, M. (2022). Selenium supplementation and crop plant tolerance to metal/metalloid toxicity. *Frontiers in Plant Science*. 12, 792-770.
- Ho, C. T., Nguyen, T. H., Lam, T. T., Le, D. Q., Nguyen, C. X., Lee, J. H., and Hur, H. G. (2021). Biogenic synthesis of selenium nanoparticles by *Shewanella* sp. HN-41 using a modified bioelectrochemical system. *Electronic Journal of Biotechnology*. 54, 1-7.
- Horobin, R. W. (2010). How do dyes impart color to different components of the tissues. *Educational guide special stains and H and E, 2nd edn. Carpinteria, California*. 159-166.
- Hu, H., Xin, J. H., Hu, H., Wang, X., Miao, D., and Liu, Y. (2015). Synthesis and stabilization of metal nanocatalysts for reduction reactions—a review. *Journal of materials chemistry A*. 3(21), 11157-11182.

- Huang, X., Chen, X., Chen, Q., Yu, Q., Sun, D., and Liu, J. (2016). Investigation of functional selenium nanoparticles as potent antimicrobial agents against superbugs. *Acta biomaterialia*, 30, 397-407.
- Huang, Z., Guo, B. J., Wong, R. N. S., and Jiang, Y. (2007). Characterization and antioxidant activity of selenium-containing phycocyanin isolated from *Spirulina platensis*. *Food Chemistry*. 100(3), 1137-1143.
- Hudzicki, J. (2009). Kirby-Bauer disk diffusion susceptibility test protocol. *American society for microbiology*. 15(1), 1-23.
- Ike, M., Takahashi, K., Fujita, T., Kashiwa, M., Fujita, M. (2000). Selenate reduction by bacteria isolated from aquatic environment free from selenium contamination. *Water Res.* 34 (11), 3019e3025.
- Ishtiaq, M., Mazhar, M. W., Maqbool, M., Hussain, T., Hussain, S. A., Casini, R., ... and Elansary, H. O. (2023). Seed priming with the selenium nanoparticles maintains the redox status in the water stressed tomato plants by modulating the antioxidant defense enzymes. *Plants*. 12(7), 1556.
- Joudeh, N., and Linke, D. (2022). Nanoparticle classification, physicochemical properties, characterization, and applications: a comprehensive review for biologists. *Journal of Nanobiotechnology*. 20(1), 262.
- Kalimuthu, K., Babu, R.S., Venkataraman, D., Bilal, M., and Gurunathan, S. (2008). Biosynthesis of silver nanocrystals by *Bacillus licheniformis*. *Colloid Surf. B*. 65: 150-153.
- Kammler, H., Mädler, L. and Pratsinis, S. (2001). Flame synthesis of nanoparticles. *Chem. Eng. Technol.* 24(6): 583-596.
- Kang, I., Kang, M., Lee, E., Seo, H. and Ahn, C. (2011). Facile, hetero-sized nanocluster array fabrication for investigating the nanostructure-dependence of nonvolatile memory characteristics. *Nanotechnology*. 22(25): 254018
- Kapur, M., Soni, K., and Kohli, K. (2017). Green synthesis of selenium nanoparticles from broccoli, characterization, application and toxicity. *Adv. Tech. Biol. Med*, 5(1), 2379-1764.
- Kathiresan, K., Alikunhi, N., Pathmanaban, S., Nabikhan, A. and Kandasamy, S. (2010). Analysis of antimicrobial silver nanoparticles synthesized by coastal strains of *Escherichia coli* and *Aspergillus niger*. *Can. J. Microbiol.* 56(12), 1050-1059.
- Khan I, Saeed K, Khan I. (2019). Nanoparticles: properties, applications and toxicities. *Arab J Chem*.12(7),908–31.

- Kim, H., Choi, B., and Kim, J. (2010). Reduction of earth pressure on buried pipes by EPS geof foam inclusions. *Geotechnical Testing Journal*. 33(4), 304-313.
- Klaus, T., Joerger, R., Olsson, E., and Granqvist, C. G. (1999). Silver-based crystalline nanoparticles, microbially fabricated. *Proceedings of the National Academy of Sciences*. 96(24), 13611-13614.
- Kumar, A., and Prasad, K. S. (2021). Role of nano-selenium in health and environment. *Journal of Biotechnology*. 325, 152-163.
- Kumar, M. A., Anandapandian, K. T. K., and Parthiban, K. (2011). Production and characterization of exopolysaccharides (EPS) from biofilm forming marine bacterium. *Brazilian archives of biology and technology*. 54, 259-265.
- Lamas, D., Lascalea, G., Juárez, R., Djurado, E., Pérez, L. and de Reza, N. (2003). Metastable forms of the tetragonal phase in compositionally homogeneous, nanocrystalline zirconia–ceria powders synthesised by gel-combustion. *J. Mat. Chem*. 13(4), 904- 910.
- Li, D.-B., Cheng, Y.-Y., Wu, C., Li, W.-W., Li, N., Yang, Z.-C., Tong, Z.-H., Yu, H.-Q., (2014). Selenite reduction by *Shewanella oneidensis* MR-1 is mediated by fumarate reductase in periplasm. *Sci. Rep.* 4, 3735.
- Lindblow-Kull, C., Kull, F.J., Shrift, A. (1985). Single transporter for sulfate, selenate, and selenite in *Escherichia coli* K-12. *J. Bacteriol.* 163, 1267–1269.
- Lupo, A., Coyne, S., and Berendonk, T. U. (2012). Origin and evolution of antibiotic resistance: the common mechanisms of emergence and spread in water bodies. *Frontiers in microbiology*. 3, 18.
- Mishra, R., Singh, E., Kumar, A., Singh, A. K., Madhav, S., Shukla, S. K., and Kumar, S. (2023). Metal pollution in marine environment: sources and impact assessment. In *Metals in Water*.175-193. Elsevier.
- Mody VV, Siwale R, Singh A, Mody HR. (2010). Introduction to metallic nanoparticles. *J Pharm Bioallied Sci*. 2(4):282.
- Mohamed, S. S., Amer, S. K., Selim, M. S., and Rifaat, H. M. (2018). Characterization and applications of exopolysaccharide produced by marine *Bacillus altitudinis* MSH2014 from Ras Mohamed, Sinai, Egypt. *Egyptian Journal of Basic and Applied Sciences*. 5(3), 204-209.
- Mohapatra, B., Sar, P., Kazy, S. K., Maiti, M. K., and Satyanarayana, T. (2018). Taxonomy and physiology of *Pseudoxanthomonas arseniciresistens* sp. nov., an

arsenate and nitrate-reducing novel *gammaproteobacterium* from arsenic contaminated groundwater, India. *PLoS One*. 13(3), e0193718.

- Mohapatra, B., Sar, P., Kazy, S. K., Maiti, M. K., and Satyanarayana, T. (2018). Taxonomy and physiology of *Pseudoxanthomonas arseniciresistens* sp. nov., an arsenate and nitrate-reducing novel *gammaproteobacterium* from arsenic contaminated groundwater, India. *PLoS One*. 13(3), e0193718.
- Morris, J. and Crane, S. (2013). Selenium toxicity from a misformulated dietary supplement, adverse health effects, and the temporal response in the nail biologic monitor. *Nutrients*. 5(4), 1024-1057.
- Mujawar, S. Y., Shamim, K., Vaigankar, D. C., and Dubey, S. K. (2019). Arsenite biotransformation and bioaccumulation by *Klebsiella pneumoniae* strain SSSW7 possessing arsenite oxidase (aioA) gene. *Biometals*. 32, 65-76.
- Mujawar, S. Y., Vaigankar, D. C., and Dubey, S. K. (2021). Biological characterization of *Bacillus flexus* strain SSA11 transforming highly toxic arsenite to less toxic arsenate mediated by periplasmic arsenite oxidase enzyme encoded by aioAB genes. *BioMetals*. 34(4), 895-907.
- Muthukannan, R. and Karuppiyah, B. (2011). Rapid synthesis and characterization of silver nanoparticles by novel *Pseudomonas* sp. “ram bt-1”. *J. Eco. Biotechnol.* 3, 24-28.
- Nagar, V., Singh, T., Tiwari, Y., Aseri, V., Pandit, P. P., Chopade, R. L., and Awasthi, G. (2022). ZnO Nanoparticles: Exposure, toxicity mechanism and assessment. *Materials Today: Proceedings*. 69, 56-63.
- Nahar, L. and Arachchige, I. (2013). Sol-Gel methods for the assembly of metal and semiconductor nanoparticles. *JSM Nanotechnol. Nanomed.* 1, 1104.
- Nangia, Y., Wangoo, N., Goyal, N., Shekhawat, G. and Suri, C.R. (2009). A novel bacterial isolate *Stenotrophomonas maltophilia* as living factory for synthesis of gold nanoparticles. *Microb. Cell Fact.* 8, 39.
- Nascimento MA, Cruz JC, Rodrigues GD, de Oliveira AF, Lopes RP. (2018). Synthesis of polymetallic nanoparticles from spent lithium-ion batteries and application in the removal of reactive blue 4 dye. *J Clean Prod.*202, 264–72
- Ng KK, Zheng G (2015). Molecular interactions in organic nanoparticles for phototheranostic applications. *Chem Rev.*115(19), 11012–42.

- Niki, E. (2010). Do free radicals play causal role in atherosclerosis? Low density lipoprotein oxidation and vitamin E revisited. *Journal of clinical biochemistry and nutrition*, 48(1), 3-7.
- Oremland, R., Herbel, M., Blum, J., Langley, S., Beveridge, T., Ajayan, P., Sutto, T., Ellis, A. and Curran, S. (2004). Structural and spectral features of selenium nanospheres produced by Se-respiring bacteria. *Appl. Environ. Microbiol.* 70(1): 52-60.
- Pan K, Zhong Q. (2016). Organic nanoparticles in foods: fabrication, characterisation, and utilization. *Annu Rev Food Sci Technol.* 7: 245–66.
- Paparella, S., Araújo, S. S., Rossi, G., Wijayasinghe, M. A. L. A. K. A., Carbonera, D., and Balestrazzi, A. (2015). Seed priming: state of the art and new perspectives. *Plant cell reports.* 34, 1281-1293.
- Pereira, A. D. E. S., Oliveira, H. C., and Fraceto, L. F. (2019). Polymeric nanoparticles as an alternative for application of gibberellic acid in sustainable agriculture: a field study. *Scientific reports.* 9(1), 7135.
- Piacenza, E., Presentato, A., Bardelli, M., Lampis, S., Vallini, G., Turner, R.J. (2019). Influence of bacterial physiology on processing of selenite, biogenesis of nanomaterials and their thermodynamic stability. *Molecules* 24.
- Pimpin, A. and Srituravanich, W. (2012). Review on micro-and nanolithography techniques and their applications. *Eng. J.* 16(1): 37-56.
- Qurashi, A. W., and Sabri, A. N. (2012). Biofilm formation in moderately halophilic bacteria is influenced by varying salinity levels. *Journal of basic microbiology.* 52(5), 566-572.
- Rahman, M. M., Feng, X., Zhang, H., Yan, X., Peng, Q., and Yu, P. (2019). Using vibrational ATR-FTIR spectroscopy with chemometrics to reveal faba CHO molecular spectral profile and CHO nutritional features in ruminant systems. *Spectrochimica Acta Part A: Molecular and Biomolecular Spectroscopy.* 214, 269-276.
- Ran, M., Wu, T., Jiao, Y., Wu, J., and Li, J. (2024). Selenium bio-nanocomposite based on extracellular polymeric substances (EPS): Synthesis, characterization and application in alleviating cadmium toxicity in rice (*Oryza sativa* L.). *International Journal of Biological Macromolecules.* 258, 129-089.
- Ravindra P. (2009). Protein-mediated synthesis of gold nanoparticles. *Mat. Sci. Eng. B* 163,93- 98.
- Saad, A. M., Sitohy, M. Z., Sultan-Alolama, M. I., El-Tarabily, K. A., and El-Saadony, M. T. (2022). Green nanotechnology for controlling bacterial load and heavy metal

accumulation in Nile tilapia fish using biological selenium nanoparticles biosynthesized by *Bacillus subtilis* AS12. *Frontiers in microbiology*. 13, 101-5613.

- Saad, Am and Moghannem, Saad and Farag, Mohamed and Shehabeldine, Amr and Salah, Mohamed. (2017). Media Optimization for Exopolysaccharide Producing *Klebsiella oxytoca* KY498625 under Varying Cultural Conditions. *International Journal of Advanced Research in Biological Sciences (IJARBS)*. 4. 16-30.
- Sabaty, M., Avazeri, C., Pignol, D., Vermeaglio, A. (2001). Characterization of the reduction of selenate and tellurite by nitrate reductases. *Appl. Environ. Microbiol.* 67, 5122–5126.
- Samant, S., Naik, M., Parulekar, K., Charya, L. and Vaigankar, D. (2018). Selenium reducing *Citrobacter freundii* strain KP6 from Mandovi estuary and its potential application in selenium nanoparticle synthesis. *Proc. Natl. Sci. India Sect. B: Bio. sci.* 88(2), 747-754.
- Keskin, N. O., Akbal Vural, O., and Abaci, S. (2020). Biosynthesis of noble selenium nanoparticles from *Lysinibacillus* sp. NOSK for antimicrobial, antibiofilm activity, and biocompatibility. *Geomicrobiology Journal*. 37(10), 919-928.
- Sathiyarayanan, G., Kiran, G. S., and Selvin, J. (2013). Synthesis of silver nanoparticles by polysaccharide bioflocculant produced from marine *Bacillus subtilis* MSBN17. *Colloids and Surfaces B: Biointerfaces*. 102, 13-20.
- Schrauzer, G.N. (2000). Selenomethionine: a review of its nutritional significance, metabolism, and toxicity. *J. Nutr.* 130, 1653–1656.
- Setty, J., Samant, S. B., Yadav, M. K., Manjubala, M., and Pandurangam, V. (2023). Beneficial effects of bio-fabricated selenium nanoparticles as seed nanopriming agent on seed germination in rice (*Oryza sativa* L.). *Scientific Reports*. 13(1), 22349.
- Shakeri, F., Zaboli, F., Fattahi, E., and Babavalian, H. (2022). Biosynthesis of selenium nanoparticles and evaluation of its antibacterial activity against *Pseudomonas aeruginosa*. *Advances in Materials Science and Engineering*. 1-10.
- Shakibaie, M., Forootanfar, H., Golkari, Y., Mohammadi-Khorsand, T., and Shakibaie, M. R. (2015). Anti-biofilm activity of biogenic selenium nanoparticles and selenium dioxide against clinical isolates of *Staphylococcus aureus*, *Pseudomonas aeruginosa*, and *Proteus mirabilis*. *Journal of Trace Elements in Medicine and Biology*. 29, 235-241.
- Sharma, S. K., Gaur, A., Saddikuti, V., and Rastogi, A. (2017). Structural equation model (SEM)-neural network (NN) model for predicting quality determinants of e-

learning management systems. *Behaviour and information technology*. 36(10), 1053-1066.

- Shenton, W., Douglas, T., Young, M., Stubbs, G. and Mann, S. (1999). Inorganic–organic nanotube composites from template mineralization of *Tobacco mosaic virus*. *Adv. Mater.* 11:253- 256.
- Shi, X. D., Tian, Y. Q., Wu, J. L., and Wang, S. Y. (2021). Synthesis, characterization, and biological activity of selenium nanoparticles conjugated with polysaccharides. *Critical Reviews in Food Science and Nutrition*. 61(13), 2225-2236.
- Shirsat, S., Kadam, A., Naushad, M. and Mane, R.S. (2015). Selenium nanostructures: microbial synthesis and applications. *RSC Adv.* 5(112): 92799-92811.
- Shrestha, S., Zhang, W., Begbie, A. J., Pukala, T. L., and Smid, S. D. (2020). Ecklonia radiata extract containing eckol protects neuronal cells against A β 1–42 evoked toxicity and reduces aggregate density. *Food and Function*. 11(7), 6509-6516.
- Silver, S., and Phung, L. T. (1996). Bacterial heavy metal resistance: new surprises. *Annual review of microbiology*. 50(1), 753-789.
- Singh, D., Singh, V., Mishra, S. B., Sharma, D., and Agarwal, V. (2022). Evaluation of anti-biofilm, anti-quorum, anti-dysenteric potential of designed polyherbal formulation: in vitro and in vivo study. *Journal of Applied Biomedicine*. 20(1).
- Skalickova, S., Milosavljevic, V., Cihalova, K., Horoky, P., Richtera, L., Adam, V. (2017). Selenium nanoparticles as a nutritional supplement. *Nutrition*. 33, 83–90.
- Sohm, J. A., Edwards, B. R., Wilson, B. G., and Webb, E. A. (2011). Constitutive extracellular polysaccharide (EPS) production by specific isolates of *Crocospaera watsonii*. *Frontiers in microbiology*. 2, 16345.
- Srivastava, N. and Mukhopadhyay, M. (2013). Biosynthesis and structural characterization of selenium nanoparticles mediated by *Zooglea ramigera*. *Powder Technol.* 244, 26-29.
- Sumithra, D., Bharathi, S., Kaviyarasan, P., and Suresh, G. (2023). Biofabrication of selenium nanoparticles using marine *Streptomyces* sp. and assessment of its antibacterial, antibiofilm, antioxidant, and in vivo cytotoxic potential. *Geomicrobiology Journal*. 40(5), 485-492.
- Tamura, K., Stecher, G., and Kumar, S. (2021). MEGA11: molecular evolutionary genetics analysis version 11. *Molecular biology and evolution*. 38(7), 3022-3027.

- Tan, L.C., Nancharaiah, Y.V., van Hullebusch, E.D., Lens, P.N. (2018). Anaerobic Treatment of Mine Wastewater for the Removal of Selenate and its Co-contaminants. *CRC Press*. 9e71.
- Tian, Y. (2008) Behaviour of bacterial extracellular polymeric substances from activated sludge: A review. *Int. J. Environ. Pollut.* 32, 78–89.
- Torres, S. K., Campos, V. L., León, C. G., Rodríguez-Llamazares, S. M., Rojas, S. M., Gonzalez, M., ... and Mondaca, M. A. (2012). Biosynthesis of selenium nanoparticles by *Pantoea agglomerans* and their antioxidant activity. *Journal of Nanoparticle Research*. 14, 1-9.
- Toshima N, Yonezawa T. (1998). Bimetallic nanoparticles—novel materials for chemical and physical applications. *New J Chem*. 22(11):1179–201.
- Turner, R.J., Weiner, J.H., Taylor, D.E. (1998). Selenium metabolism in *Escherichia coli*. *Biometals*. 11, 223–227.
- Ullah, H., Lun, L., Rashid, A., Zada, N., Chen, B., Shahab, A., ... and Wong, M. H. (2023). A critical analysis of sources, pollution, and remediation of selenium, an emerging contaminant. *Environmental Geochemistry and Health*. 45(5), 1359-1389.
- Vaigankar, D. C. (2020). Biosynthesis and characterization of Selenium and Tellurium nanoparticles by marine bacteria (Doctoral dissertation, Goa University).
- Wadhvani, S. A., Gorain, M., Banerjee, P., Shedbalkar, U. U., Singh, R., Kundu, G. C., and Chopade, B. A. (2017). Green synthesis of selenium nanoparticles using *Acinetobacter* sp. SW30: optimization, characterization and its anticancer activity in breast cancer cells. *International journal of nanomedicine*. 6841-6855.
- Wadhvani, S.A., Shedbalkar, U.U., Singh, R., Chopade, B.A. (2016). Biogenic selenium nanoparticles: current status and future prospects. *Appl. Microbiol. Biotechnol.* 100, 2555–2566.
- Wang, D., Rensing, C., and Zheng, S. (2022). Microbial reduction and resistance to selenium: mechanisms, applications and prospects. *Journal of hazardous materials*. 421, 126684.
- Wang, D., Xia, X., Wu, S., Zheng, S., Wang, G. (2019). The essentialness of glutathione reductase GorA for biosynthesis of Se (0)-nanoparticles and GSH for CdSe quantum dot formation in *Pseudomonas stutzeri* TS44. *J. Hazard. Mater.* 366, 301–310.

- Wang, Y., Wang, H., and Chen, H. (2023). Response of aerobic activated sludge to edible oil exposure: extracellular polymeric substance (EPS) characteristics and microbial community. *Journal of Environmental Management*. 335, 117571.
- Weisburg, W. G., Barns, S. M., Pelletier, D. A., and Lane, D. J. (1991). 16S ribosomal DNA amplification for phylogenetic study. *Journal of bacteriology*. 173(2), 697-703.
- Wells, M., McGarry, J., Gaye, M.M., Basu, P., Oremland, R.S., Stolz, J.F. (2019). Respiratory selenite reductase from *Bacillus selenitireducens* strain MLS10. *J. Bacteriol.* 201, e00614–e00618.
- Wingender, J., Neu, T. R., and Flemming, H. C. (1999). What are bacterial extracellular polymeric substances? *Springer Berlin Heidelberg*.1-19.
- World Health Organization (WHO) (2011) Guidelines for drinkingwater quality, 4th edn. WHO, *Geneva*.
- Yu, H. H., Song, Y. J., Yu, H. S., Lee, N. K., and Paik, H. D. (2020). Investigating the antimicrobial and antibiofilm effects of cinnamaldehyde against *Campylobacter* spp. using cell surface characteristics. *Journal of food science*. 85(1), 157-164.

APPENDIX

Appendix I

Media composition

1. Nutrient Agar: HiMedia

Ingredients	g/L
Peptone	5
Yeast extract	1.5
Sodium chloride	5
HM peptone B#	1.5
Agar	15
Distilled water	1000 ml
pH	7.4±0.2

2. Zobell Marine Agar: HiMedia

Ingredients	g/L
Peptone	5
Yeast extract	1
Ferric citrate	0.100
Sodium chloride	19.45
Magnesium chloride	8.80
Sodium sulphate	3.240
Calcium chloride	1.800
Potassium chloride	0.550
Sodium bicarbonate	0.160
Potassium bromide	0.080
Strontium chloride	0.034
Boric acid	0.022
Sodium silicate	0.004
Sodium fluoride	0.0024
Ammonium nitrate	0.0016
Disodium phosphate	0.008
Agar	15
Distilled water	1000 ml
pH	7.6±0.2

3. Mueller Hinton Agar: HiMedia

Ingredients	g/L
Meat infusion	2.0
Acidcase	17.5
Starch	1.5
Agar	17.0
Distilled water	1000 ml
pH	7.3±0.2

4. Nutrient Broth: HiMedia

Ingredients	g/L
Peptone	5
Yeast extract	3
Sodium chloride	5
HM peptone B#	1.5
Yeast extract	1.5
Distilled water	1000 ml
pH	7.4±0.2

5. Zobell Marine Broth: HiMedia

Ingredients	g/L
Peptone	5
Yeast extract	1
Ferric citrate	0.100
Sodium chloride	19.45
Magnesium chloride	8.80
Sodium sulphate	3.240
Calcium chloride	1.800
Potassium chloride	0.550
Sodium bicarbonate	0.160
Potassium bromide	0.080
Strontium chloride	0.034
Boric acid	0.022
Sodium silicate	0.004
Sodium fluoride	0.0024
Ammonium nitrate	0.0016
Disodium phosphate	0.008
Distilled water	1000 ml
pH	7.6±0.2

6. Saline: HiMedia

Ingredients	g/L
Sodium chloride	0.85
Distilled water	100 ml

Appendix II

Biochemical test media composition

1. Sugar medium: HiMedia

Ingredients	g/L
Peptone	0.1
Sodium chloride	0.5
Phenol red	5ml of 0.2%
Distilled water	1000 ml
pH	7.2±7.4

2. Hugh-Leifsons Glucose medium: HiMedia

Ingredients	g/L
Peptone	2
Sodium chloride	30
Yeast extract	0.50
Dextrose	10
Bromothymol blue	0.015
Agar	3
Distilled water	1000 ml
pH	7.4±0.2

3. Nitrate Broth: HiMedia

Ingredients	g/L
Peptone	5
Potassium nitrate	1
HM peptone B#	3
Distilled water	1000 ml
pH	7.0±0.2

a) Reagent A

Ingredients	g/L
Sulfanilic acid	3.46
Distilled water	20 ml

a) Reagent B

Ingredients	g/L
Alpha- naphthylamine	2.86
Distilled water	20 ml

4. Motility medium

Ingredients	g/L
Nutrient agar	0.56
Distilled water	20 ml

5. Indole production medium: HiMedia

Ingredients	g/L
Tryptone	10
Sodium chloride	5
Distilled water	1000 ml
pH	7.5±0.2

6. Methyl red and Voges Proskauer: HiMedia

Ingredients	g/L
Buffered peptone	7
Dextrose	5
Dipotassiumhydro phosphate	5
Distilled water	1000 ml
pH	6.9±0.2

a) Barrit's reagent A

Ingredients	g/L
Alpha- naphthol	1
Distilled water	20 ml

a) Barrit's reagent B

Ingredients	g/L
Potassium hydroxide	8
Distilled water	20 ml

7. Citrate utilization media: HiMedia

Ingredients	g/L
Magnesium sulphate	0.2
Ammonium hydrogen phosphate	1
Dipotassium hydrogen phosphate	1
Sodium citrate	2
Sodium chloride	5
Bromothymol blue	0.08
Agar	15
Distilled water	1000 ml
pH	6.8±0.2

8. EPS medium

Ingredients	g/L
Zobell Marine Agar	5.525
Congo red	8 ml
Distilled water	100 ml

9. Gram's staining

a) Crystal violet: HiMedia

Ingredients	Quantity
Ammonium oxalate	8 gm
Crystal violet	10 gm
Alcohol	100 ml
Distilled water	900 ml

b) Gram's iodine: HiMedia

Ingredients	Quantity
Iodine	1 gm
Potassium iodide	2 gm
Distilled water	300 ml

c) Decolorizer: HiMedia

Ingredients	Quantity
Ethanol	95 ml
Distilled water	5 ml

d) Safranin: HiMedia

Ingredients	Quantity
Safranin powder	20 mg
Distilled water	100 ml

Appendix III

Other Chemicals

1. Prepare a stock solution of Sodium selenite

Ingredients	g/L
Sodium selenite	17.29
Distilled water	100 ml

2. Phosphate Buffered Saline (PBS)

Ingredients	g/L
Sodium chloride	4
Potassium chloride	0.1
Dipsodium hydrogen phosphate	0.72
Potassium Dihydrogen phosphate	0.12
Distilled water	500 ml
pH	7.4

Appendix IV

1. PCR reaction mixture

Component Concentration Quantity	Concentration	
Template DNA	50 ng/ μ L	4 μ L
Master mix	2X	25 μ L
Forward primer	20 mM	2 μ L
Reverse primer	20 mM	2 μ L
Deionized water	-	17 μ L
Total volume	50 μ L	

2. Agarose Gel Electrophoresis

a) 0.8 % and 1 % agarose

Weigh 0.8 g and 1.0 g and dissolve in 100 mL of 1X TAE buffer to prepare 0.8 % and 1 % agarose respectively. Melt the solution in microwave oven until clear, transparent solution is obtained. Add ethidium bromide to a final concentration of 0.5 μ g/mL and cast the gel.

b) Ethidium Bromide

Add 1.0 g of ethidium bromide to 100 mL of deionized water. Stir on magnetic stirrer for several hours to ensure that the dye has dissolved. Transfer the solution to amber coloured bottle and store at room temperature.

c) Gel Loading Buffer

0.05 % (w/v) Bromophenol blue

40 % (w/v) Sucrose

0.1M Ethylenediaminetetraaceticacid (EDTA) (pH 8.0)

0.5 % (w/v) Sodium dodecyl sulphate

d) 10X Tris EDTA (TE) Buffer (pH 8.0)

Tris Chloride 100 mM

EDTA 10 mM

Sterilize for 20 min at 15 psi.

3. Electrophoresis buffer (pH > 13)

a) Stock solution

10 N NaOH: 200 g of NaOH pellets were dissolved in 500 mL DDW. This solution was dispersed in 27 mL aliquots in tightly capped tubes and was stored at ambient temperature (28-34 $^{\circ}$ C).

200 mM EDTA: 14.89 g of EDTA was dissolved in 200 mL DDW, the pH was adjusted to 10 and stored at ambient temperature (28-34 $^{\circ}$ C).

b) Working solution

The working solution was prepared by mixing 27 mL of 10 N NaOH, 4.5 mL of 200 mM EDTA and 1 mL of DMSO. The working solution was prepared fresh before each run.

4. Stain

Ingredients	µg/ml
Ethidium bromide	15
Distilled water	1 ml

Appendix V

Antibiotic assay standard disc chart

Name of antibiotics (dose)	Inhibitory zone diameter to nearest millimeter (mm)		
	Sensitive (S)	Moderately sensitive (MS)	Resistant (R)
Amoxicillin (30 μ g/disk)	≥ 18	14–17	≤ 13
Cloxacillin (5 μ g/disk)	≥ 25	22–24	≤ 21
Cephalothin (30 μ g/disk)	≥ 18	15–17	≤ 14
Cephradine (25 μ g/disk)	≥ 18	13–17	≤ 12
Cefuroxime (30 μ g/disk)	≥ 23	15–22	≤ 14
Cefixime (5 μ g/disk)	≥ 19	16–18	≤ 15
Kanamycin (30 μ g/disk)	≥ 18	14–17	≤ 13
Streptomycin (10 μ g/disk)	≥ 15	12–14	≤ 11
Neomycin (30 μ g/disk)	≥ 17	13–16	≤ 12
Vancomycin (30 μ g/disk)	≥ 12	10–11	≤ 9
Erythromycin (15 μ g/disk)	≥ 23	14–22	≤ 13
Azithromycin (15 μ g/disk)	≥ 18	14–17	≤ 13
Ciprofloxacin (15 μ g/disk)	≥ 21	16–20	≤ 15
Levofloxacin (5 μ g/disk)	≥ 17	14–16	≤ 13
Tetracycline (30 μ g/disk)	≥ 15	12–14	≤ 11
Doxycycline (30 μ g/disk)	≥ 14	11–13	≤ 10
Cotrimoxazole (25 μ g/disk)	≥ 16	11–15	≤ 10
Chloramphenicol (30 μ g/disk)	≥ 18	13–17	≤ 12

Antibiotics	Disc content	Diameter of zone of inhibition (mm)		
		Resistant (mm or less)	Intermediate (mm)	Sensitive (mm or more)
Neomycin	30 mcg	12	13-16	17
Gentamicin	10 mcg	12	13-14	15
Vancomycin	30 mcg	14	15-16	17
Ampicillin	10 mcg	13	14-16	17
Bacitracin	10 units	8	9-12	13
Erythromycin	15 mcg	13	14-22	23
Penicillin G	10 units	14	--	15
Streptomycin	10 mcg	11	12-14	15
Chloramphenicol	30 mcg	12	13-17	18

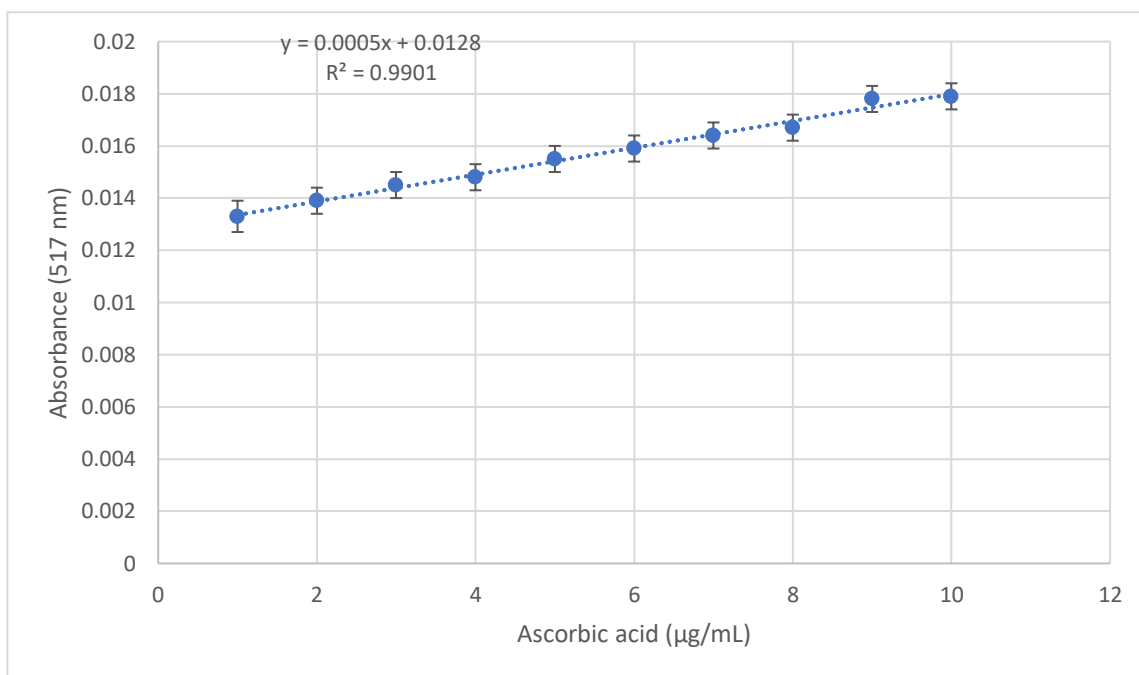
Appendix VI**Standard curve**

Fig. A: Calibration curve of ascorbic acid for estimation of DPPH free radical scavenging activity.

Values are mean \pm (standard error) for three independent experiments.

SEMINAR ATTENDED

Attended one day State level seminar on “Sustainable Energy Development And Renewable Energy Technologies: Perspectives And Challenges” also, participated in Poster Competition and was awarded 1st prize in Post Graduate category, held on 7th March 2024, organised by Department of Physics, P.E.S’s R.S.N College of Arts and Science at Farmagudi, Ponda Goa.



Presented poster at P.E.S’s R.S.N College of Arts and Science at Farmagudi, Ponda Goa.



Awarded 1st prize in Poster Competition